Australian Government
Bureau of Meteorology

Changes to Fire Weather in Queensland

A report from the Australian Bureau of Meteorology, prepared for Queensland Fire and Emergency Services

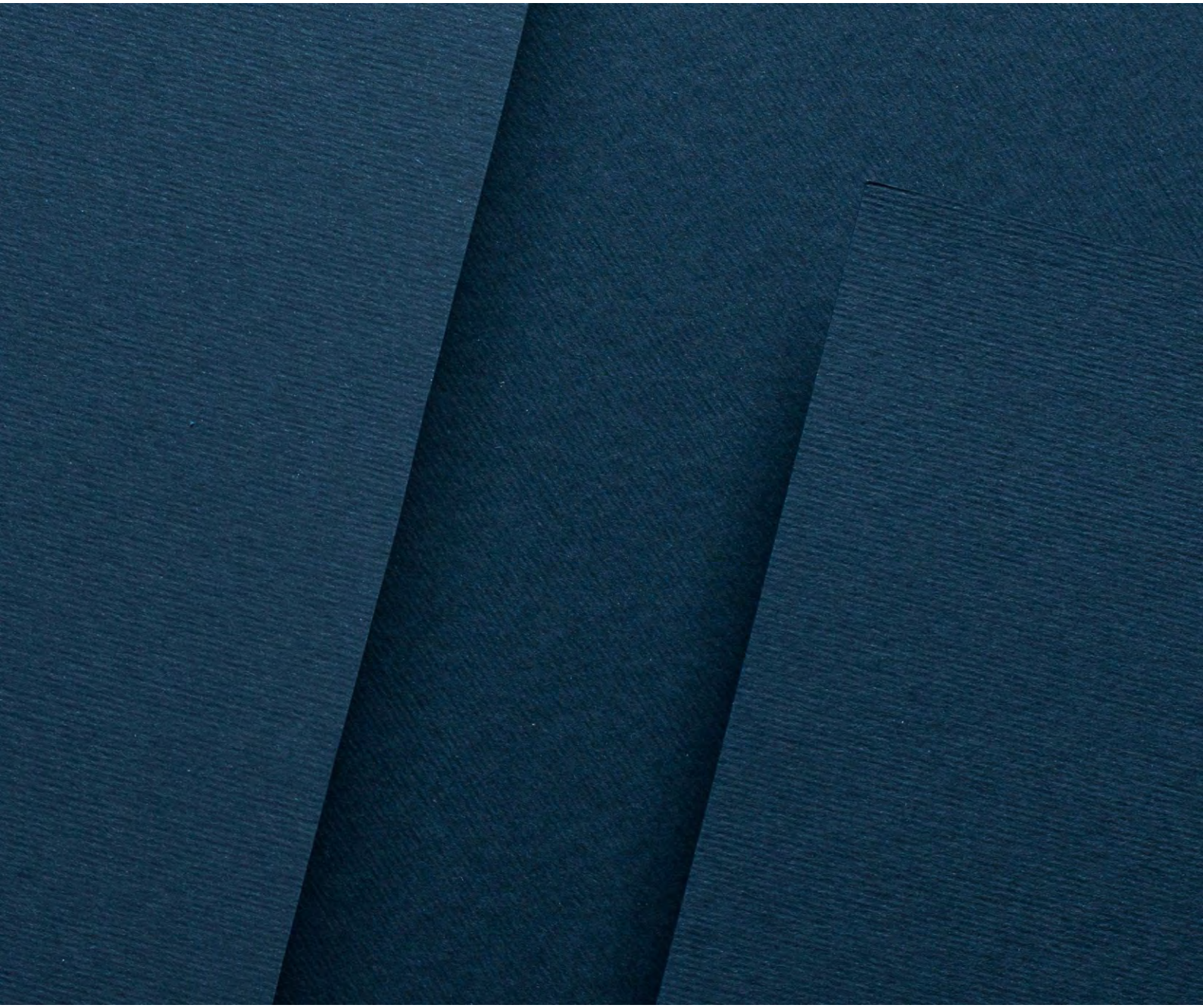

This report is the product of ongoing collaboration between the Bureau of Meteorology and Queensland Fire and Emergency Services (QFES). The Bureau acknowledges, in particular, the contribution of the Community Resilience and Risk Mitigation Branch within QFES.

Bureau contact for this report:

Dr David Jones
Manager Climate Services
Bureau of Meteorology
GPO Box 1289 Melbourne Vic 3001, Australia
Phone: +61 3 9669 4085
Email: david.jones@bom.gov.au

QFES contact for this report:

Office of the Assistant Commissioner, Emergency Management and Community Capability
Queensland Fire and Emergency Services
GPO Box 1425 Brisbane QLD 4001, Australia
Mail Cluster 14.11
Phone: +61 7 3635 3745
Email: emcc.assistantcommissioner@qfes.qld.gov.au

Table of Contents

Executive Summary

This report describes long-term changes in fire-weather conditions for Queensland across the period 1950-2018, as characterised by the Mark V McArthur daily Forest Fire Danger Index (FFDI), together with an assessment of changes in other relevant climatic variables (rainfall, temperature). The report looks at these changes in the Statewide context, but also focusses on nine subregions. The report uses the daily FFDI dataset of Dowdy (2018), which is available from 1950 through to the present, and that availability dictates the choice of study period. This dataset is a gridded dataset, at 0.05° resolution. Each grid point FFDI value is therefore representative of an area of approximately 5 km × 5 km, and so complete consistency with collocated site data (e.g., from a single automatic weather station) is not to be expected.

Key messages:

- Annually averaged maximum temperatures have risen across the period 1950-2018 for most of Queensland (Figure 17, Table 2), with the highest values being in the southwest of the State where the changes exceed +2°C.
- Annual rainfall has risen over most of the far west and far north of the State across the study period, but fallen across the remainder of the State, particularly along the east coast where the declines exceed 100 mm (Figure 18, Table 2). It should be noted that Australian rainfall shows significant interdecadal variability.
- Annual accumulated FFDI, a proxy for average daily FFDI, has risen across most of the State, and particularly so in the south (Figure 20, Table 3). The largest subregional changes in percentages terms are in the southeast (South East Coast 51%, Wide Bay and Burnett 42%). For the Central South subregion, it is 27%.
- Annual highest daily FFDI has risen strongly in the south of the State, with increases of 15 FFDI points and higher seen along the southern border. Falls in annual highest daily FFDI are seen in the far west (Figure 21), reaching 15 FFDI points.
- The annual incidence of FFDI ≥ 25 days has risen across most of the State (Figures ES1 and 22, Table 3). In State-averaged terms, Queensland is now seeing an additional 29 FFDI ≥ 25 days per year. The largest subregional changes in percentages terms are in the southeast (South East Coast 254%, Wide Bay and Burnett 187%). For the Cape York Peninsula subregion, it is 109%.

- In Statewide terms, FFDI ≥ 25 days are occurring earlier in Spring than before (Figure 42). There are some suggestions that this is happening in the two southeast subregions (South East Coast, Wide Bay and Burnett), although such Spring days remain relatively infrequent. The signs are stronger and clearer in the inland subregions (Central South, Central, North West, South West), although in the South West subregion the change is also intruding upon the late winter.

There are strong indications that the changes in Queensland's fire-weather characteristics have *not* been uniform across the study period. Instead, the changes have been more rapid in recent decades. Figure ES1 (also Figure 32) shows the Statewide annual incidence of FFDI ≥ 25 days across 1950-2018. The *lowess*-regression calculation shows that most of the change has arisen in the last three decades. A comparison of Figures 22 and 29, looking at the linear trends across the periods 1950-2018 and 1989-2018 supports this conclusion.

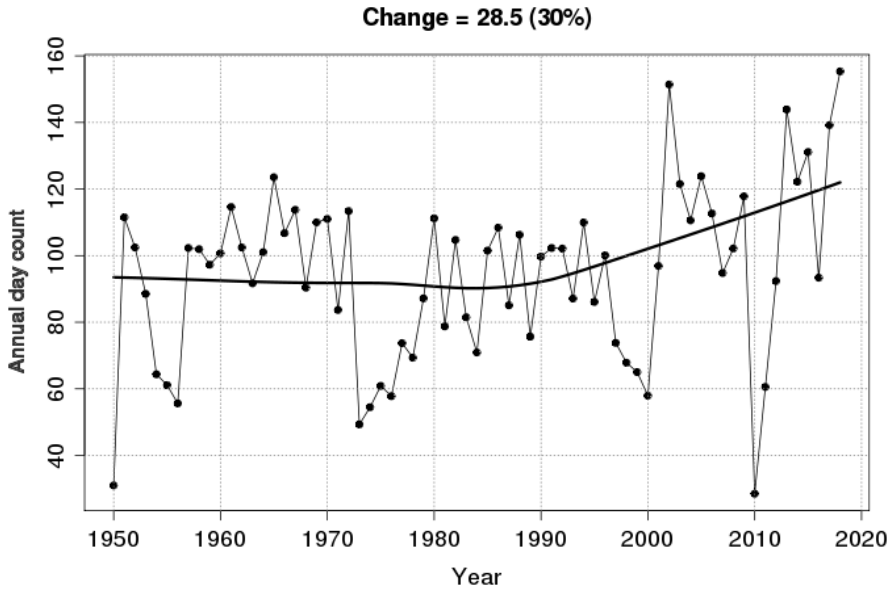

Figure ES1: Time series of annual FFDI ≥ 25 days for Queensland across the period 1950 to 2018. A *lowess* regression is superimposed. This calculation is also shown in Figure 32.

Current climate-change projections for future trends in the FFDI and related fire-weather characteristics across Queensland are somewhat limited at the time of writing, although new results are beginning to become available (Dowdy et al. 2019). This report therefore includes some details of previously published climate-change projections for rainfall and temperature taken from the CSIRO and Bureau of Meteorology (2015) *Climate Change in Australia* work,

along with FFDI projections at five indicative Queensland locations (CSIRO and Bureau of Meteorology 2015ea and CSIRO and Bureau of Meteorology 2015na). They suggest a strong likelihood that annual maximum temperatures will continue to rise rapidly across Queensland in the coming decades, with a lower likelihood that annual rainfall will decline in the southeast (Figures 46 to 54). Annually accumulated FFDI and days of severe FFDI are both projected to rise (Tables 5 and 6).

Although the Dowdy (2018) daily gridded FFDI dataset only goes back to 1950, attempts have been made to estimate the behaviour of annually aggregated FFDI statistics for the decades prior to 1950. These estimates suggest that the magnitudes of the 1950-2018 changes shown in this report would likely have been slightly lower if the earlier (pre-1950) daily data had been available. On the other hand, they do support the previously noted finding that most of the changes have occurred in the last three decades.

17 September 2019

Australian Government
Bureau of Meteorology

QUEENSLAND FIRE AND EMERGENCY SERVICES

Introduction

Bushfires have had severe impacts in Australia, encompassing loss of life (human, other animal, forest), ecological damage, and large economic costs (e.g., Crompton et al. 2010). Anthropogenic climate change, chiefly driven through increased greenhouse gas concentrations in the atmosphere, is having an impact on Australian weather patterns, including the frequency and severity of dangerous fire-weather conditions.

Wildfire (i.e., bushfire, grassfire) activity depends on a range of factors in addition to weather and climate. Fire ignitions, fire suppression, fuel state and structure have large uncertainties and are not easily quantified over suitably long periods. However, many climatological studies have focussed on the weather conditions that influence fire activity (referred to as fire-weather conditions), given the ability to quantify long-term changes in many of these factors with a useful degree of confidence, including for historical trends. The fire-weather conditions at different times of the year can provide a useful metric of "fire season" severity, noting that the ability to suppress fires and losses suffered tend to vary closely with fire-weather parameters.

This report focusses on how fire-weather conditions in Queensland are changing, looking primarily at historical changes that have already occurred based on observations. The analysis presented here is derived from a dataset of fire-weather conditions based on observations (Dowdy 2018). The report should be considered a first-pass analysis, noting that future work should incorporate a range of complementary datasets and methods, so as to more broadly sample the uncertainty space around the influence of climate change on bushfire risk factors.

A limited amount of climate change projection information of basic climate variables (maximum temperature, rainfall), derived from the *Climate Change in Australia* project (CSIRO and Bureau of Meteorology 2015) is included in the *Looking Forward* section. That project did not report geographically on a State/Territorial basis, instead focussing on more climatologically based geographical regions. Further, its direct reporting on projected FFDI changes is limited to five indicative locations in Queensland (data taken from CSIRO and Bureau of Meteorology 2015ea and CSIRO and Bureau of Meteorology 2015na). At these locations, fire-weather conditions are projected to increase across the coming decades. The *Climate Change in* Australia results are the principal ones available and relevant to

Queensland at the time of writing, but it is noted that the modelling represented here is at least four years old, and that the current generation of comparable modelling is still being assessed. A new assessment at the national spatial scale (Dowdy et al. 2019) has just been published.

This report for the most part adopts an investigative framework very similar to that used by the Bureau of Meteorology in respect of fire-weather changes in another State (Bureau of Meteorology 2018a), supplemented by additional approaches as required.

Data and Methods

Climatologies and changes in the observed Mark V daily McArthur Forest Fire Danger Index (FFDI) are calculated using the Dowdy (2018) dataset. This dataset consists of gridded daily FFDI at 0.05° grid spacing (i.e., around 4 to 5 km) from January 1950 to the present. It is updated in near real time (typically at a few days' delay). Contributing components to the FFDI calculation are daily drought factor (DF), daily maximum temperature, daily afternoon (3 pm) relative humidity and daily afternoon (3 pm) 10-metre windspeed. The daily maximum temperatures in the FFDI calculation are sourced from the Bureau of Meteorology's operational daily maximum temperature analyses (Jones et al. 2009), with windspeed based on reanalysis data, as detailed in Dowdy (2018). The maximum temperature component of the calculation is available back to 1910 in gridded form, while the drought factor component is available back to 1911.

The FFDI is used here to provide an indication of fire-weather conditions, with higher values representing more dangerous conditions under which fires are more likely to start, spread, be more difficult to suppress, and have higher impacts and consequences. Values are grouped into the following categories: *Low/Moderate* (0-11), *High* (12-24), *Very High* (25-49), *Severe* (50-74), *Extreme* (75-99) and *Catastrophic* (100+). The FFDI provides a measure of how easy fire suppression is likely to be, and has been related to the likelihood of property losses (Blanchi et al. 2010; Harris et al. 2012).

The FFDI is calculated across the entire country in the dataset, irrespective of whether there is any actual forest present at a particular location, as the intended purpose of this dataset was to provide a spatially and temporally consistent measure of fire-weather conditions for broad-scale climatological analysis. The dataset is based on a long period of observations throughout Australia, designed to be complementary to other approaches such as datasets based on point locations from individual observing stations or based on modelling.

This study divides Queensland into nine subregions, obtained by aggregating one or more of the Bureau's rainfall districts. The nine subregions are:

1. South East Coast,
2. Wide Bay and Burnett,
3. Central Coast,
4. North Coast,
5. Cape York Peninsula,
6. Central South,
7. Central,
8. North West, and
9. South West.

These subregions are shown in Figures 1 and A1; see also Figures B1, C1, ..., J1 in the Regional Fact Sheets section, where the contributing rainfall districts are listed. A national map of the Australian rainfall districts is available online[1]. Figures 1 also shows the Queensland Fire and Emergency Services (QFES) regions (in black outline), for reference, but those QFES regions have not been used in this study. The sampling of the 0.05° FFDI grids is done at 0.125° resolution, which necessitates some interpolation of the grids. That interpolation is performed using the method of bicubic polynomial interpolation. The 0.125° is the resolution of the rainfall districts points lattices used operationally within the Bureau's Climate Monitoring Group at the time of the study. The bicubic polynomial interpolation method is likewise the operational method used within the Climate Monitoring Group, so in this respect, the methods used in this study are consistent with current operational practice. Only continental grid points are used in the calculations described here: off-shore island grid points are not included.

[1] www.bom.gov.au/climate/cdo/metadata/maps/raindist.pdf

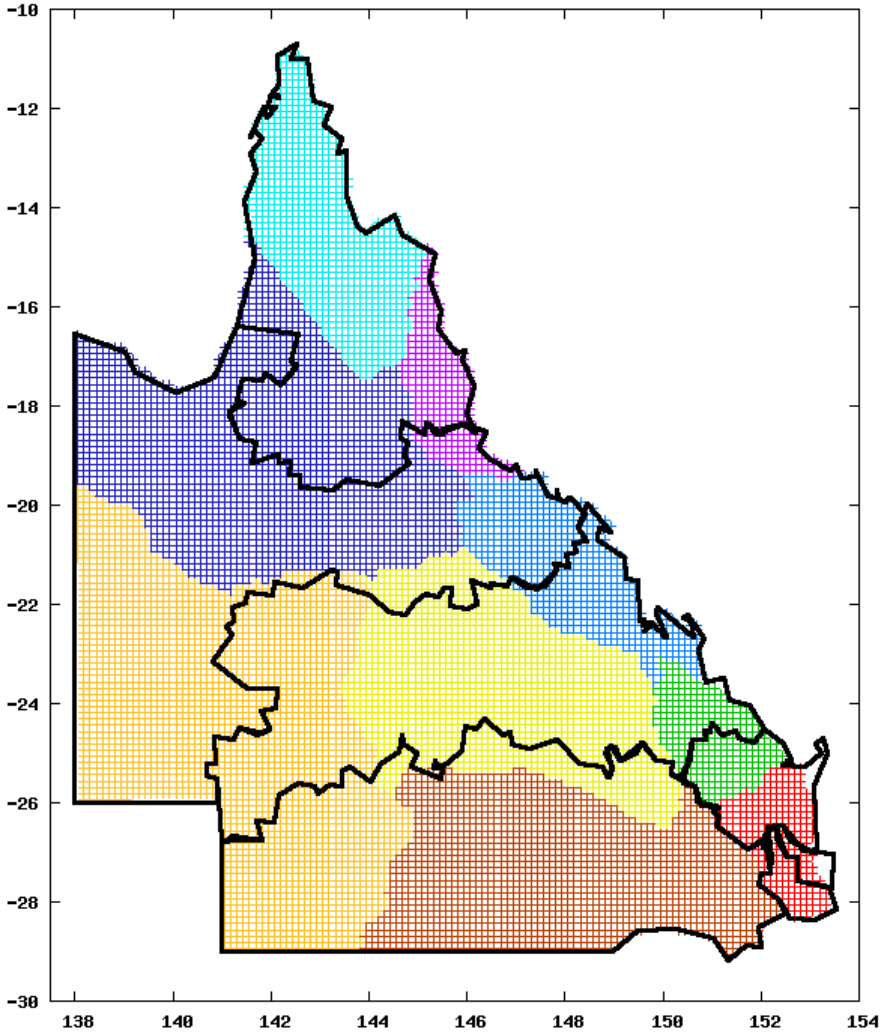

Figure 1: Map of the nine subregions used in this study: South East Coast (red), Wide Bay and Burnett (green), Central Coast (blue), North Coast (magenta), Cape York Peninsula (cyan), Central South (brown), Central (yellow), North West (dark blue) and South West (gold). Off-shore islands are not included in the calculations. Regional boundaries are superimposed (black lines), for the Brisbane, Central, Far Northern, North Coast, Northern, South Eastern and South Western QFES regions.

These nine subregions are used to create time series of relevant fire-weather variables, which are then subjected to a range of time-series analysis techniques. Changes in area-averaged time series are calculated by fitting a *lowess* (local regression) model to the time series, and calculating the change as {last point on the regression line} − {first point on the regression line}. The *lowess* regressions are performed using the statistics computer

program *R* and employ a span parameter value of $f = 0.8$. The span parameter functions somewhat like the width of a moving-average window, in that larger values result in smoother regressions. The *lowess* regression technique is used in preference to ordinary least squares (OLS) linear regression because it can empirically diagnose departures from linearity in the time series, and thereby indicate whether or not the observed climate change is accelerating or decelerating. It is known that many Australian climate variables show changes which are non-linear in time, either through showing acceleration (e.g., Australian annual mean temperature; CSIRO and Bureau of Meteorology 2018) or the appearance of step changes (e.g., southwest and southeast Australian rainfall; Fawcett et al. 2010).

The use of OLS linear regression is however retained for the gridded calculations shown in the maps because an implementation of the *lowess* methodology is not currently available for use on the gridded datasets. Hence for the mapped changes (e.g., Figure 17), linear trends are calculated using OLS linear regression.

Since the daily FFDI dataset only goes back to 1950, an attempt is made to characterise the broad-scale FFDI behaviour for the decades prior using what meteorological data are available. The time series of annual accumulated FFDI averaged across Queensland and the nine subregions is reconstructed back to 1911, using OLS linear regression models with the time series of annual rainfall, annual maximum temperature and annual drought factor as predictors. These three climate variables are all available back to 1911 (the annual maximum temperature being actually available back to 1910 and the annual rainfall back to 1900). Letting these three time series be denoted x_1, x_2 and x_3, respectively, and the FFDI time series y, for each region four different hindcasting models were considered:

- $y = a_0 + a_1 x_1 + a_2 x_2 + a_3 x_3$
- $y = a_0 + a_1 x_1^{1/2} + a_2 x_2 + a_3 x_3$
- $y = a_0 + a_1 x_1 + a_2 x_2 + a_3 x_3 + a_4 x_1 x_2 + a_5 x_2 x_3 + a_6 x_3 x_1$
- $y = a_0 + a_1 x_1^{1/2} + a_2 x_2 + a_3 x_3 + a_4 x_1^{1/2} x_2 + a_5 x_2 x_3 + a_6 x_3 x_1^{1/2}$.

The coefficients a_0, a_1, ..., a_6 are constants to be estimated in the fitting of the model.

In two of the four models, the rainfall time series appears linearly in the model. In the other two models, the rainfall time series appears in square-root form. This is because it is unlikely that annual accumulated FFDI scales entirely linearly with annual rainfall, with the taking of the square root or cube root of rainfall totals being found to be a useful operation in other

contexts. The model amongst the four which yields the highest adjusted R-squared value between the observed and reconstructed annual accumulated FFDI values across the data period 1950-2018 is the one which is adopted. All terms in the model are retained in the calculation, whether or not the coefficients are statistically significant, but obviously statistical insignificance is associated with small contribution to the resultant model.

The primary purpose for attempting these estimations of the pre-1950 FFDI is not to make definitive assessments of the behaviour of the pre-1950 FFDI, rather to assess whether there are likely to be substantial end effects associated with the FFDI dataset starting in 1950. [By this is meant whether or not the inclusion/exclusion of the 1930s and 1940s data changes to a substantial amount the estimates of the 1950-2018 changes.] Accordingly some caution should be taken in comparing the pre-1950 reconstructions with the post-1949 observations. [There could also be end effects associated with the inclusion/exclusion of post-2018 data, but for obvious reasons they cannot be quantified at the time of writing.]

Queensland maps shown in this report employ the cylindrical equidistant projection.

Observed Climatology

The climatological calculations presented in this section are based on the last thirty years (1989-2018), unless otherwise indicated. Thirty-year periods are commonly used for calculations of this nature. The current World Meteorological Organization standard climatological period is still 1961-1990 at the time of writing, but in significant respects the pattern of global warming has rendered that standard period obsolete. Seasonal and annual climatologies are prepared by computing separately and initially monthly climatologies, which are then summed or averaged (as required) to calculate the seasonal and annual climatologies.

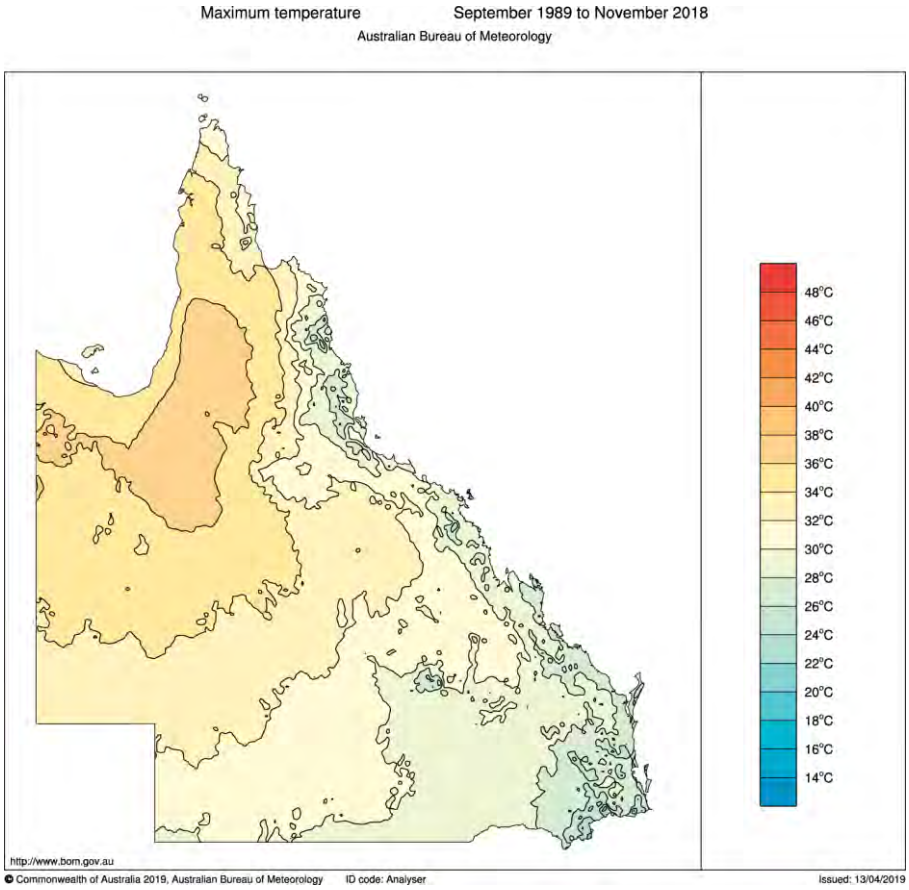

Figure 2: Climatological Spring mean maximum temperature across Queensland for the period 1989-2018.

Figure 2 shows the climatological mean maximum temperature for Spring (September to November) across Queensland. Average maximum temperatures range from below 24 °C in the southeast to above 36 °C in the northwest. Average temperatures are generally cooler

along east-coastal parts east of the Great Dividing Range, the exception being in the far north, on Cape York Peninsula. Average temperatures are also cool in the elevated parts of the southeast, inland of the coastal plains.

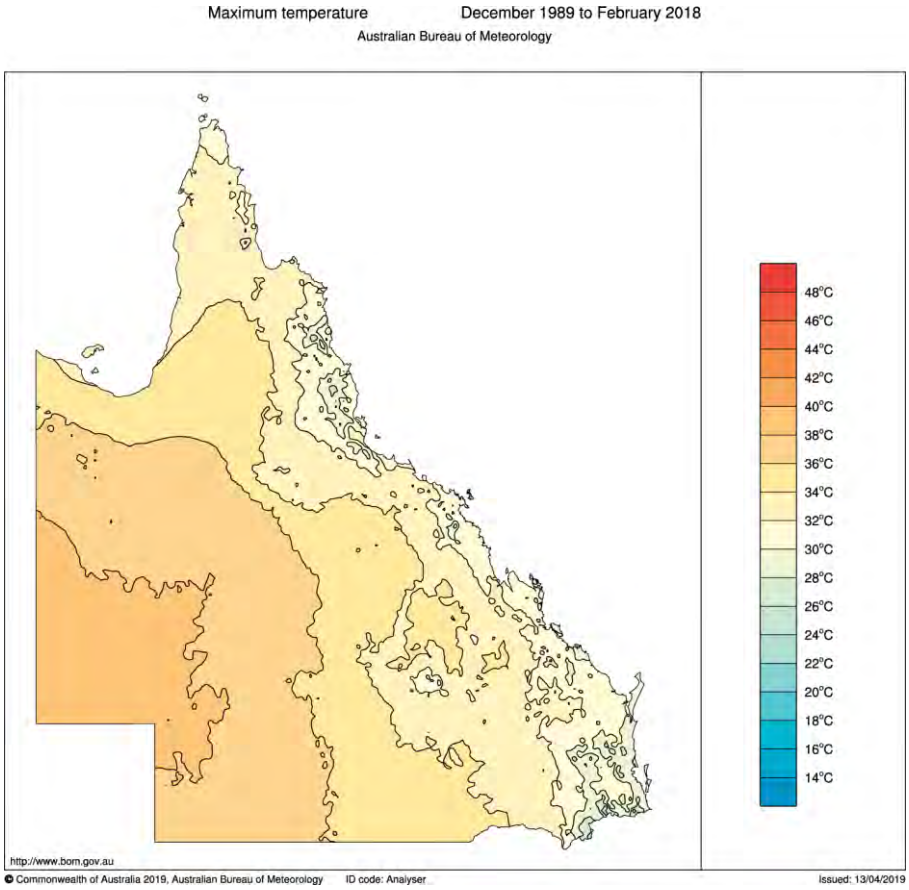

Figure 3: Climatological Summer mean maximum temperature across Queensland for the period 1989-2018.

Figure 3 shows the climatological mean maximum temperature for Summer (December to February) across Queensland. Average maximum temperatures range from below 28 °C in the southeast to above 38 °C in the west.

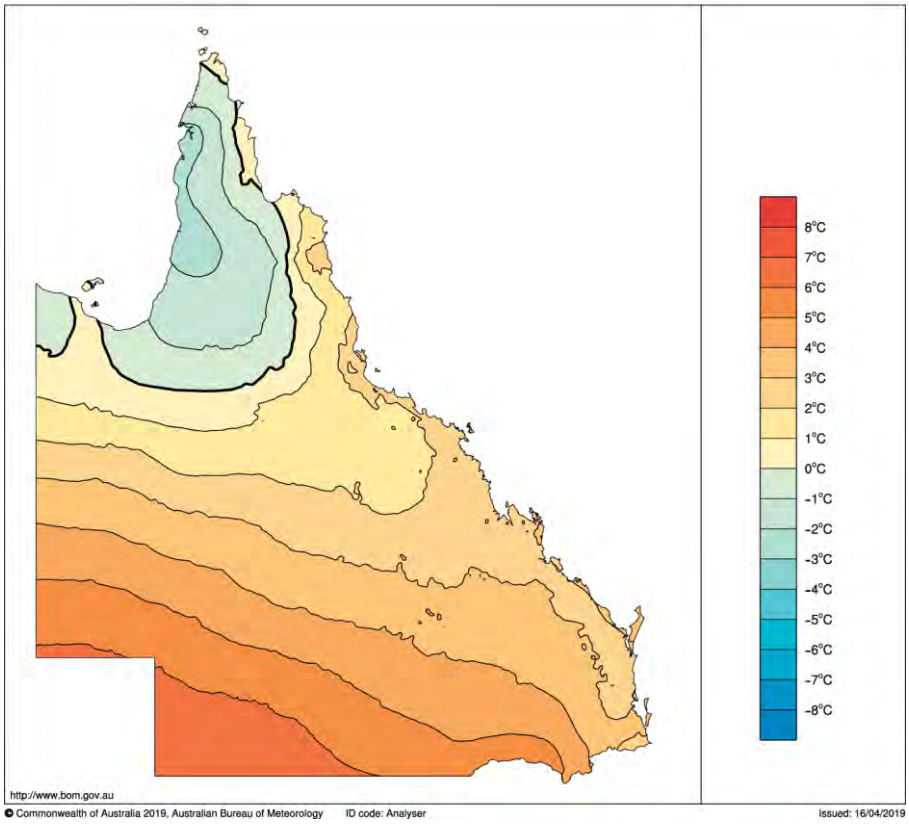

Figure 4: Change in the climatological mean maximum temperature from Spring to Summer across Queensland for the period 1989-2018. Positive values indicate Summer being hotter than Spring.

Figure 4 shows the change in climatological mean maximum temperature across Queensland from Spring to Summer. Positive values in the figure mean Summer is hotter than Spring, negative values the other way around. As expected, Summer is hotter than Spring over most of the State, and much hotter in the southwest of the State, but in the far north around the Gulf of Carpentaria, this is not the case. The Summers there are on average cooler than the Springs. This has implications for the climatological FFDI.

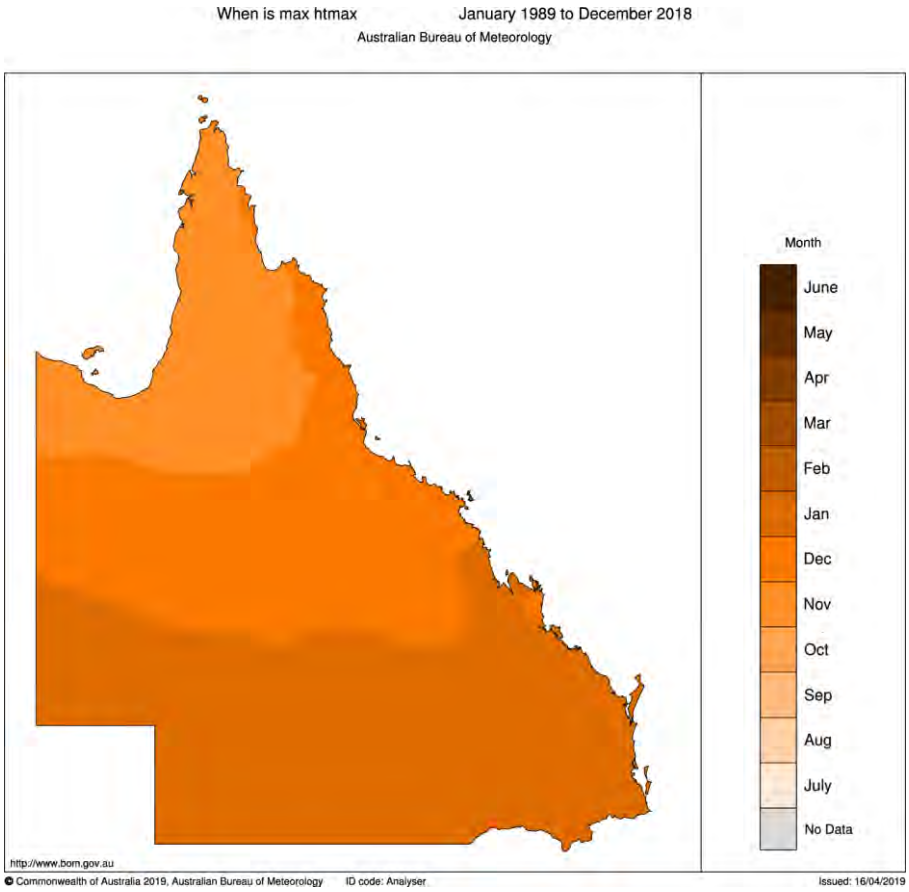

Figure 5: Month of the highest average monthly maximum temperature across Queensland for the period 1989-2018.

Figure 5 shows which month has the highest average monthly maximum temperature across the period 1989-2018. On Cape York Peninsula and around the Gulf of Carpentaria, November is typically the hottest month. Across central Queensland it is typically December, but across southern Queensland it is January.

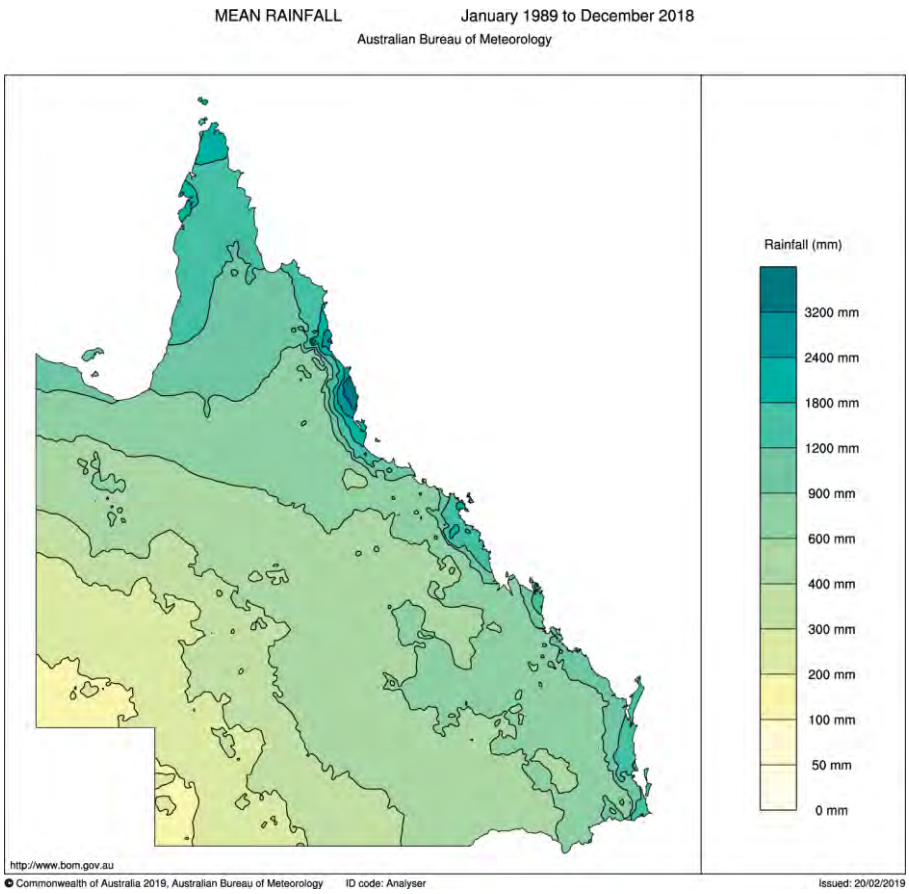

Figure 6: Climatological annual rainfall across Queensland for the period 1989-2018.

Figure 6 shows the climatological annual rainfall across Queensland. Average annual rainfall is generally highest in the north and along the east coast where it exceeds 600 mm, and generally lowest in the southwest where it drops below 200 mm. This is part of a general pattern to Australian rainfall: climatological rainfall declines with increasing distance from the coastline (Bureau of Meteorology 2008). The climatologically wettest part of Queensland is between Cairns and Tully, where average annual rainfall exceeds 3200 mm. These high rainfalls arise as a consequence of onshore flows of very moist air meeting elevated topography close to the coast. An additional effect of this aspect to the meteorology is the much lower average annual rainfall on the western (lee) side of that topography (Bureau of Meteorology 2008).

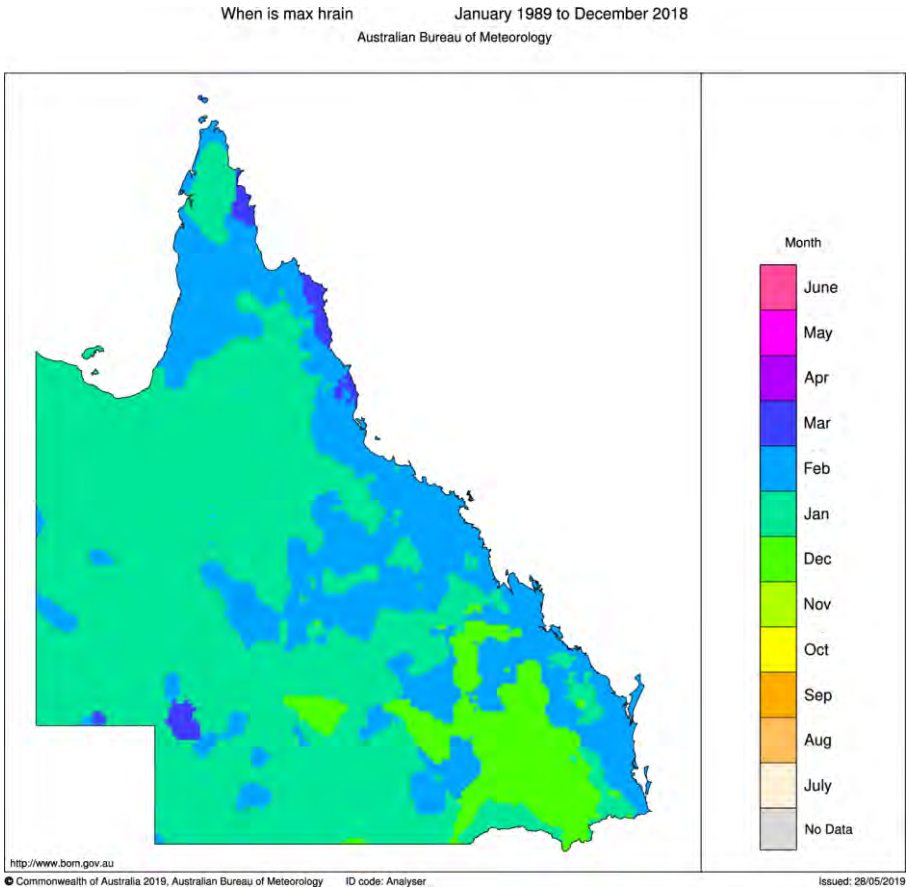

Figure 7: Month of the highest average monthly rainfall across Queensland for the period 1989-2018.

Figure 7 shows which month has the highest average monthly rainfall across the period 1989-2018. Over most of inland Queensland, January is the wettest month on average, although in the inland southeast it is December. On Cape York Peninsula and along the east, February is the wettest month on average, although in scattered parts of the north coast it is March.

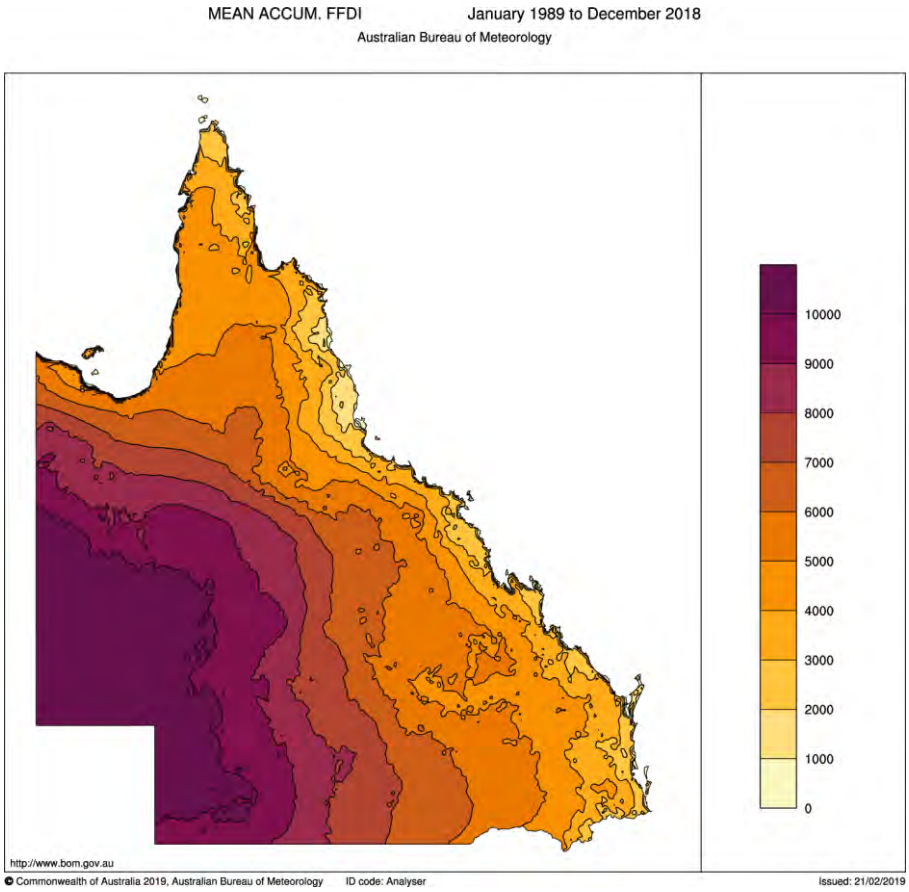

Figure 8: Climatological annual accumulated FFDI across Queensland for the period 1989-2018.

Figure 8 shows the climatological annual accumulated FFDI across Queensland. This calculation involves summing the daily FFDI values at each location in each year to produce an annual accumulation, which is then averaged across the thirty-year climatological study period adopted for this report (1989-2018). The climatological annual accumulation gives an indication of the overall severity of the fire weather experienced, as measured by the FFDI. Average annual accumulated FFDI values are typically lowest along the east coast and highest in the southwest and central west. An annual accumulated FFDI of 10000 (the highest contour shown in Figure 8) corresponds to an average daily FFDI of 27 (the bottom end of the *Very High* range).

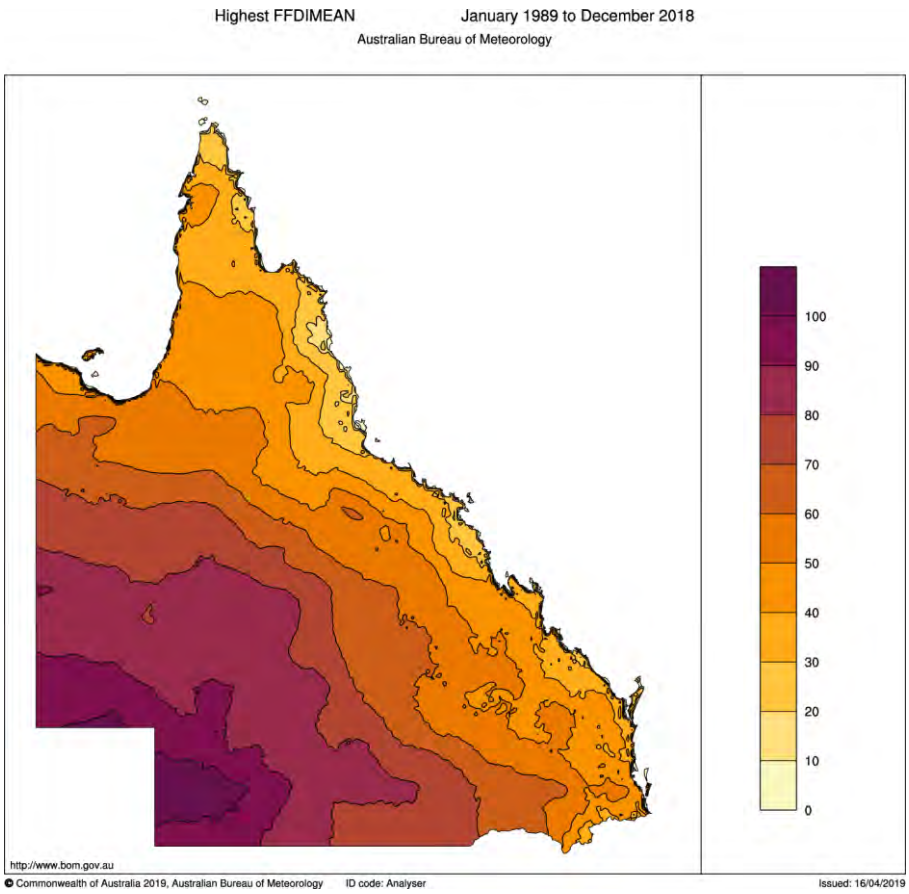

Figure 9: Climatological annual highest daily FFDI (in FFDI units) across Queensland for the period 1989-2018.

Figure 9 shows the average annual highest daily FFDI across Queensland for the period 1989-2018. The average annual highest daily FFDI is an indicator of the expected worst fire weather in a given year. Peak values are in the far southwest where they exceed 100 FFDI points. They fall away to the east and north, to below 30 around Cairns and Cooktown. Much of the east-coastal fringe experiences average annual highest daily FFDI values between 20 and 40 FFDI points.

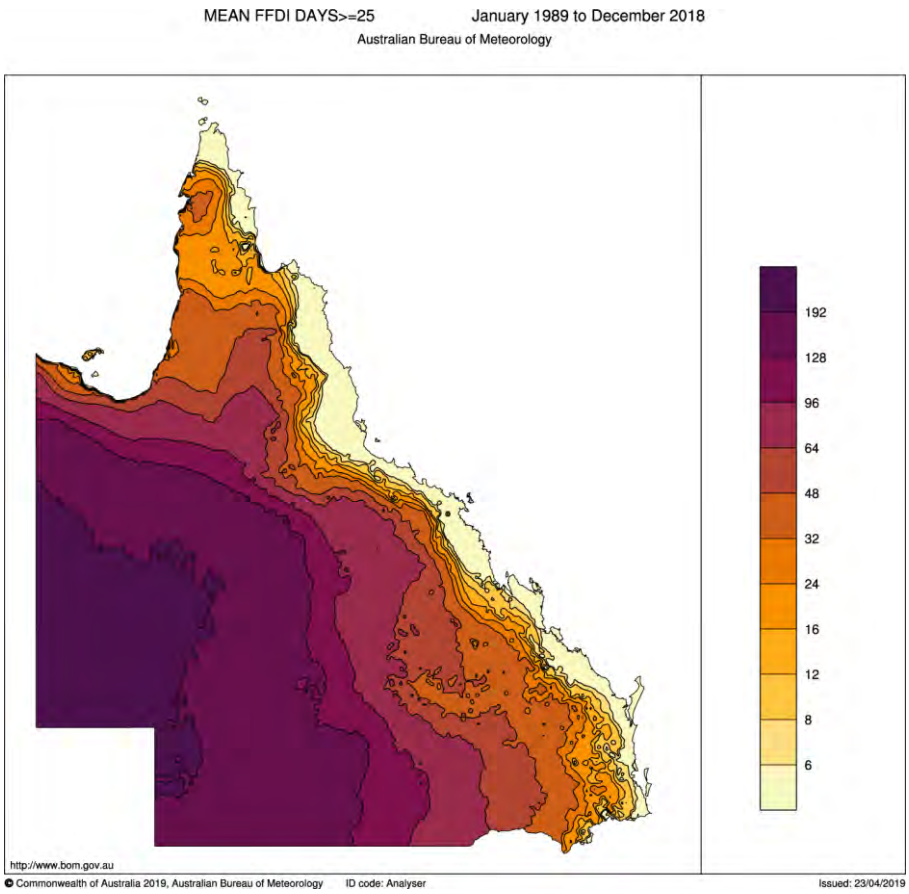

Figure 10: Climatological annual FFDI ≥ 25 days across Queensland for the period 1989-2018.

Figure 10 shows the climatological annual number of days with FFDI ≥ 25 across Queensland. FFDI ≥ 25 days are most frequent in the southwest and central west, where they occur more frequently than one day in two (182.5 days per year), and least frequent along the east-coastal fringe where they average less than six days per year. The lower values near the coast reflect the generally higher humidity, higher rainfall (and hence lower fuel dryness) and lower maximum temperatures.

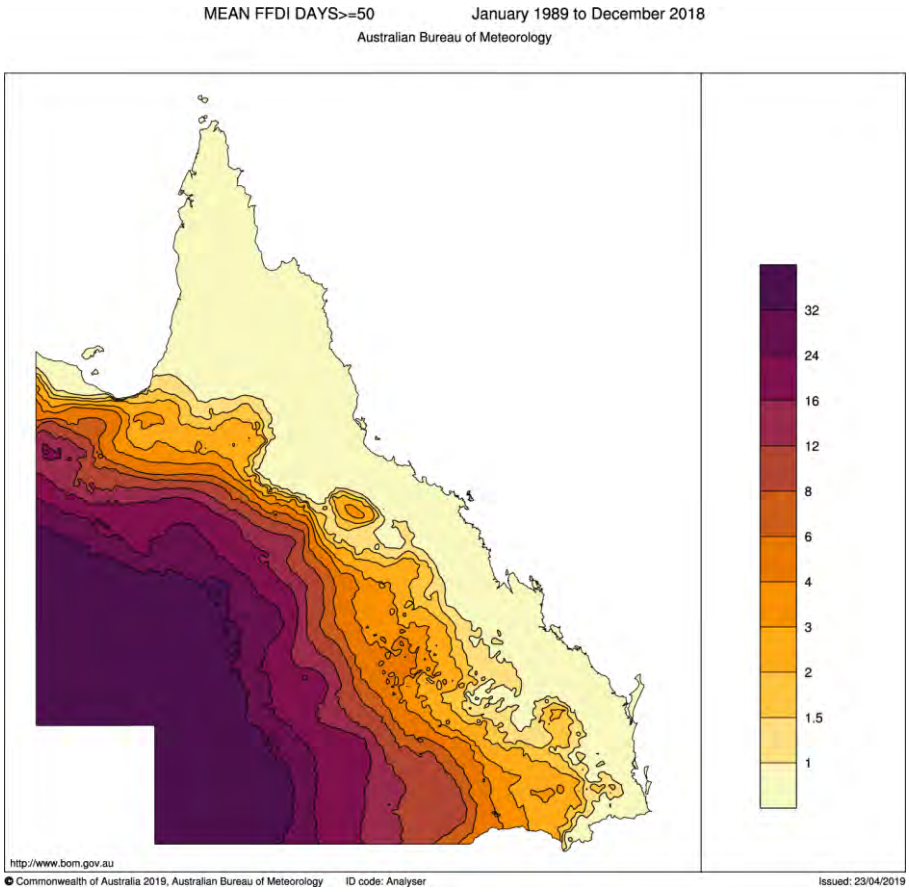

Figure 11: Climatological annual FFDI ≥ 50 days across Queensland for the period 1989-2018.

Figure 11 shows the climatological annual number of days with FFDI ≥ 50 across Queensland (i.e., the *Severe* category and upwards). FFDI ≥ 50 days are most common in the southwest and central west, where they exceed 32 days per year on average, and least common along the east coast and Cape York Peninsula, where they occur on average less than one day per year. Figures E4 and F4 in the Regional Fact Sheets section show that FFDI ≥ 50 days in the far north of the State are very infrequent, and do not occur at all in many years.

Seasonality

There is a pronounced seasonality to the fire-weather season across Queensland, with considerable variation in the timing of the peak fire-weather period. This aspect of the climatology will be explored in a little detail, as the results will impact upon subsequent enquiry into whether or not the fire-weather season has expanded or contracted over the study period. Figure 12 shows the climatological monthly means and medians for accumulated monthly FFDI averaged across the nine study subregions. Table 1 summarises the results.

In climatological terms, there is a typically clear peak of maximum fire-weather activity, comprising a single month, as measured by the FFDI. When this occurs will be influenced by opposing factors; the seasonal cycle of temperature which preferences a Summer maximum in most parts of the State *versus* the seasonal cycle of rainfall which preferences the driest part of the year. Over most of the State this balances towards October (Figure 14; also in State-averaged terms and almost all the subregions when subregionally averaged), although in the southeast corner it is September, but in the inland south it is December, as Spring and early Summer rainfall is lighter and unreliable. In the tropical north, the onset of the northern wet season opposes the tendency of Summer to be the time of maximum fire-weather activity, with the consequence of that maximum shifting earlier to October in climatological terms.

On the other hand in much of the State, there are two months, February (wetter) and June (cooler), which are climatologically quieter than the surrounding months. In some parts where this happens, one of those two months is distinctly the quieter, but in the southeast corner they are almost equally quiet in terms of fire weather, and it depends on whether one uses the mean or median to determine the climatologically quietest month for fire weather. It should be noted that because these calculations involve the accumulated FFDI, February being the shortest month is at a slight temporal "disadvantage" in the comparison, with its accumulations being automatically deflated by around 10 per cent compared to the neighbouring months of January and March.

Region	Minimum	Maximum
Queensland	June	October
South East Coast	February	September
Wide Bay and Burnett	June	October
Central Coast	February	October
North Coast	February	October
Cape York Peninsula	February	October
Central South	June	October
Central	June	October
North West	February	October
South West	June	October

Table 1: Climatological timing of the minima and maxima for mean monthly accumulated FFDI (based on data for 1989 to 2018). For the equivalent results at finer spatial scales, see Figures 14 and 16.

The complexity in the seasonal cycle is shown by the regional FFDI sequences. It is apparent that the progression of the fire-weather season changes quite substantially as one moves from southwest Queensland (lower in Winter, higher in Summer) to the north and west. In the tropics the cycle is dominated by rainfall, with lower values during the wet (monsoon) season, and higher values during Spring in the build up to the wet season. It is worth noting, however, that high values are sometimes seen in Summer across many of the regions when the Summer-season rainfall fails (for example, as happened in parts of Queensland in Summer 2018/2019).

Queensland **Cape York Peninsula**

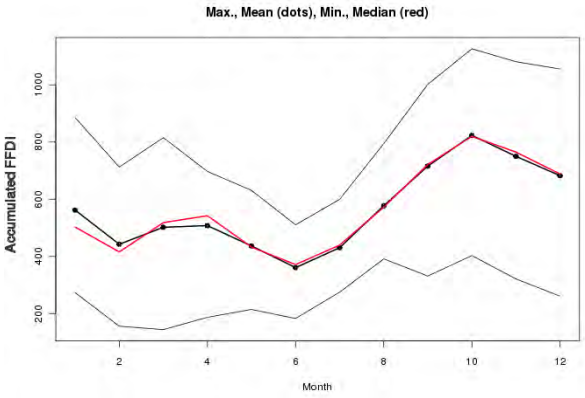

South East Coast

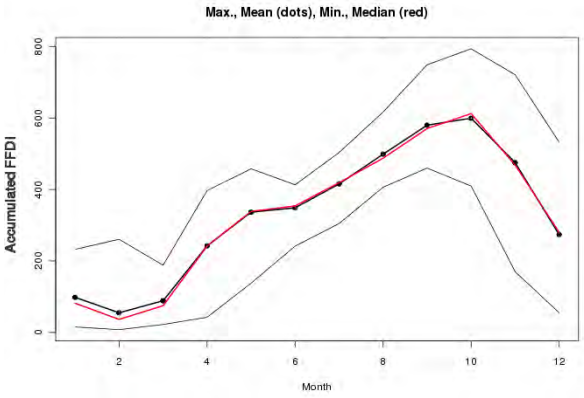

Central South

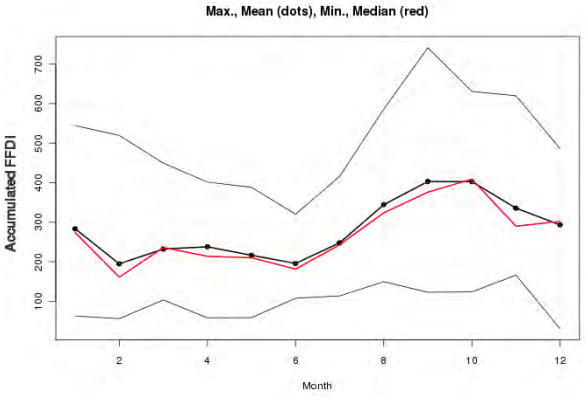

Wide Bay and Burnett

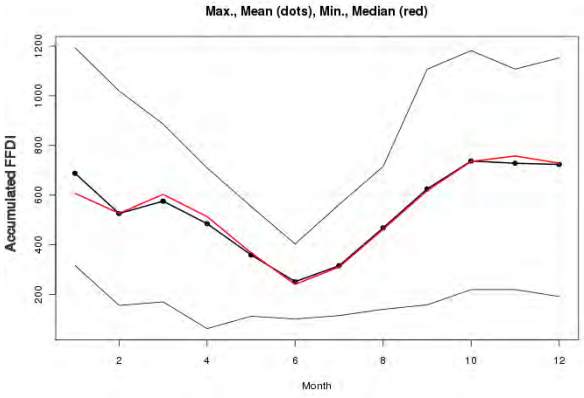

Central

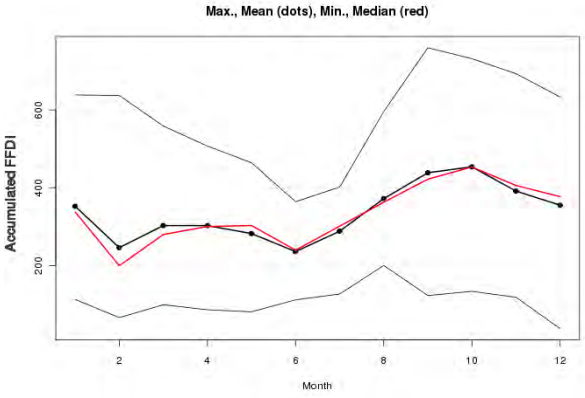

Central Coast

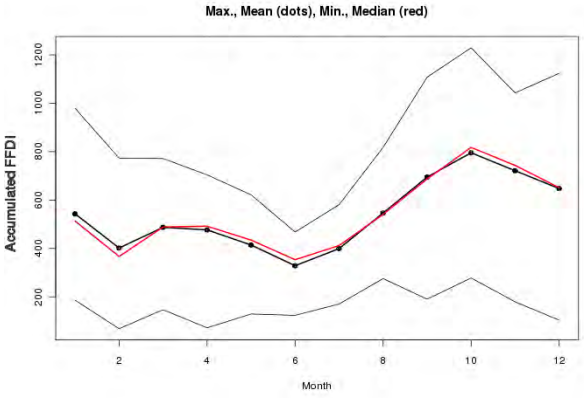

North West

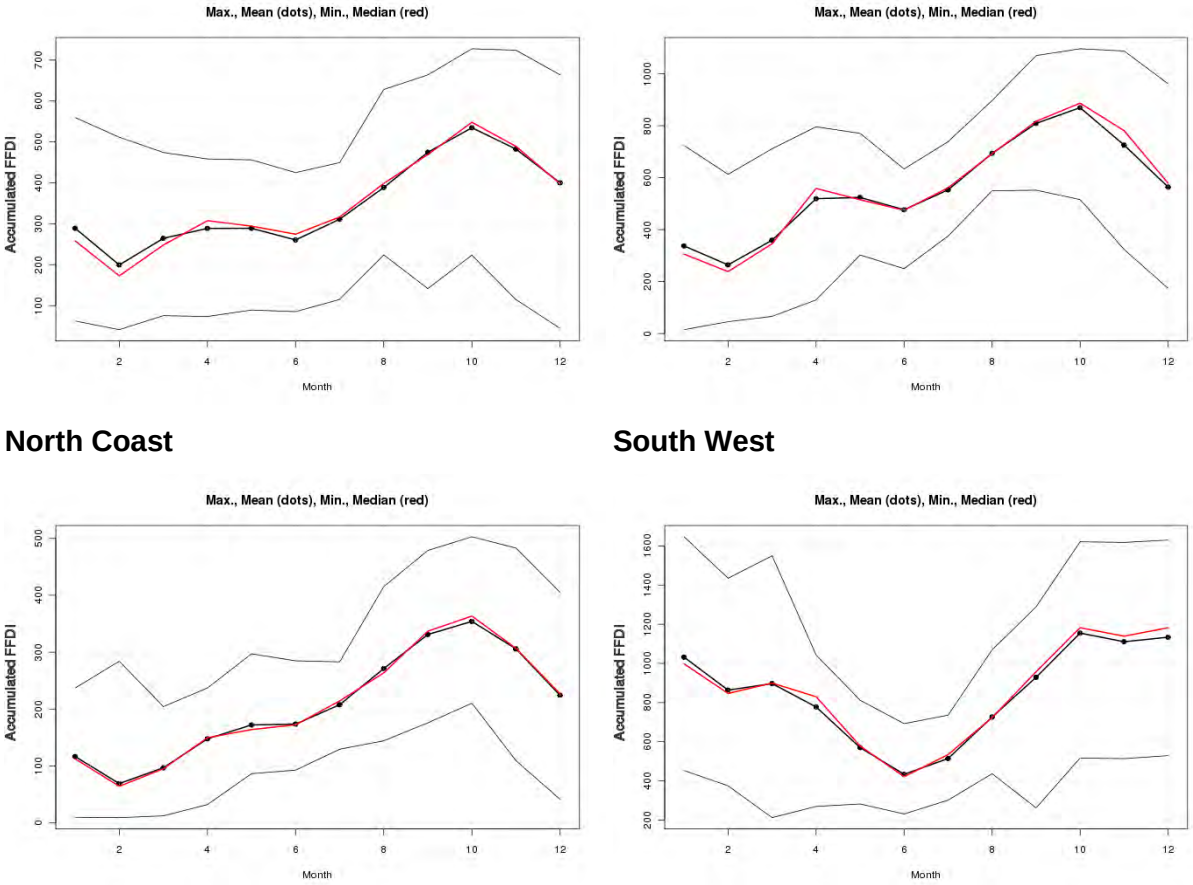

North Coast **South West**

Figure 12: Monthly mean (thick black line with dots), median (blue line), maximum (upper black line) and minimum (lower black line) accumulated FFDI across the period 1989 to 2018.

Figure 13 shows the corresponding results for climatological numbers of FFDI ≥ 25 days, again calculated across the period 1989-2018. The results presented in this figure emphasise the all-year-round nature of the fire-weather climatology in many parts of Queensland. At the FFDI ≥ 25 days level of fire-weather intensity, only two of the subregions (North Coast and Cape York Peninsula) show a clear break to the fire weather, both in March.

Queensland **Cape York Peninsula**

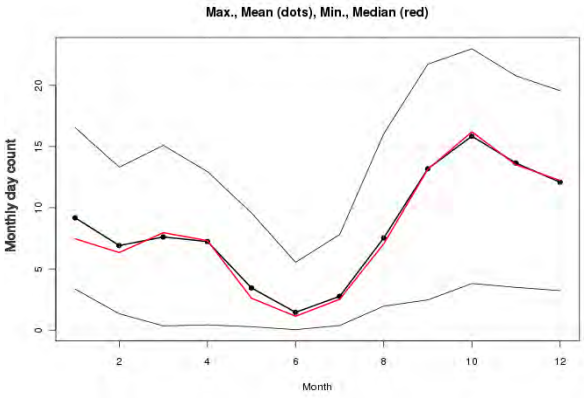

South East Coast

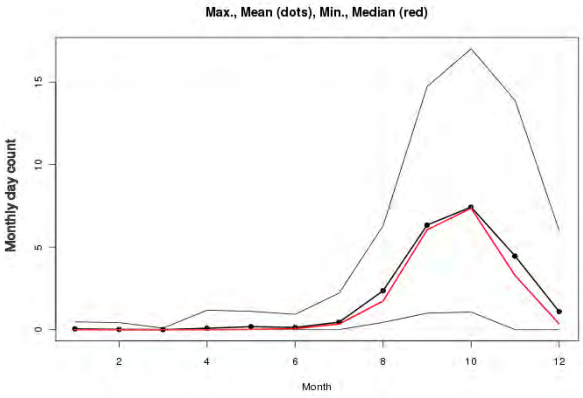

Central South

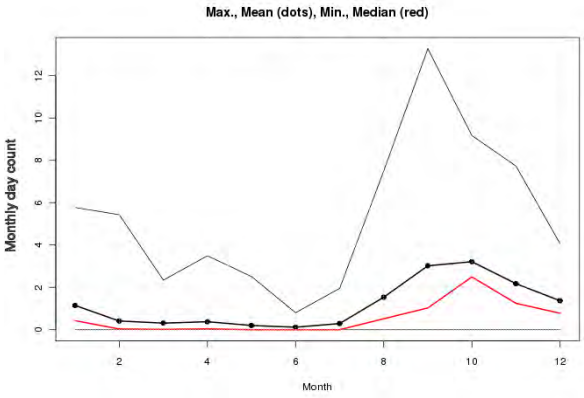

Wide Bay and Burnett

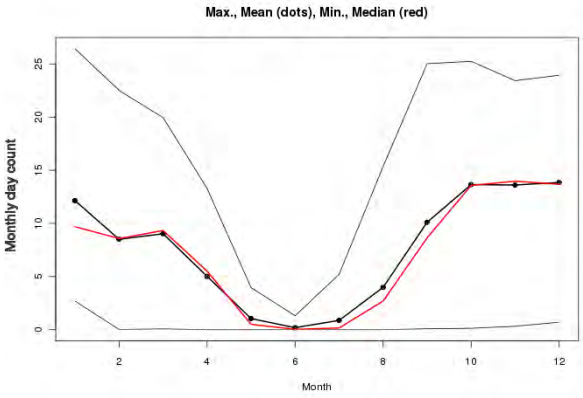

Central

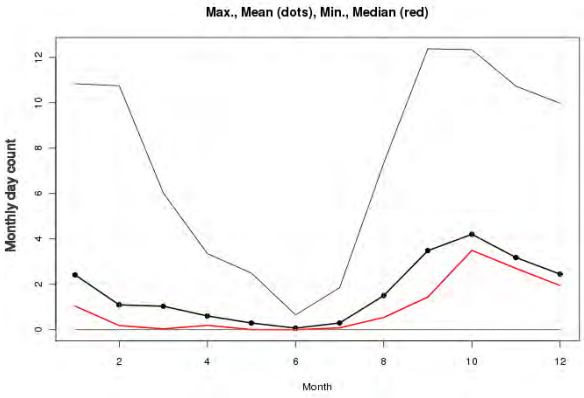

Central Coast

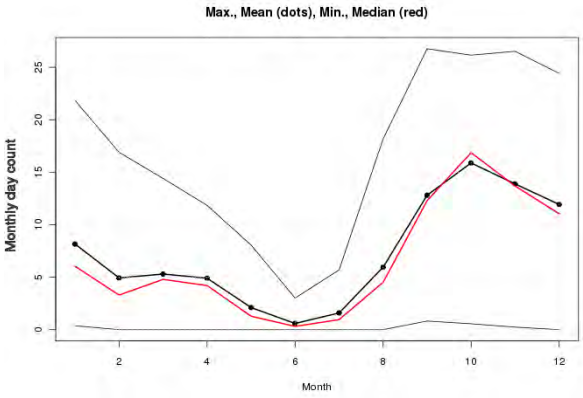

North West

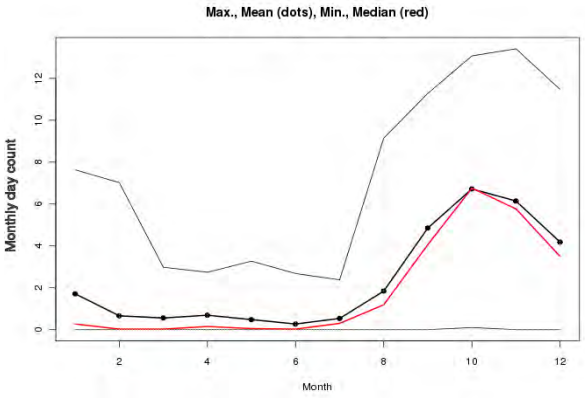

North Coast

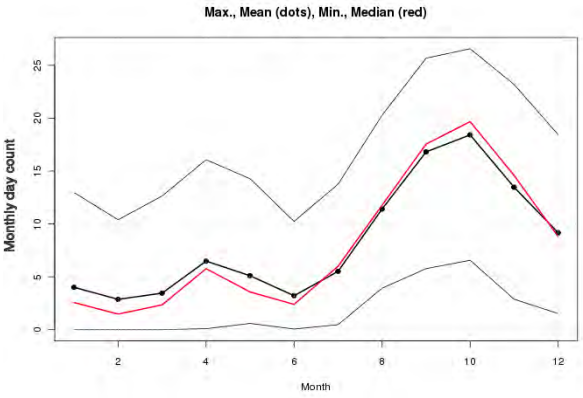

South West

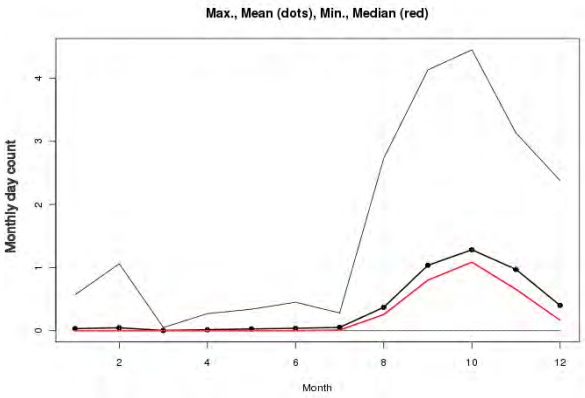

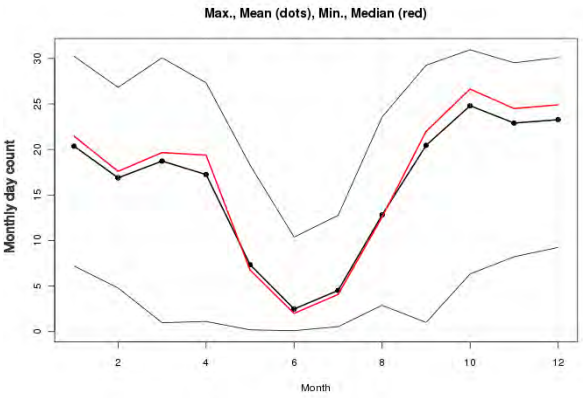

Figure 13: Monthly mean (thick black line with dots), median (blue line), maximum (upper black line) and minimum (lower black line) FFDI ≥ 25 days across the period 1989 to 2018.

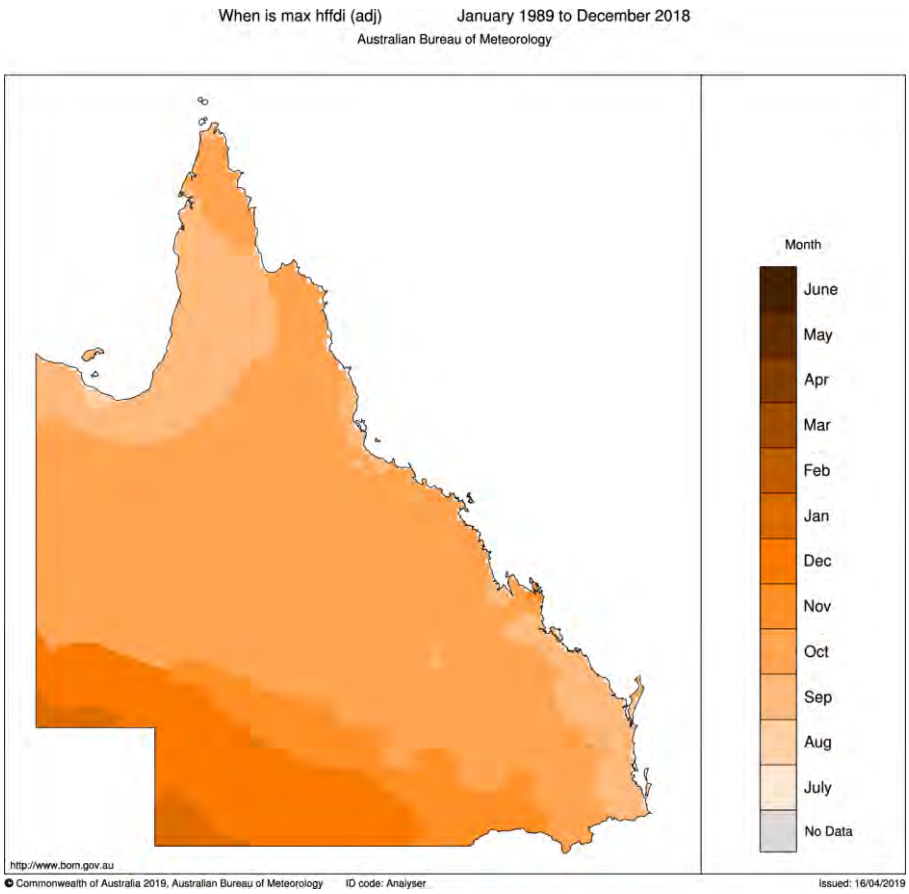

Figure 14: Month of the highest average daily FFDI across Queensland for the period 1989-2018.

Figure 14 shows the month of the highest average daily FFDI across Queensland for the period 1989-2018. Around the Gulf of Carpentaria, the most active month for fire weather is September, apart from a small region at the southern end of the Gulf. September is also the most active month for the southeast coastal strip and a few other scattered places, but for most of Queensland October is the most active month. This shades into November and December in the south and January in the far southwest. The areas in the south where December is the most active month are not large enough to make December the most active month in area-averaged terms for the Central South and South West subregions (Table 1).

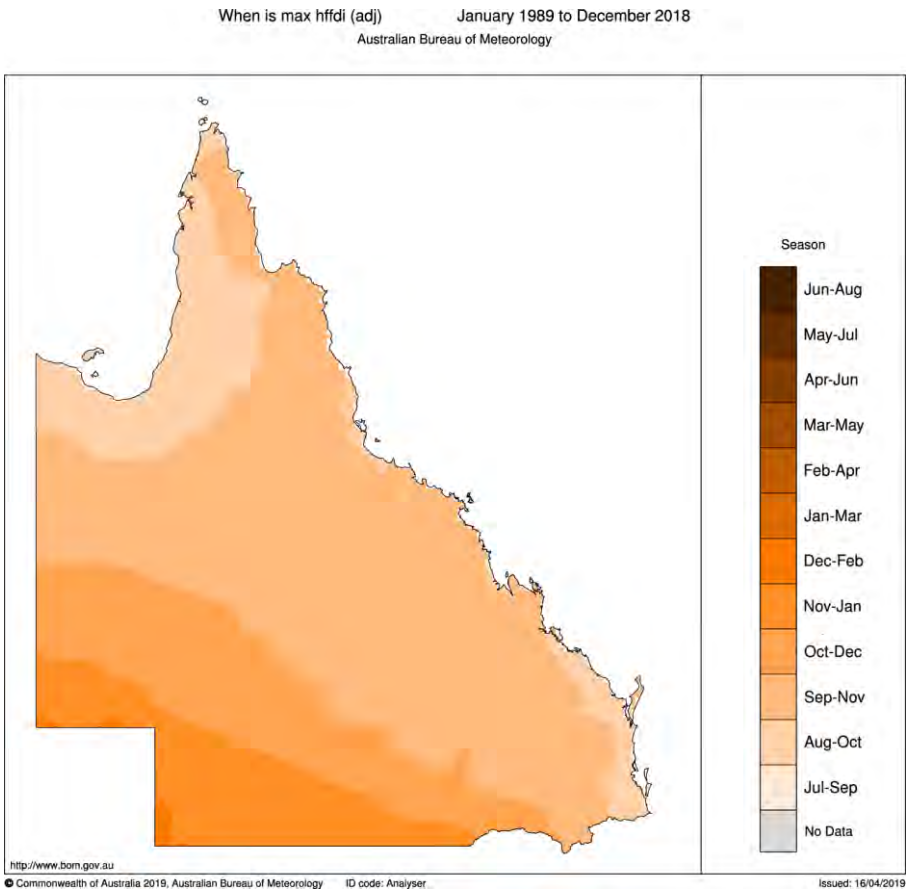

Figure 15: Season of the highest average daily FFDI across Queensland for the period 1989-2018.

This pattern of change to the fire-weather climatology is even more clearly seen when it is the most active season that is mapped. Figure 15 shows the season of the highest average daily FFDI across Queensland for the period 1989-2018. In the southeast coastal strip and around the Gulf of Carpentaria, August-October is the most active season. Over most of Queensland it is Spring (September-November), grading through October-December and November-January, to Summer (December-February) in the far southwest.

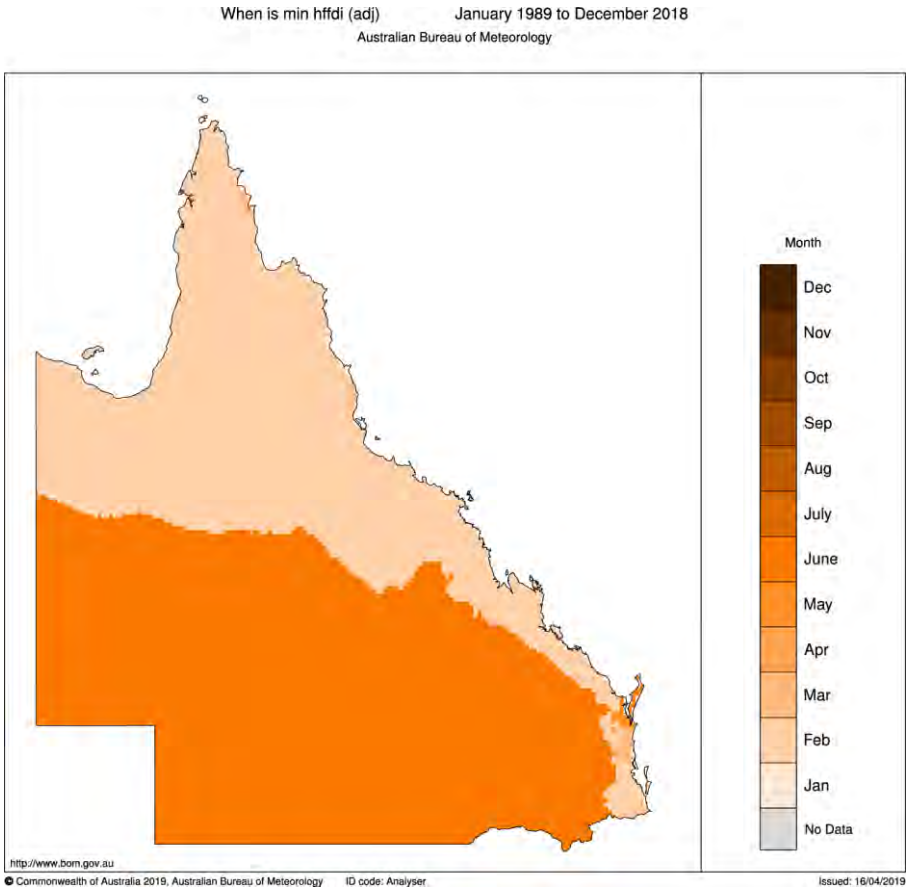

Figure 16: Month of the lowest average daily FFDI across Queensland for the period 1989-2018.

Figure 16 shows the month of the lowest average daily FFDI across Queensland for the period 1989-2018. Over the north and east coast, February is the quietest month in fire-weather terms, while over the inland south it is June. There are some slight departures from this on and south of Fraser Island.

Observed Changes

This section on observed changes is divided into five parts. The first two parts looks generally at mapped trends, over different periods. The third part looks at temporal patterns in the spatial averages. The fourth part looks at the expansion of the fire-weather season. The fifth part presents a sequence of fact sheets, one of each of the nine study subregions, summarising the changes in the fire-weather characteristics.

Spatial Patterns (1950-2018)

Figure 17 shows the linear trend in annual maximum temperature across Queensland for the period 1950 to 2018, as calculated from the Bureau of Meteorology's operational monthly maximum temperature analyses (Jones et al. 2009). The Bureau of Meteorology typically uses the analyses of its Australian Climate Observations Reference Network - Surface Air Temperature (ACORN-SAT) curated temperature dataset to report on Australian temperature changes over decadal time scales, but the whole-network operational monthly analyses are used instead in this report because they employ the same analysis methodology and temperature observations network as the analogous daily temperature analyses that have been used in the construction of the gridded daily FFDI dataset used in this report.

Trend in maximum temperature Annual 1950-2018

Australian Bureau of Meteorology

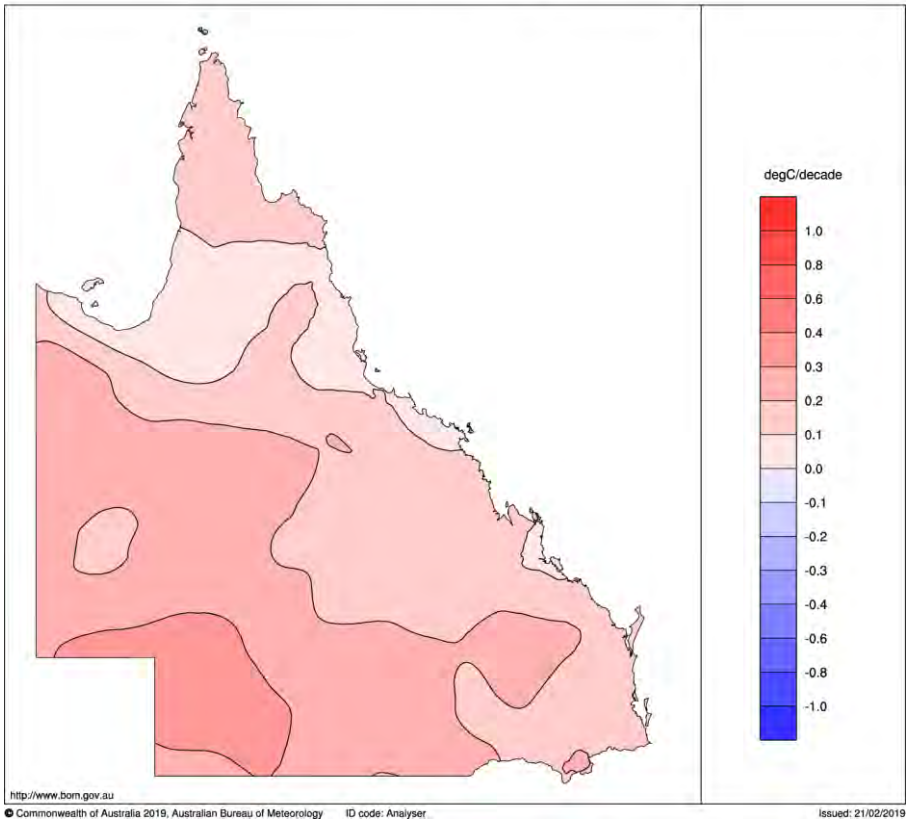

 ID code: Analyser issued: 21/02/2019

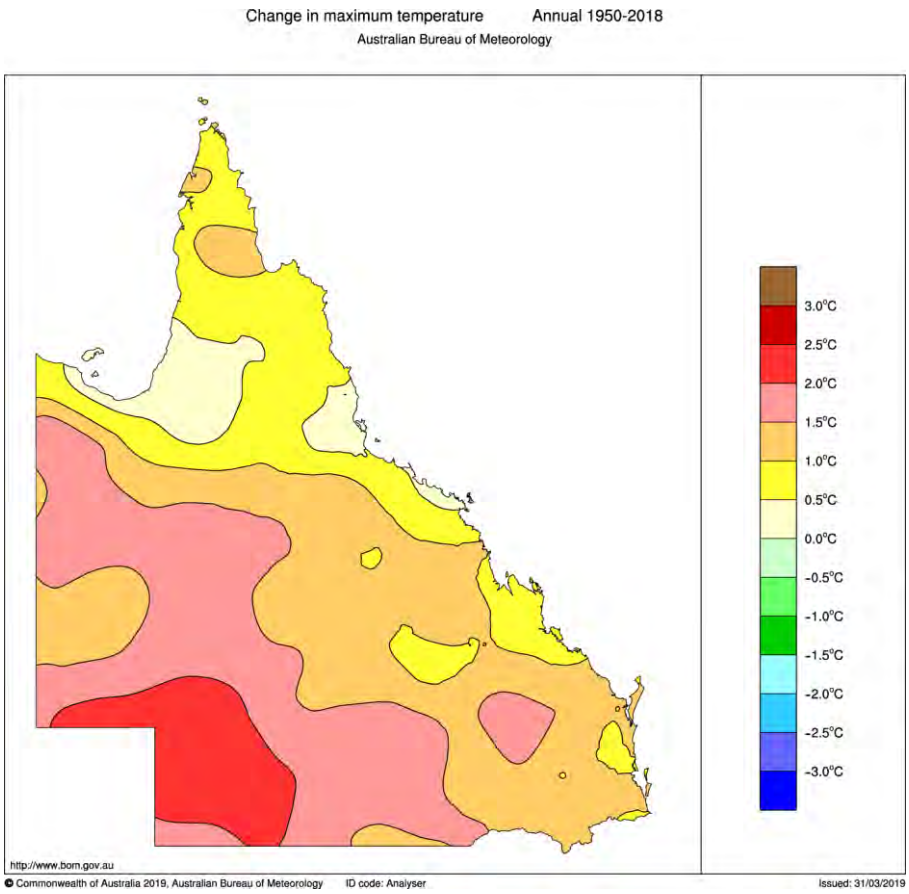

Figure 17: Trend in annual maximum temperature (in °C per decade, top) and total linear temperature change (in °C, bottom) across Queensland for the period 1950-2018.

Annual maximum temperatures have been rising at between 0.2 and 0.4 °C/decade across the southwestern half of the State, and between 0.0 and 0.2 °C/decade across the northeastern half of the State. This means that total temperature rises have been between 1.5 and 2.5 °C across the southwestern half of the State, and between 0.0 and 1.5 °C across the northeastern half of the State since 1950. No falls in annual maximum temperature are reported across this period.

Table 2 shows the total linear change in annual maximum temperature across the period 1950 to 2018, calculated at the grid-point level as {last point on the linear-regression line} − {first point on the linear-regression line}. Statewide, annual maximum temperatures have risen by 1.30 °C across the period 1950 to 2018, with the subregional rises ranging from 0.53 °C in the North Coast subregion to 1.83 °C in the South West subregion. The other results shown in Table 2 are discussed in the following paragraph.

Region	Maximum temperature	Mean rainfall	Rainfall	Highest FFDI
Queensland	+1.30	634	-32	+4
South East Coast	+1.09	930	-162	+14
Wide Bay and Burnett	+1.15	747	-124	+8
Central Coast	+0.92	807	-148	+1
North Coast	+0.53	1473	-18	-2
Cape York Peninsula	+0.83	1298	+89	+5
Central South	+1.56	489	-77	+14
Central	+1.22	536	-120	+7
North West	+1.01	712	+38	+1
South West	+1.83	290	+2	-3

Table 2: Linear change in annual maximum temperature (second column, in °C), annual rainfall (fourth column, in mm), annual highest daily FFDI (fifth column, in FFDI units) across the period 1950 to 2018. Changes in maximum temperature are rounded to two decimal places. Changes in rainfall and highest daily FFDI are rounded to whole numbers. Average annual rainfall (in mm) across the period 1989-2018 are shown in the third column for comparison, also rounded to whole numbers.

Trend in rainfall Annual 1950-2018

Australian Bureau of Meteorology

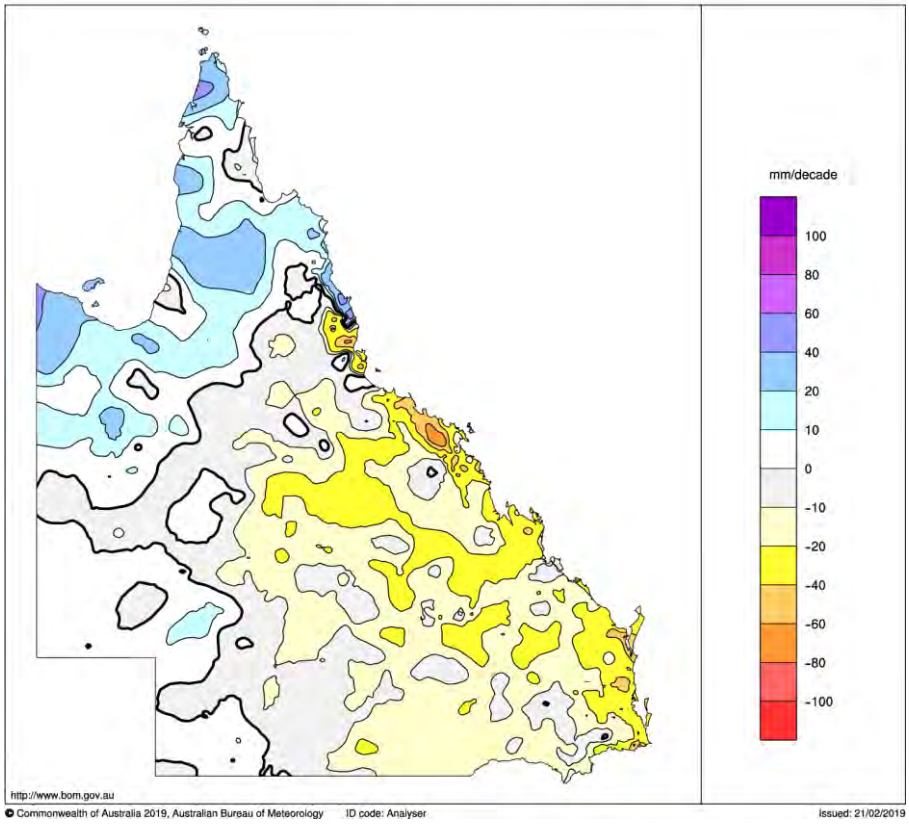

 ID code: Analyser issued: 21/02/2019

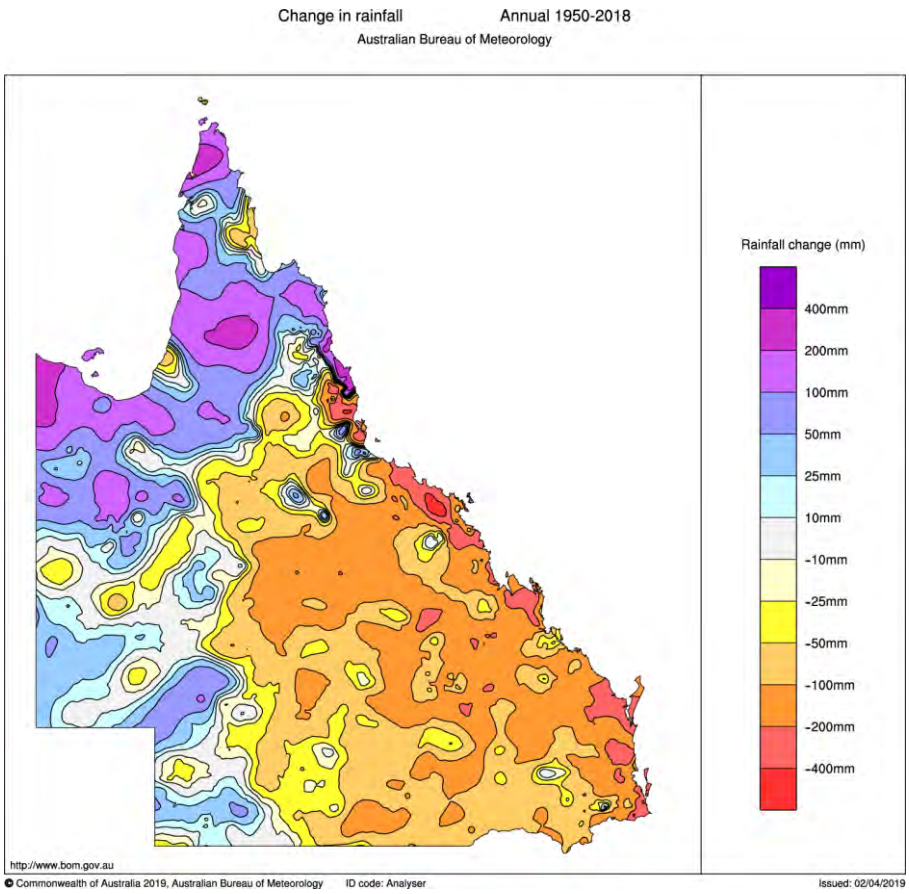

Figure 18: Trend in annual rainfall (in millimetres per decade, top) and total linear change (in millimetres, bottom) across Queensland for the period 1950-2018.

Figure 18 shows the linear trend in annual rainfall across Queensland for the period 1950 to 2018, as calculated from the Bureau of Meteorology's operational high-resolution monthly rainfall analyses (Jones et al. 2009). Trends in annual rainfall are negative across a large part of the southeast of the State, but positive in the tropical north. They are quite small in the southwest of the State. Figure 18 also shows the trends expressed as total linear changes. These total linear changes, as averaged across the study subregions, are shown in Table 2. The Statewide change is a decline of 32 mm with the subregional changes ranging from a decline of 162 mm in the South East Coast subregion to an increase of 89 mm in the Cape York Peninsula subregion. For the Central subregion, the decline of 120 mm represents a decline of 22% relative to the 1989-2018 mean of 536 mm.

It should be noted that the choice of trend period in Figure 18 reflects the FFDI data availability, not the rainfall data availability, and that over the full period of rainfall data availability (1900-2018) the linear trend in annual rainfall is somewhat different. Over the

longer period, the linear trends are weak over most of the State, except in the far north where they remain positive.

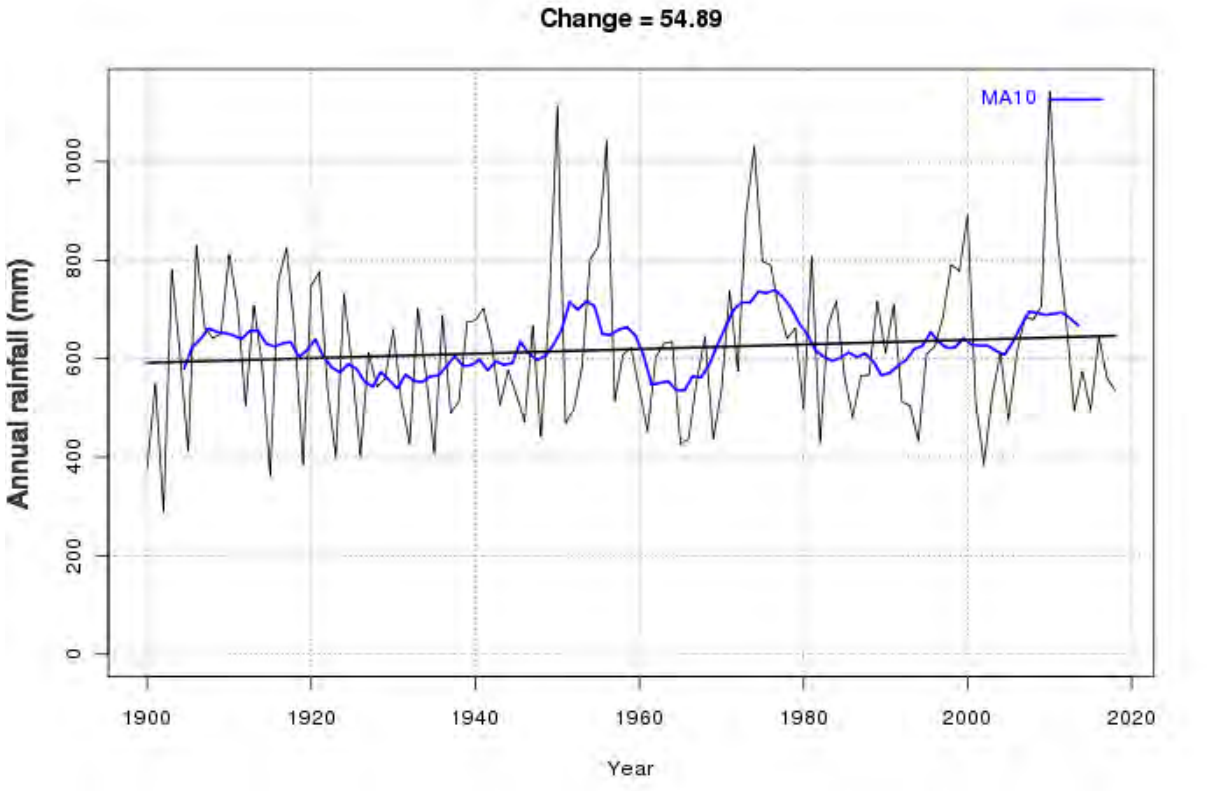

Figure 19: Average annual rainfall across Queensland (1900-2018), in millimetres, with the OLS linear trend line and a 10-year moving average (blue line). The linear modelling suggests Queensland annual rainfall has risen by around 55 millimetres across the period of the data. 1902 was the driest year (289 mm), with 2010 being the wettest year (1142 mm). The 1950s and 1970s were notably wet periods. New monthly rainfall analyses currently under development at the Bureau of Meteorology, using a different analysis approach from that of Jones et al. (2009), now extend back to 1880. The new analyses suggest that the 1880s and 1890s were a rather wet period for Queensland, comparable to the 1970s. The inclusion of the extra twenty years of data turns the weak positive change (+55 mm) shown in the figure into an even weaker negative change (−17 mm), of approximately half the magnitude of that seen here. Again, this is a reminder that the calculation of trends in annual rainfall across Queensland is affected to a substantial degree by the choice of the period used in the calculation, because of the significant variability on decadal time scales.

Figure 19 shows annual rainfall averaged across Queensland for the period 1900-2018, together with the OLS linear trend and a 10-year moving average. This is the full period of record in terms of the gridded monthly rainfall analyses of Jones et al. (2009). A significant degree of decadal to interdecadal variability can be seen in the time series of Queensland annual rainfall. The 1950s were rather wetter than the 1920s, 1930s, and 1940s. The picture turned drier again in the 1960s, while the 1970s were the wettest sustained period since Federation. Drier conditions returned in the 1980s and 1990s. Although this amounts to an increase in annual rainfall of around 55 mm averaged across the State, this result should be treated with a degree of caution, given the observed variability. In other words, it might not persist into the future as more data arrive.

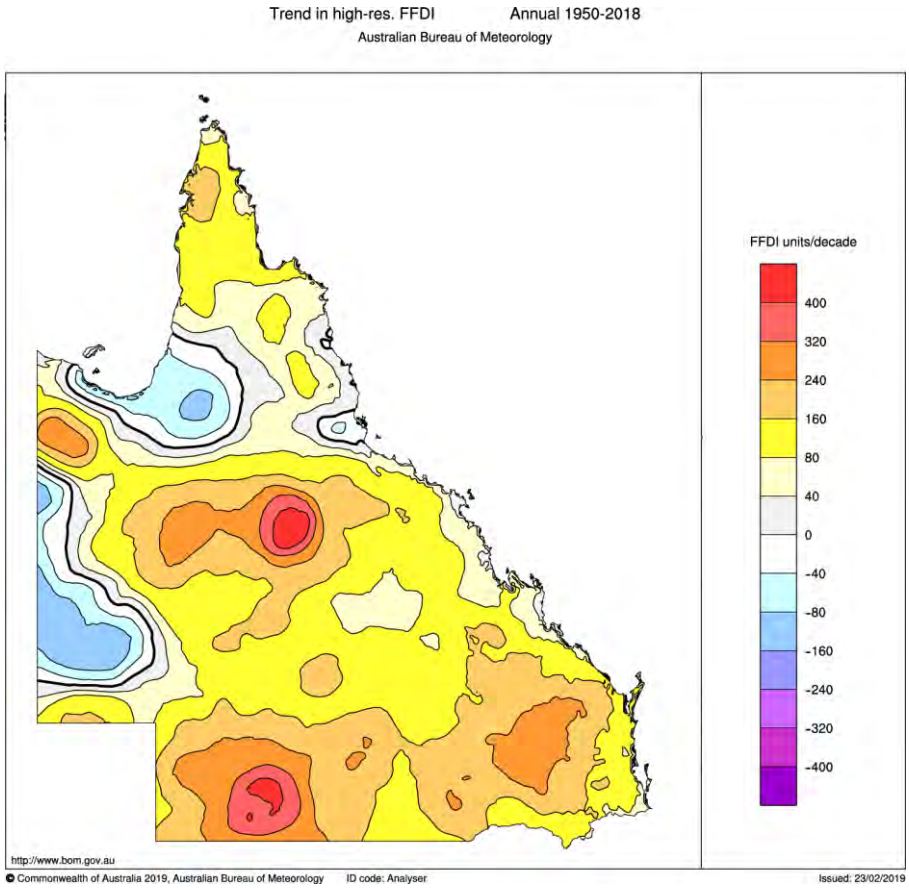

Figure 20: Trend in annual accumulated FFDI across Queensland for the period 1950-2018 (in FFDI units per decade).

Figure 20 shows the linear trend in annual accumulated FFDI across Queensland for the period 1950 to 2018. The trends are positive across most of the State, although with exceptions in the north and west. A comparison of Figure 20 with Figure 18 indicates that the declines in annual accumulated FFDI seen in the north and west cannot be ascribed solely to

the annual rainfall changes. For example, parts of the western negative patch in Figure 20 have seen very little overall change in annual rainfall.

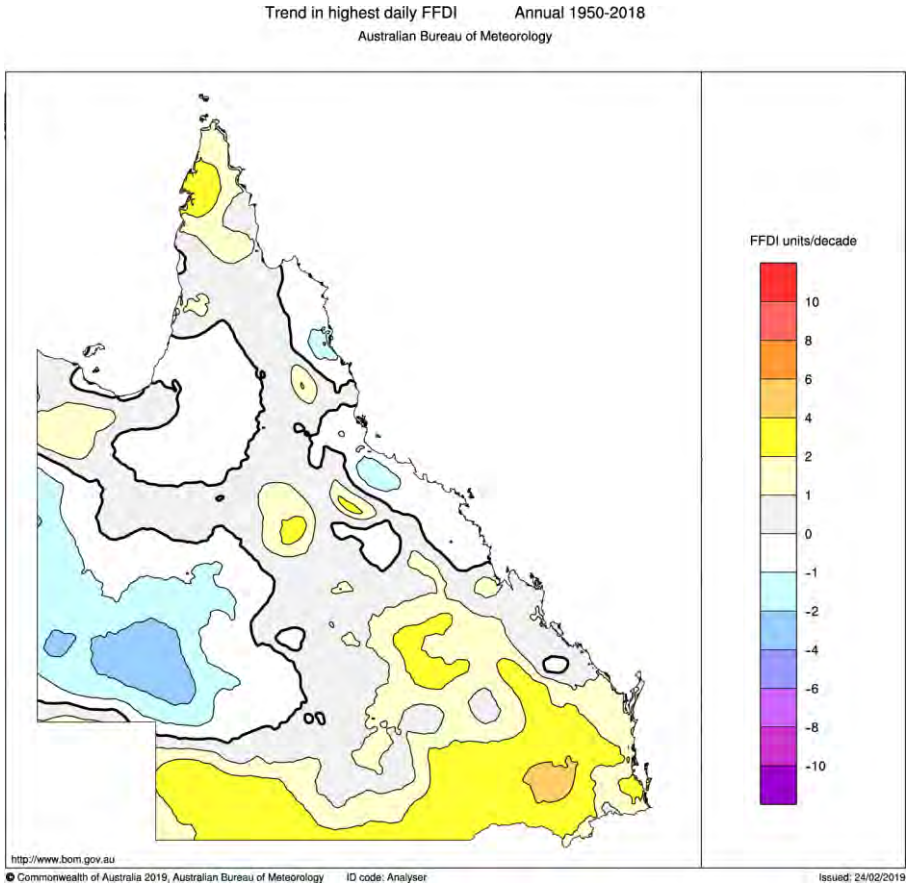

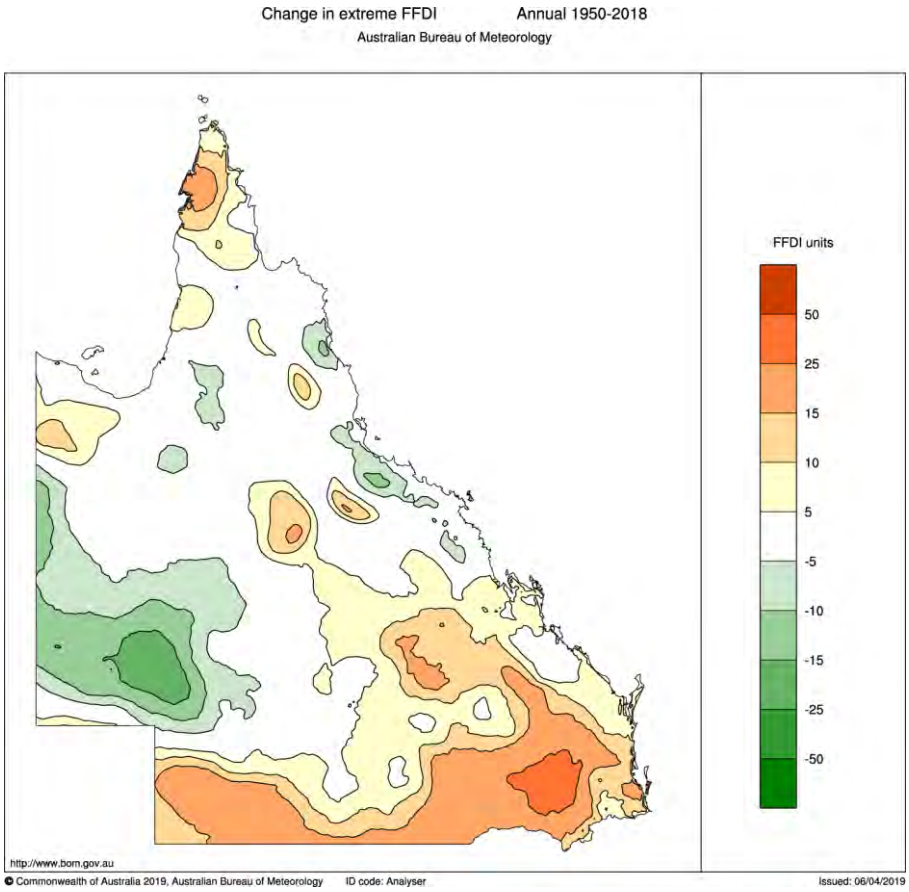

Figure 21: Linear trend in annual highest daily FFDI (in FFDI units per decade, top) and total linear change (in FFDI units, bottom) across Queensland for the period 1950-2018.

Figure 21 shows the linear trend in the highest daily FFDI in the calendar year across Queensland for the period 1950-2018. Over most of Queensland the trend is patchy, in some places positive, other places negative, and in many places weak. Over southern Queensland the trend is more consistently positive, and at the Queensland/New South Wales border it mostly exceeds 2 FFDI units per decade (implying a total linear increase of more than 15 FFDI units). This aspect of the trend extends across the border into a large part of western New South Wales and western Victoria (not shown), indicating that it is part of a larger pattern of change (of increasing fire-weather severity).

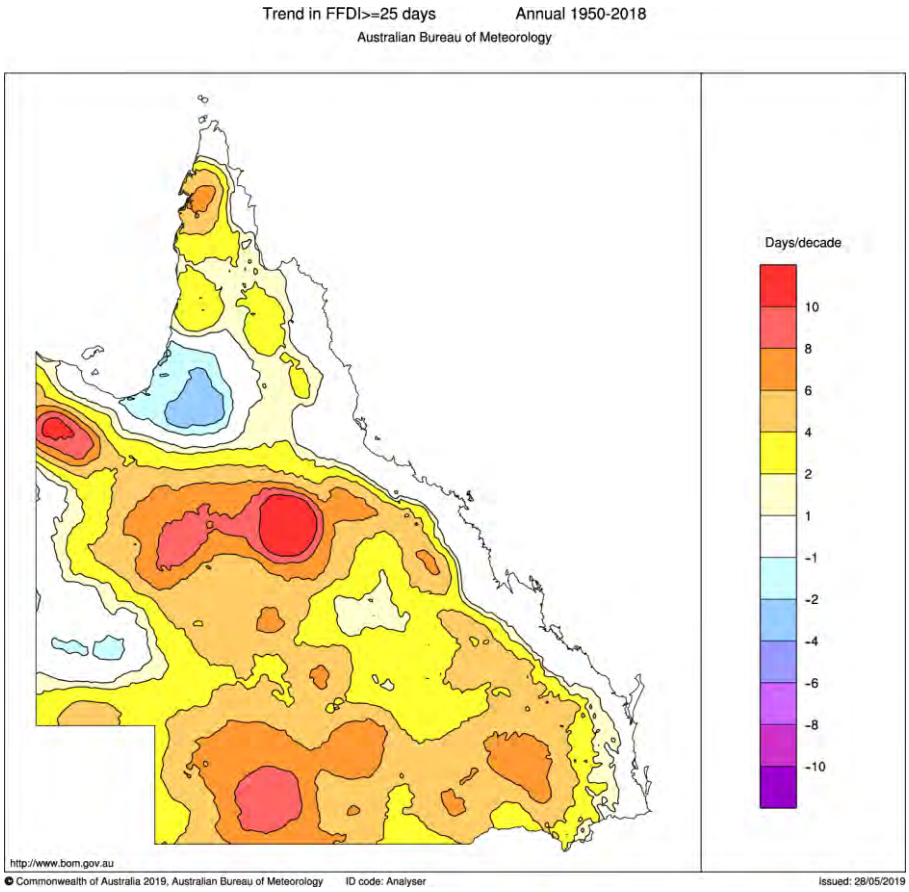

Figure 22: Trend in annual FFDI ≥ 25 days across Queensland for the period 1950-2018 (in days per decade).

Figure 22 shows the linear trend in annual FFDI ≥ 25 days across Queensland for the period 1950 to 2018. The large-scale features in Figure 22 are similar to those of Figure 20 for annual accumulated FFDI, but the distinction between east and west of the Great Dividing Range is more emphatic in Figure 22.

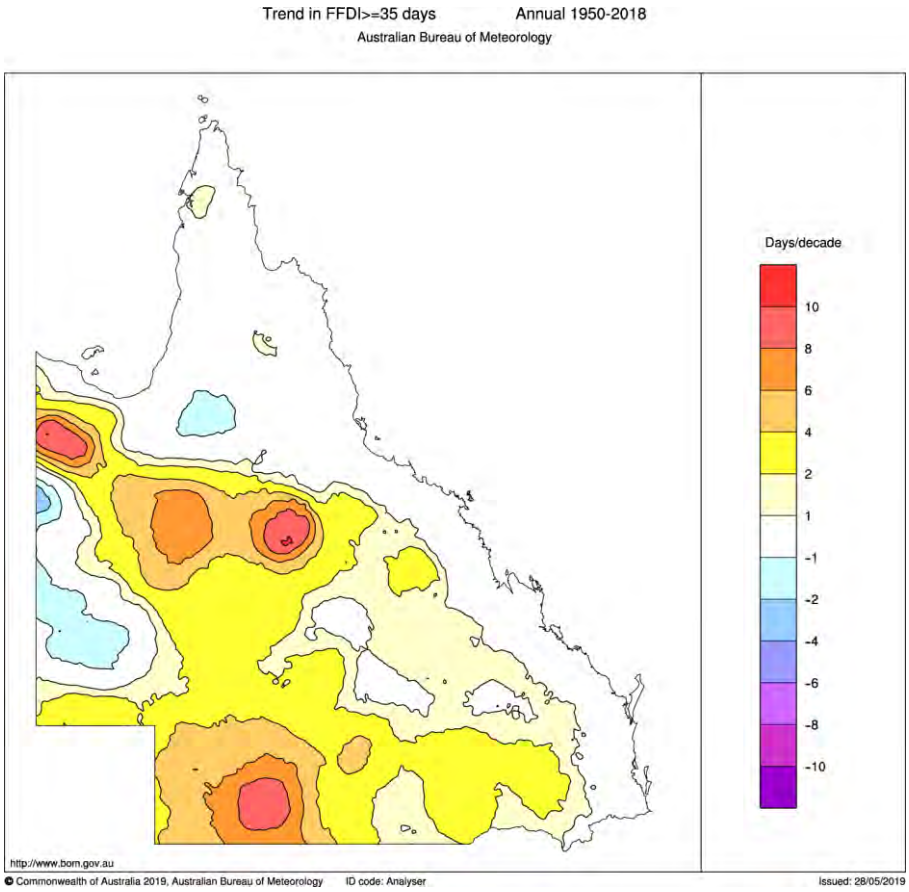

Figure 23: Trend in annual FFDI ≥ 35 days across Queensland for the period 1950-2018 (in days per decade).

Figure 23 shows the linear trend in annual FFDI ≥ 35 days across Queensland for the period 1950 to 2018. The pattern in Figure 23 is fairly similar to that of Figure 22, except in the far north where the lower frequency of FFDI ≥ 35 days relative to FFDI ≥ 25 days causes a noticeable difference.

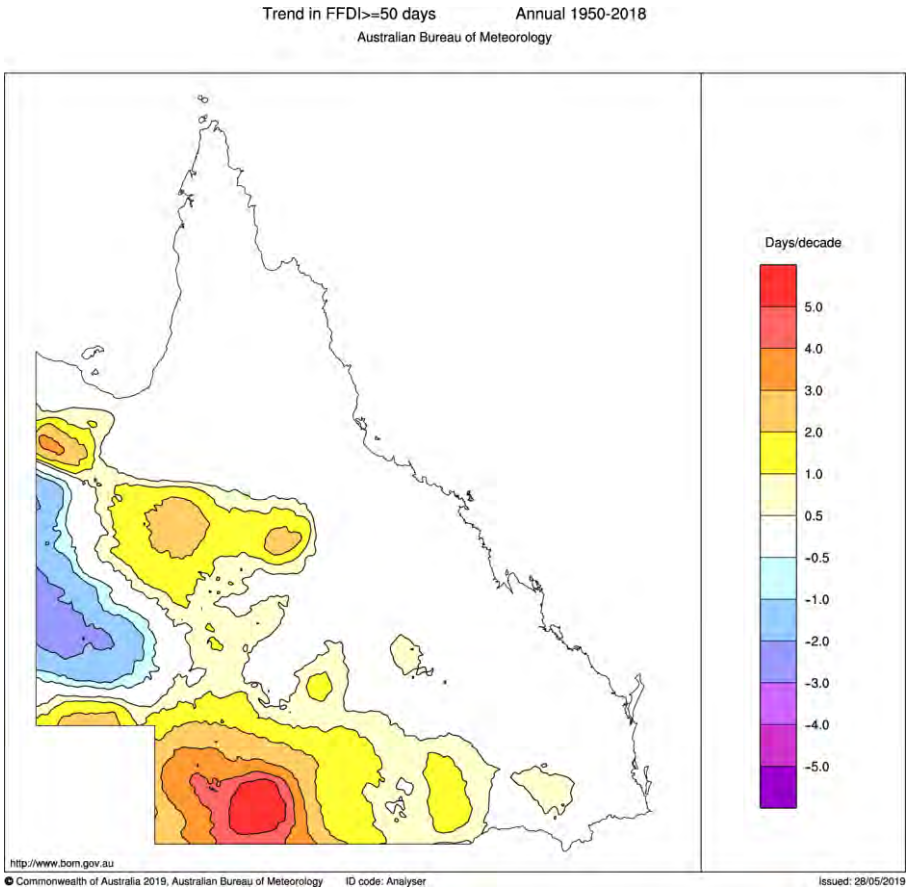

Figure 24: Trend in annual FFDI ≥ 50 days across Queensland for the period 1950-2018 (in days per decade).

Figure 24 shows the linear trend in annual FFDI ≥ 50 days across Queensland for the period 1950 to 2018. The large-scale pattern in Figure 24 is somewhat different from that of Figure 22, in part because FFDI ≥ 50 days in eastern and northern Queensland are climatologically infrequent (see Figure 11) and the resulting trends are consequently weak.

Table 3 shows the changes in annual accumulated FFDI across the period 1950 to 2018, in both actual and percentage terms, as estimated using the *lowess*-regression modelling. These numbers are taken from the figures shown in the Regional Fact Sheets section below. Annual accumulated FFDI has risen across the period 1950 to 2018 in all nine subregions (percentage increases range from 9% in the South West subregion to a quite remarkable 51% in the South East Coast subregion), as well as Statewide (14%). Table 3 also shows the changes in annual FFDI ≥ 25 days across the same period. Incidences of FFDI ≥ 25 days have risen across all subregions, and for some of them by substantial amounts. Across the Cape York Peninsula subregion, the incidence of FFDI ≥ 25 days has doubled, while in the South East Coast subregion, the incidence has more than tripled, with the Wide Bay and

Burnett subregion not quite tripling its incidence. It is noteworthy that in all nine subregions the percentage increase in the incidence of FFDI ≥ 25 days exceeds the percentage increase in annual accumulated FFDI. This outcome is not surprising, as the incidence of FFDI ≥ 25 days is in effect sampling the upper tail of the distribution of daily FFDI values under the background of a rising mean of the distribution. [Percentage increases in the annual accumulated FFDI (shown) should match the percentage increases in the average daily FFDI (not shown).]

Region	Change in FFDI		Change in FFDI ≥ 25 days	
	Actual	Percentage	Actual	Percentage
Queensland	905	14%	29	30%
South East Coast	1255	51%	13	254%
Wide Bay and Burnett	1271	42%	17	187%
Central Coast	682	18%	16	85%
North Coast	256	11%	1	25%
Cape York Peninsula	768	21%	16	109%
Central South	1532	27%	44	63%
Central	944	16%	30	41%
North West	700	11%	29	31%
South West	936	9%	32	17%

Table 3: *Lowess*-modelled changes in annual accumulated FFDI (actual and percentage) and changes in annual FFDI ≥ 25 days (actual and percentage) across the period 1950 to 2018. Actual and percentage changes in the table have been rounded to integer values.

Spatial Patterns (1989-2018)

This section presents trends and changes over the past thirty years (1989-2018). These supplement the full-period results shown in the previous section.

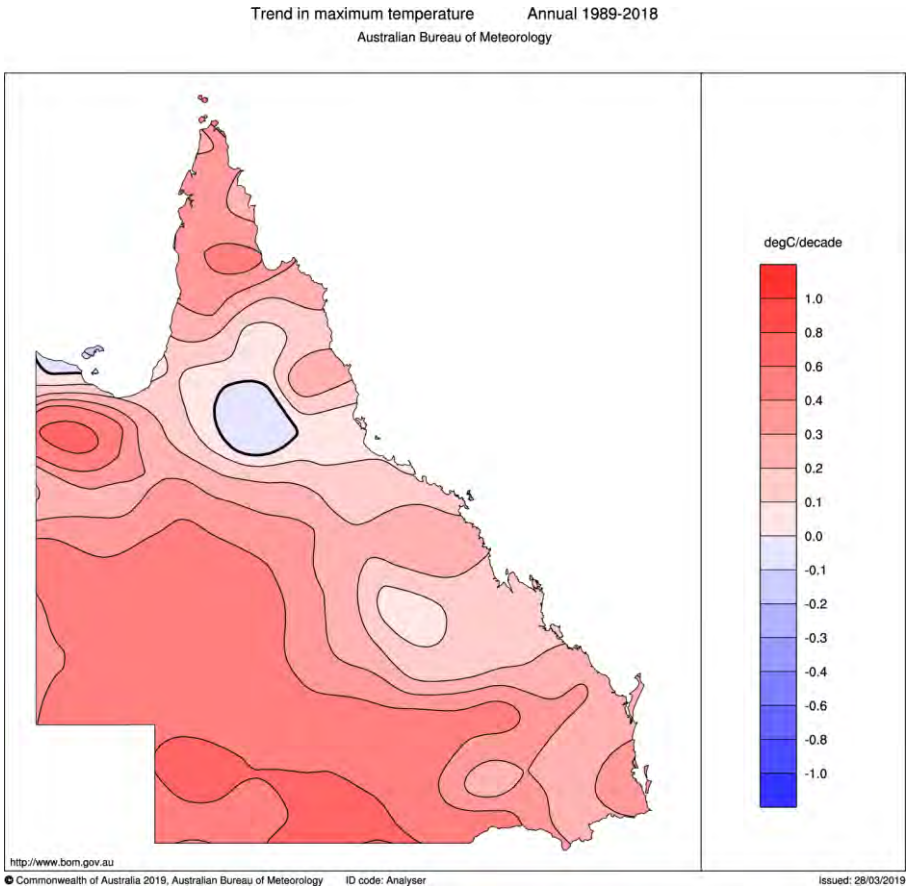

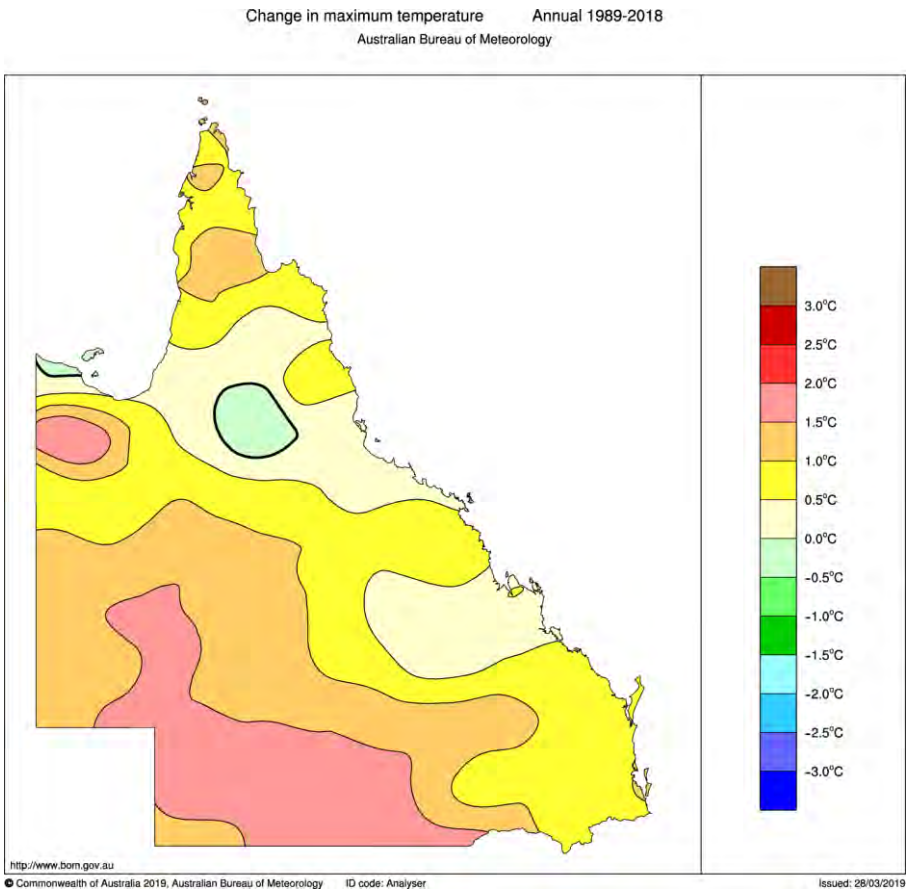

Figure 25: Linear trend in annual maximum temperature (in °C per decade, top) and total linear temperature change (in °C, bottom) across Queensland for the period 1989-2018.

Figure 25 shows the linear trend and total linear change in annual maximum temperature across Queensland for the period 1989 to 2018, as calculated from the Bureau of Meteorology's operational monthly maximum temperature analyses (Jones et al. 2009). Annual maximum temperatures have risen by between 1 and 2 °C across the southwestern half of the State, with smaller changes over most of the rest of the State. In some small areas, average annual maximum temperatures have fallen slightly over the past 30 years.

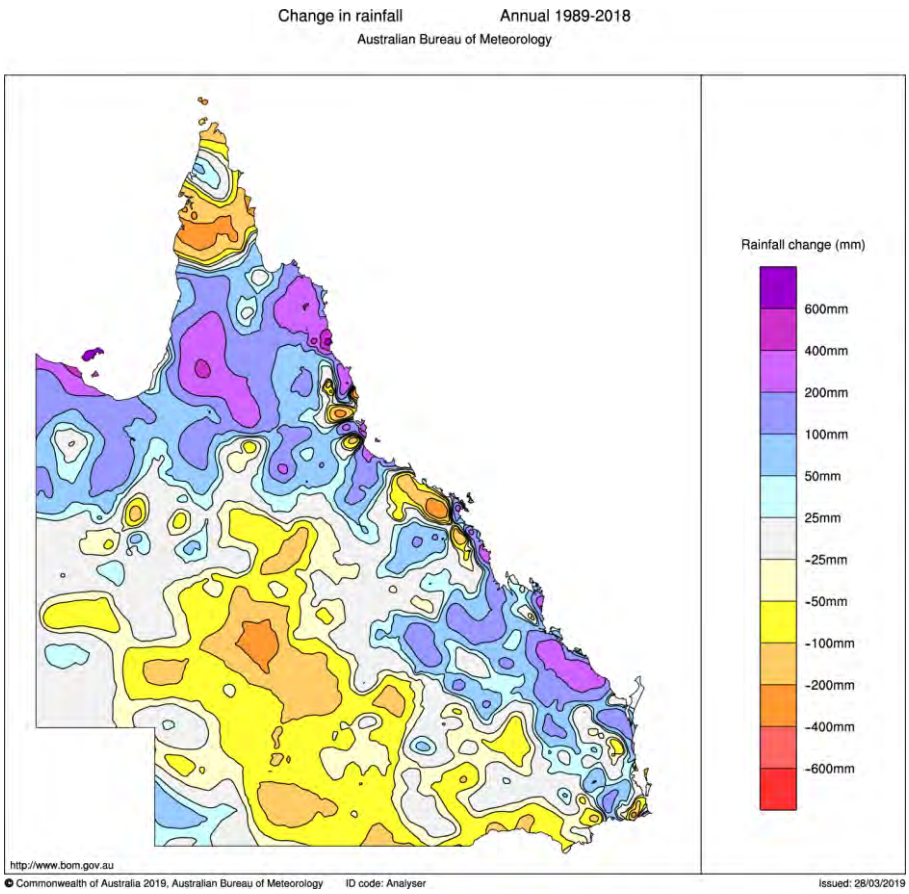

Figure 26: Linear change in annual rainfall across Queensland for the period 1989-2018 (in millimetres).

Figure 26 shows the linear change in annual rainfall across Queensland for the period 1989 to 2018, as calculated from the Bureau of Meteorology's operational monthly rainfall analyses (Jones et al. 2009). Across the past 30 years, the pattern of rainfall change is mixed. In the southern to central inland, annual rainfall has declined by up to 200 mm, with widespread declines of more than 50 mm. In contrast, annual rainfall has increased over much of the east coast and tropical north. These changes, over the last 30 years, should be treated with a degree of caution. To a significant degree, they reflect the interannual and interdecadal nature of Queensland rainfall (see Figure 19).

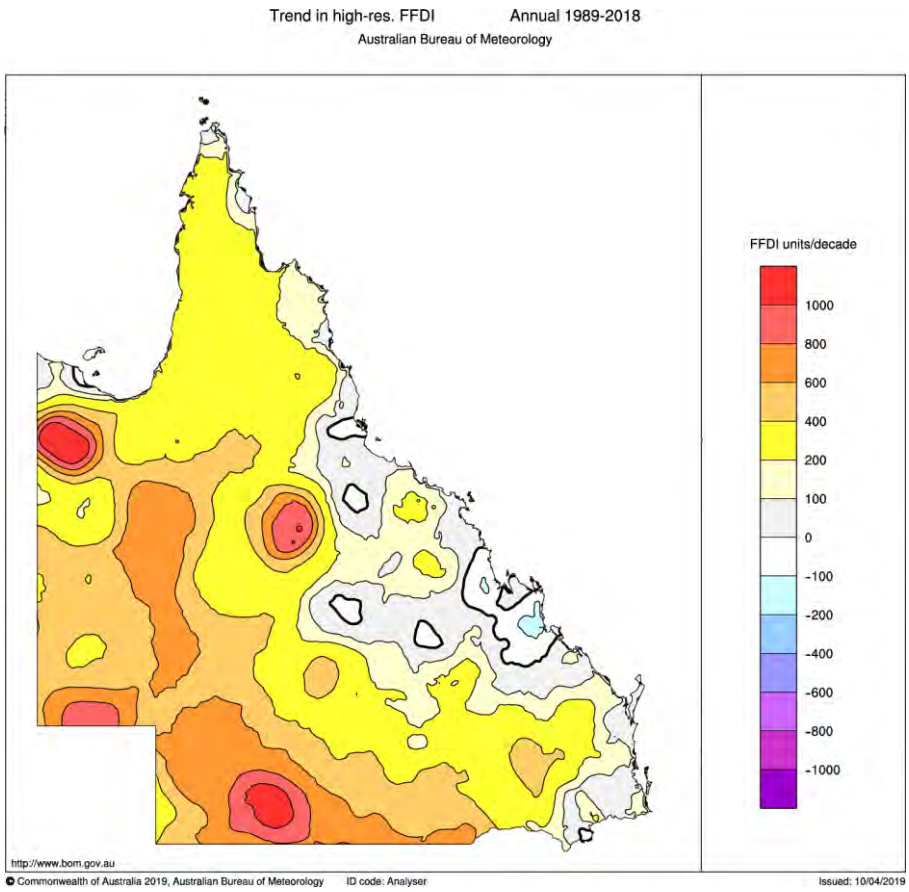

Figure 27: Trend in annual accumulated FFDI across Queensland for the period 1989-2018 (in FFDI units per decade).

Figure 27 shows the linear trend in annual accumulated FFDI across Queensland for the period 1989-2018 (in FFDI units per decade). Note that the contouring in Figure 27 is different from that in Figure 20, as the calculated trends are somewhat larger over the shorter period. Trends are generally stronger in the southwest half of the State than they are in the northeast half. Trends are generally weak in the southern and central parts of the east coast.

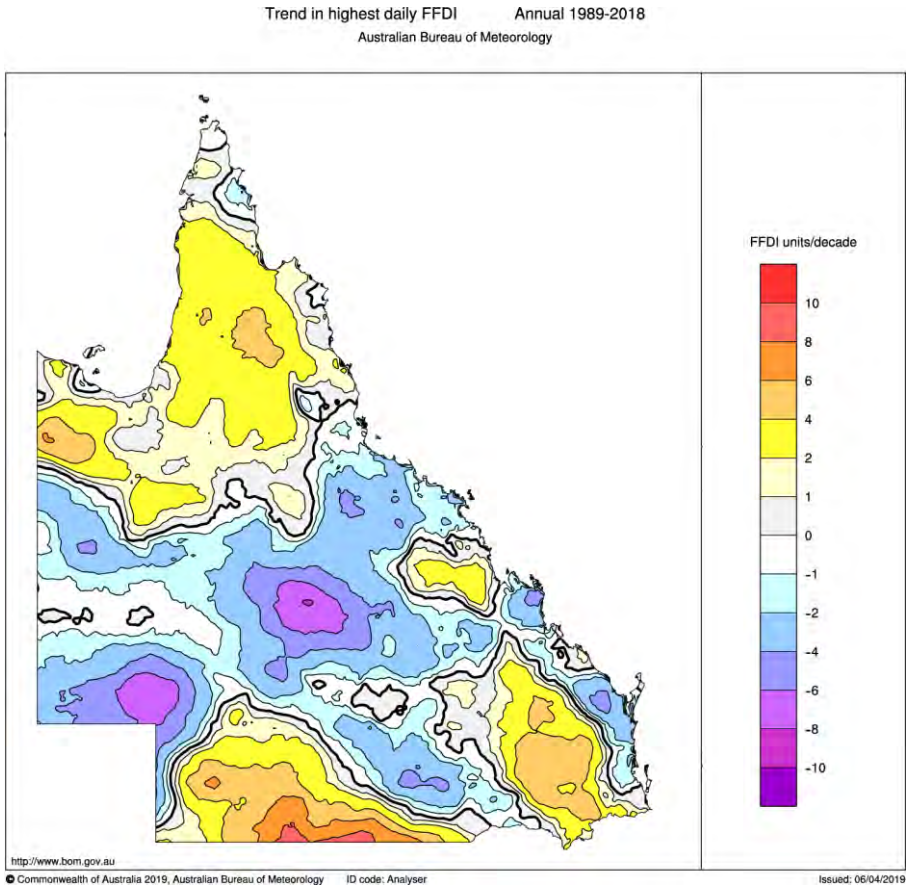
Trend in highest daily FFDI Annual 1989-2018
Australian Bureau of Meteorology
FFDI units/decade
10
8
6
4
2
1
0
-1
-2
-4
-6
-8
-10
http://www.bom.gov.au
© Commonwealth of Australia 2019, Australian Bureau of Meteorology ID code: Analyser
Issued: 06/04/2019

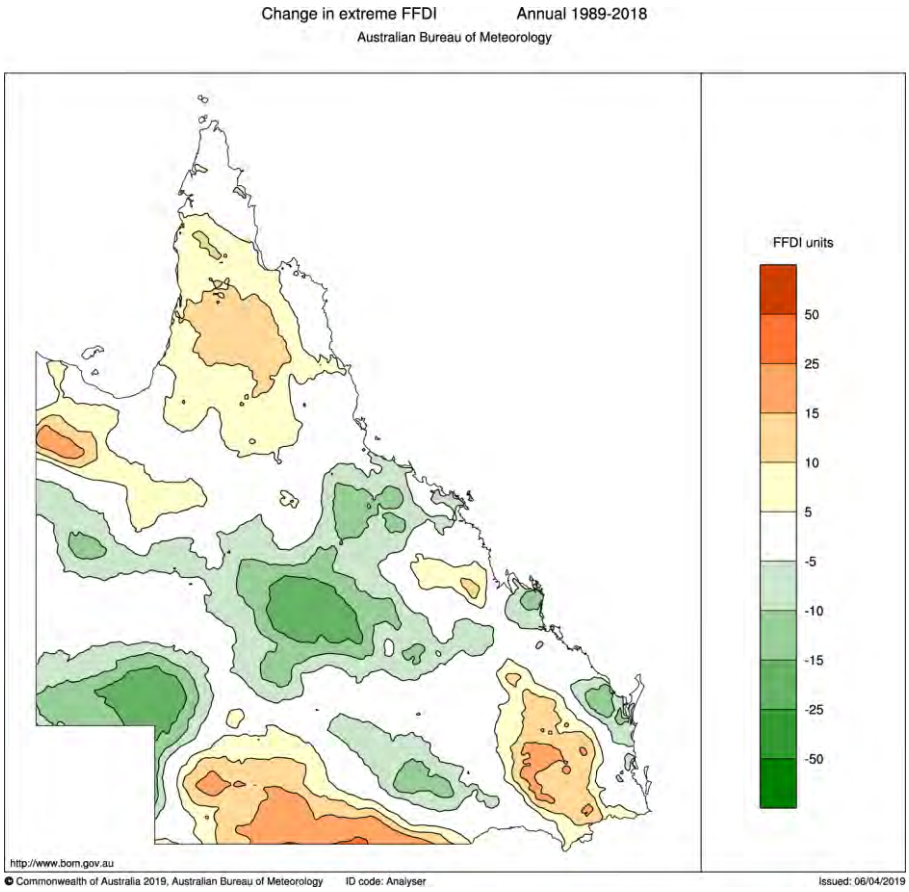

Figure 28: Linear trend in annual highest daily FFDI (in FFDI units per decade, top) and total linear change (in FFDI units, bottom) across Queensland for the period 1989-2018.

Figure 28 shows the linear trend in the highest daily FFDI across the period of 1989-2018 (in FFDI units per decade), and the total linear change (in FFDI units). The trend is patchy across the last thirty years, with rises of 15 points in parts of the south and northwest, but falls of comparable magnitude in the southwest and centre.

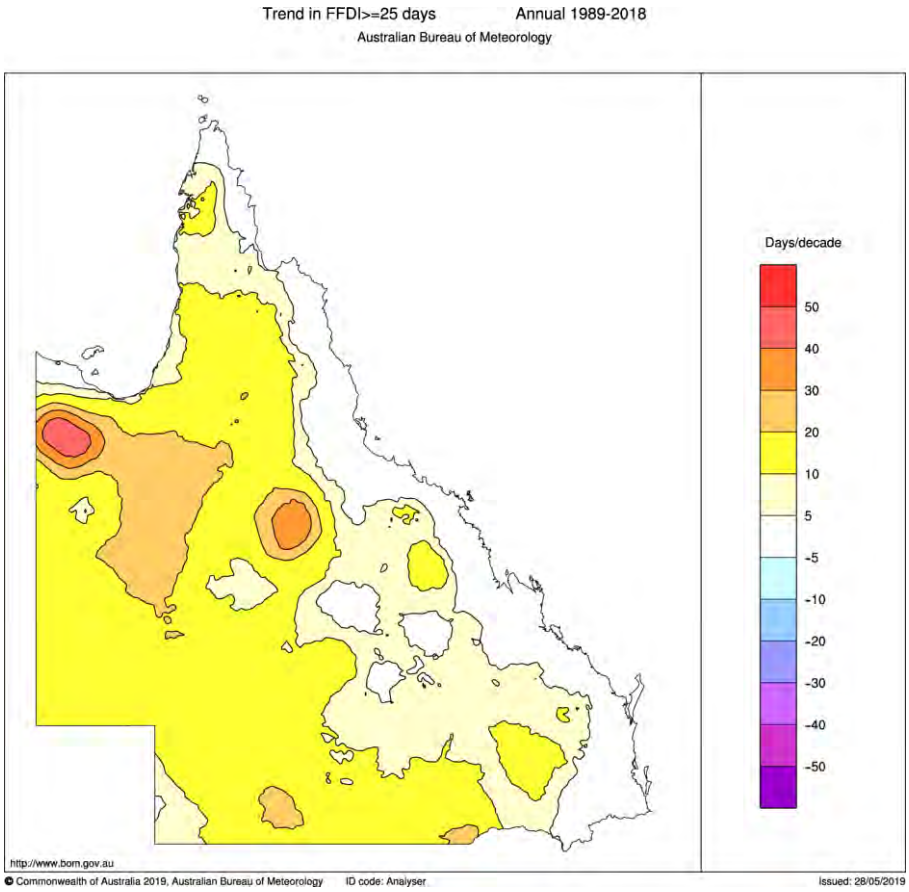

Figure 29: Trend in annual FFDI ≥ 25 days across Queensland for the period 1989-2018 (in days per decade).

Figure 29 shows the trend in the annual number of FFDI ≥ 25 days across the period 1989-2018. FFDI ≥ 25 days have increased at the rate of at least 10 days per decade over a large part of western Queensland. Trends have been weak along the east coast. The pattern of change in Figure 29 is on the whole much stronger than that shown in Figure 22 for the whole period 1950-2018 (note the different contouring arrangements). The temporal pattern of change seen below in Figure 32 indicates that this difference in the trends is the result of an overall acceleration in the arrival of FFDI ≥ 25 days.

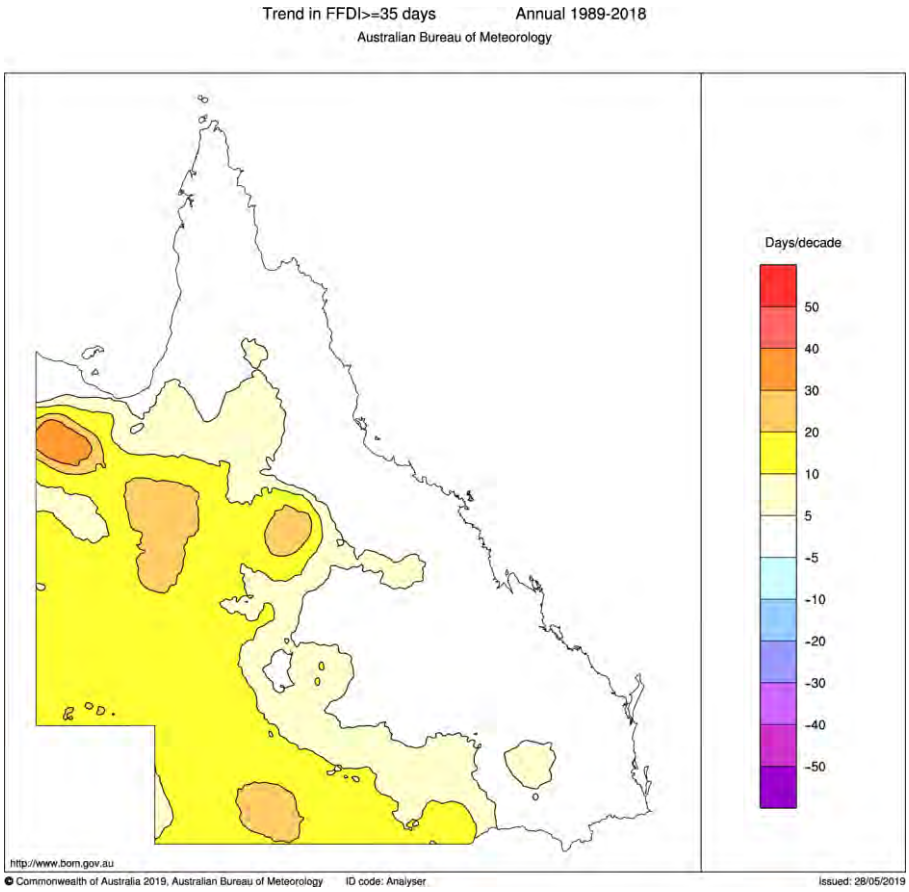

Figure 30: Trend in annual FFDI ≥ 35 days across Queensland for the period 1989-2018 (in days per decade).

Figure 30 shows the trend in the annual number of FFDI ≥ 35 days across the period 1989-2018. Trends exceed 10 days per decade over quite a lot of western Queensland, although naturally not as much as in Figure 29. Trends a broadly weak along the east coast and Cape York Peninsula.

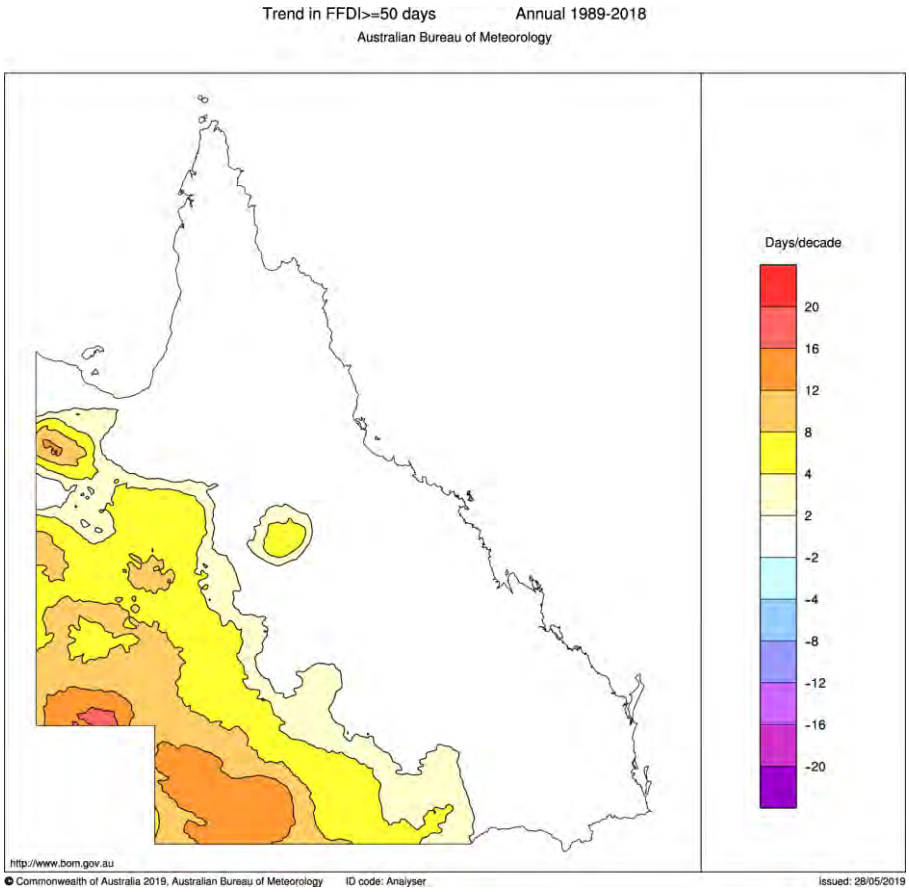

Figure 31: Trend in annual FFDI ≥ 50 days across Queensland for the period 1989-2018 (in days per decade).

Figure 31 shows the trend in the annual number of FFDI ≥ 50 days across the period 1989-2018. Noting the different contouring from Figure 30, Figure 31 shows an expanded area in the east with weak trends. A large area of the southwest shows trends above 4 days per decade.

Table 4 shows the *lowess* changes in annual accumulated FFDI and FFDI ≥ 25 days averaged across Queensland and the nine subregions for the last thirty years (1989-2018). These changes are calculated from the *lowess* regressions calculated across the entire period (1950-2018), for which the analogous results are shown in Table 3, rather than from separate regressions calculated across just these thirty years. [Doing the calculation in this manner makes the result less susceptible to the end effects of the interdecadal variability.] Across the last thirty years, annual accumulated FFDI (and therefore daily FFDI) has risen by 15%, with the subregional changes ranging from 9% in the Central Coast subregion to 21% in the South East Coast subregion. Across the last thirty years, annual FFDI ≥ 25 days have risen by 33% (30 days), with the subregional changes ranging from 24% in the South West

subregion to 108% in the South East Coast subregion. This means the annual occurrence of FFDI ≥ 25 days has more than doubled in the South East Coast subregion, with a near doubling in the Cape York Peninsula subregion.

Region	Change in FFDI		Change in FFDI ≥ 25 days	
	Actual	Percentage	Actual	Percentage
Queensland	952	15%	30	33%
South East Coast	639	21%	9	108%
Wide Bay and Burnett	457	12%	11	76%
Central Coast	379	9%	11	48%
North Coast	327	14%	2	71%
Cape York Peninsula	568	15%	15	98%
Central South	1218	20%	33	41%
Central	647	10%	21	27%
North West	851	13%	36	42%
South West	1522	15%	43	24%

Table 4: *Lowess*-modelled changes in annual accumulated FFDI (actual and percentage) and changes in annual FFDI ≥ 25 days (actual and percentage) across the period 1989 to 2018. Actual and percentage changes in the table have been rounded to integer values.

Temporal Patterns

This section looks at temporal patterns in the changes, in contrast to the previous two sections that looked at spatial patterns.

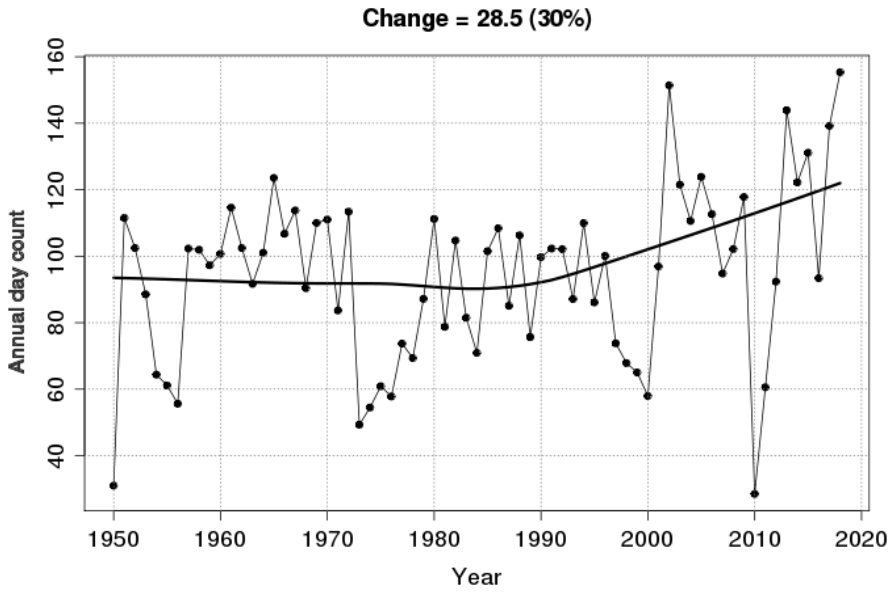

Figure 32: Time series of annual FFDI ≥ 25 days for Queensland across the period 1950 to 2018. A *lowess* regression is superimposed.

Figure 32 shows the time series of annual FFDI ≥ 25 days for Queensland across the period 1950 to 2018. A *lowess* regression has been superimposed to diagnose the trend, which shows a substantial departure from linearity. This modelling diagnoses little change across first four decades of the dataset (1950 to 1990), followed by increasing incidence in the last three decades. The years of lowest incidence of FFDI ≥ 25 days are 2010, followed by 1950. The year of highest incidence is 2018. The fact of the first year in the time series being the second-lowest value and the last year being the highest value may have a slight (inflating) impact on the diagnosed change (an increase of 30% in the incidence across the study period). Prior to the 21st Century, the Statewide-averaged total of FFDI ≥ 25 days had only once exceeded 120 days. During the 21st Century, this level of incidence has been exceeded in eight years.

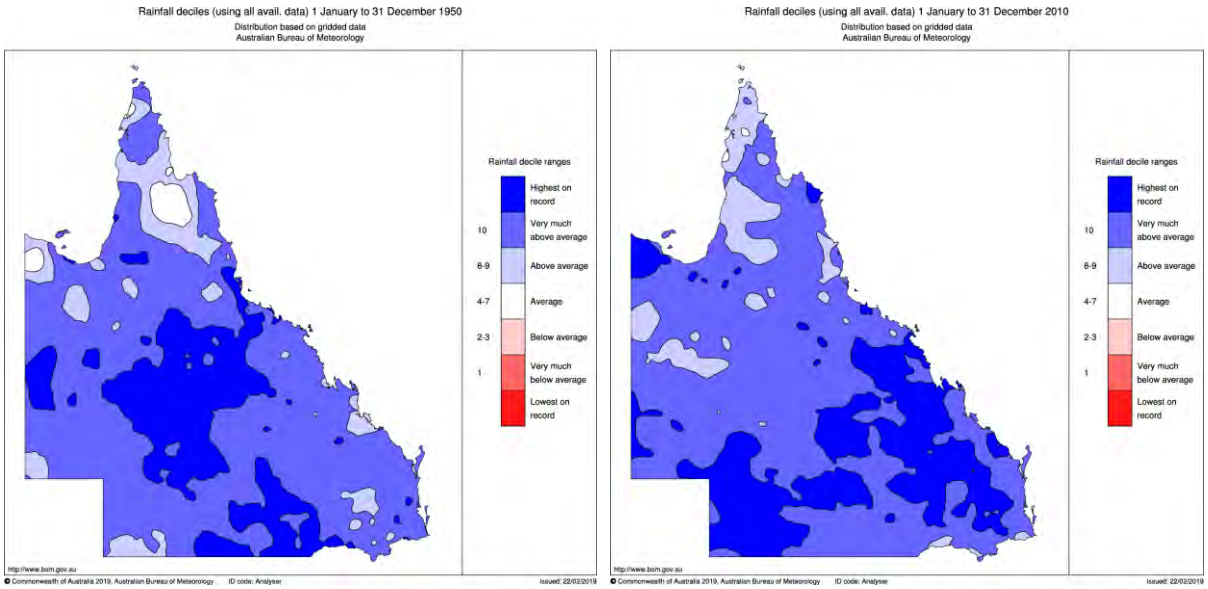

Figure 33: Rainfall deciles for 1950 (left) and 2010 (right). The calculation uses annual rainfalls from 1900 to 2018. 1950 had the second-lowest incidence of FFDI ≥ 25 days averaged across Queensland, while 2010 had the lowest incidence of FFDI ≥ 25 days.

That 2010 and 1950 had very low incidences of FFDI ≥ 25 days can be ascribed in part to those years being very wet years across Queensland (see Figure 33). Those wet years can in turn be ascribed to the state of the El Niño-Southern Oscillation. 2010 saw the end of the 2009/2010 El Niño and the start of the 2010/2011 La Niña (Ganter 2011), the transition from one to the other occurring at the usual time in the southern hemispheric Autumn. 1950 was likewise dominated by La Niña conditions in the tropical Pacific.

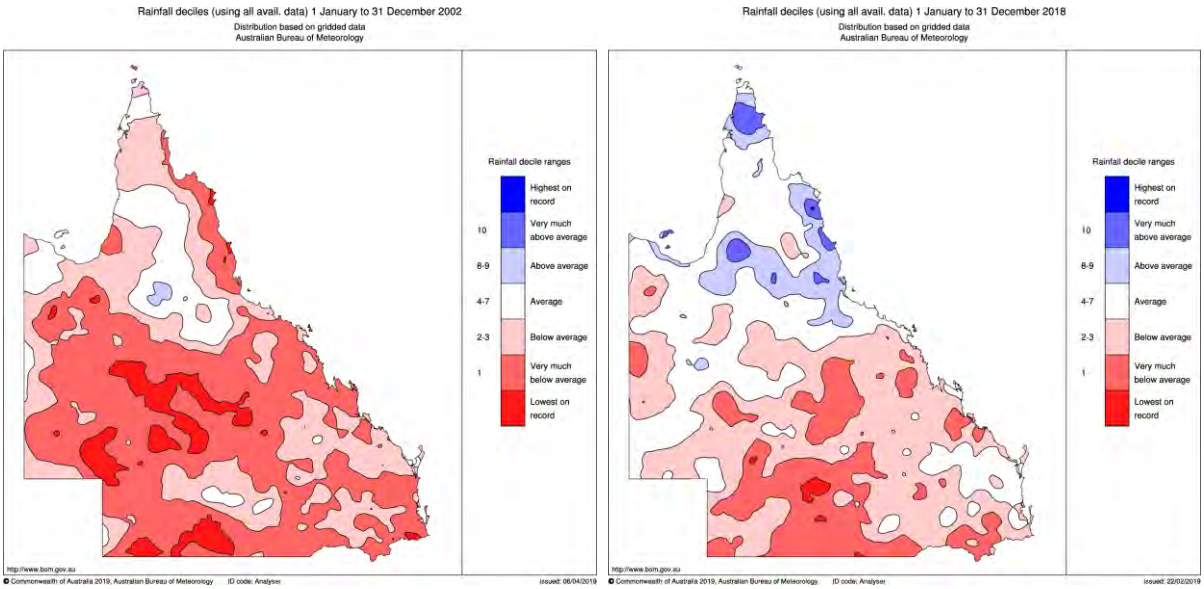

Figure 34: Rainfall deciles for 2002 (left) and 2018 (right). The calculation uses annual rainfalls from 1900 to 2018. 2018 had the highest incidence of FFDI ≥ 25 days averaged across Queensland, while 2002 had the second-highest incidence of FFDI ≥ 25 days.

Analogously the very high incidence of such days in 2018 can be ascribed in part to that year being a somewhat dry year (see Figure 34) across Queensland, although evidently other factors are playing a part (e.g., 2018 was the fourth-warmest year on record for annually averaged maximum temperature across Queensland). 2018 was characterised by a transition from a weak negative phase of the El Niño-Southern Oscillation (i.e., La-Niña-like, but not strong enough to be called La-Niña) conditions to a weak positive phase (i.e., El-Niño-like, but not strong enough to be called El-Niño) in the tropical Pacific, while 2002 (the year of the second-highest incidence of FFDI ≥ 25 days) was unambiguously an El Niño year (Fawcett and Trewin 2003, Jones 2003).

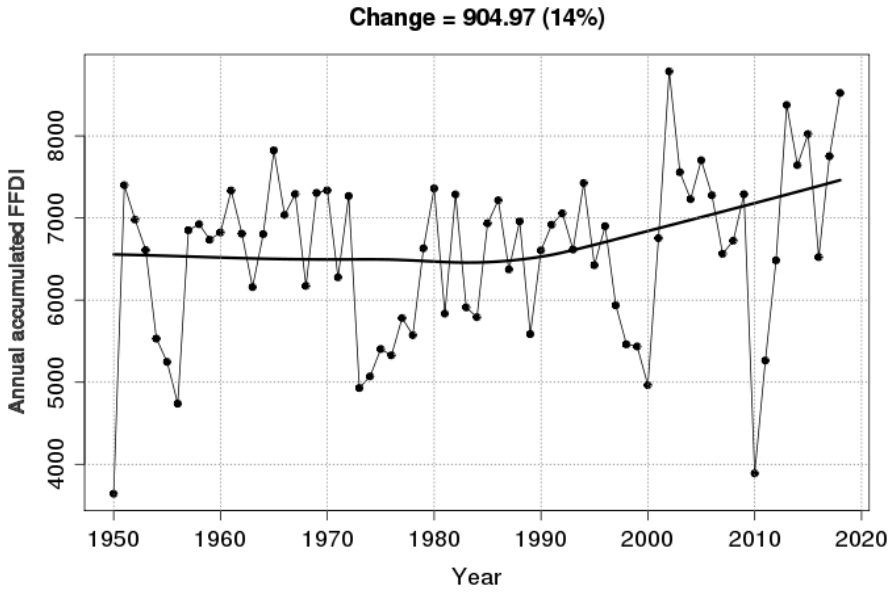

Figure 35: Time series of annual accumulated FFDI averaged across Queensland for the period 1950 to 2018. A *lowess* regression is superimposed.

Figure 35 shows the time series of annual accumulated FFDI across the period 1950 to 2018 for Queensland. The temporal pattern here is similar to that of Figure 32 (i.e., decades of little change followed by decades of increasing activity), although the two highest and two lowest years have their ranks swapped in each case (2002 is highest on record for annual accumulated FFDI while 2018 is highest on record for annual FFDI ≥ 25 days; likewise 1950 is lowest on record for annual accumulated FFDI while 2010 is lowest on record for annual FFDI ≥ 25 days).

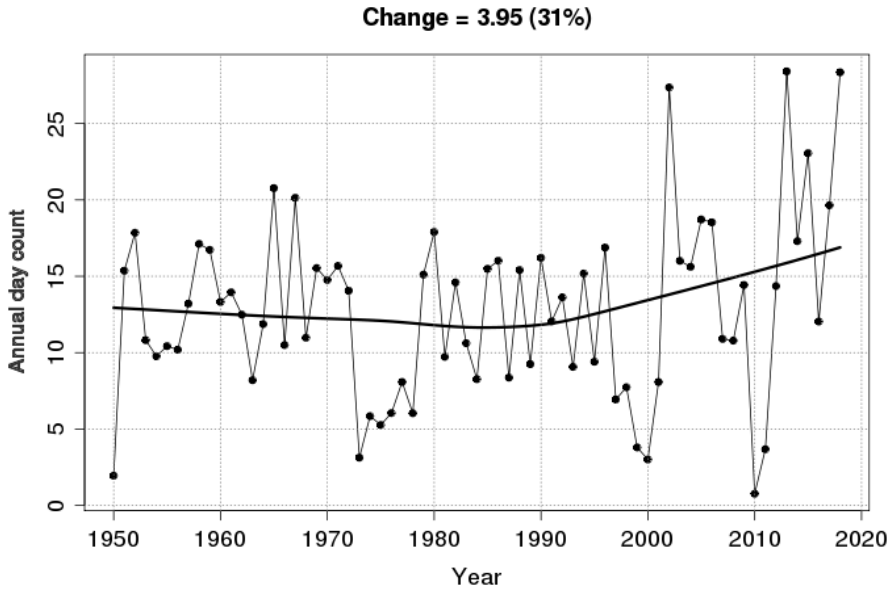

Figure 36: Time series of annual FFDI ≥ 50 days for Queensland across the period 1950 to 2018. A *lowess* regression is superimposed.

Figure 36 shows the time series of FFDI ≥ 50 days across the period 1950 to 2018 for Queensland. The *lowess* regression diagnoses a slight decline in the incidence of FFDI ≥ 50 days from the 1950s to the 1980s, followed by a rebound. This amounts to an overall increase of 31% in the annual incidence. Prior to the 21st Century, the Statewide annual incidence had only twice exceeded 20 days, and had not exceeded 25 days at all. In the 21st Century, the 20-day total has been exceeded four times, and the 25-day total three times. Particularly high values occurred in 2002, 2013 and 2018, each being well above anything in the prior 50 years.

As indicated in the Data and Methods section, since the Dowdy (2018) FFDI dataset only goes back to 1950, an attempt will now be made to estimate the annual accumulated FFDI across Queensland prior to 1950, using annual rainfall, annual maximum temperature and annual drought factor, to obtain an indication of the behaviour of the FFDI in the decades prior to the 1950s. The annual rainfall is available from 1900, annual maximum temperature from 1910 (both of these from the Jones et al. (2009) dataset), and annual drought factor from 1911 (from the Dowdy (2018) dataset). Accordingly, reconstructions are attempted for the period 1911 to 1949.

Queensland

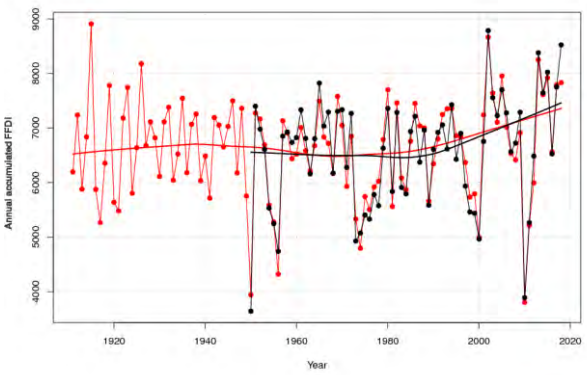

Cape York Peninsula

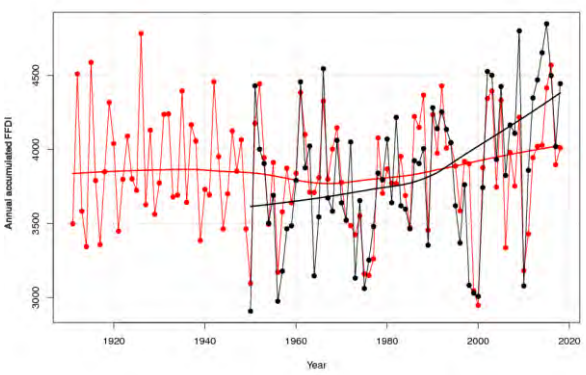

South East Coast

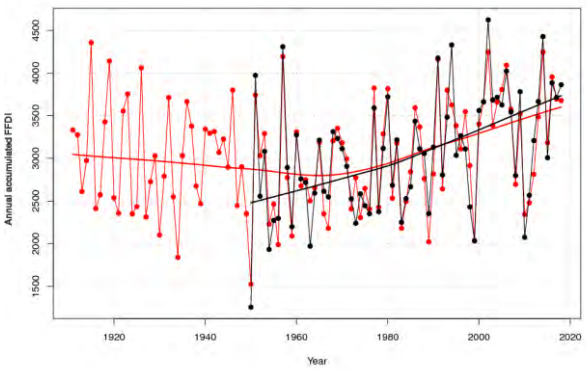

Central South

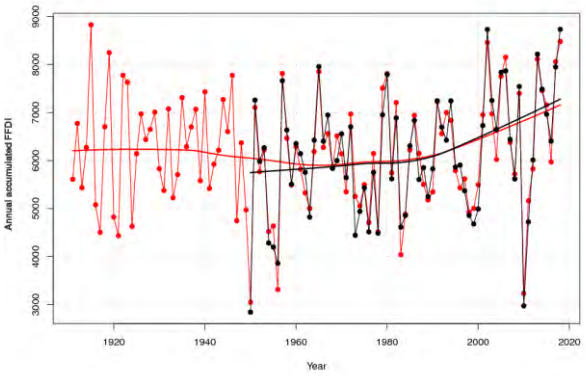

Wide Bay and Burnett

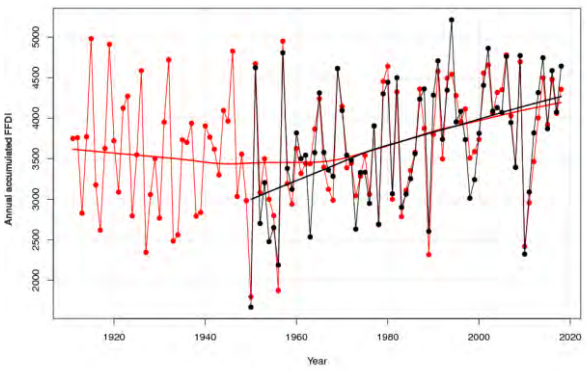

Central

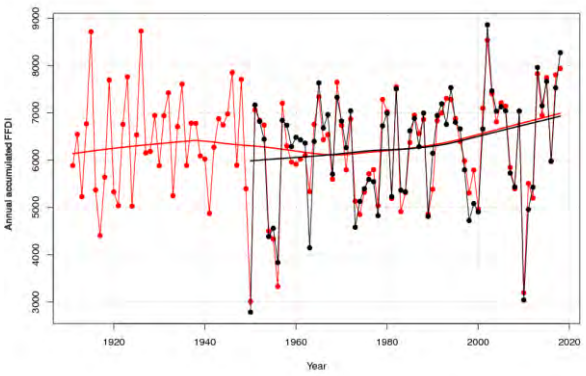

Central Coast

North West

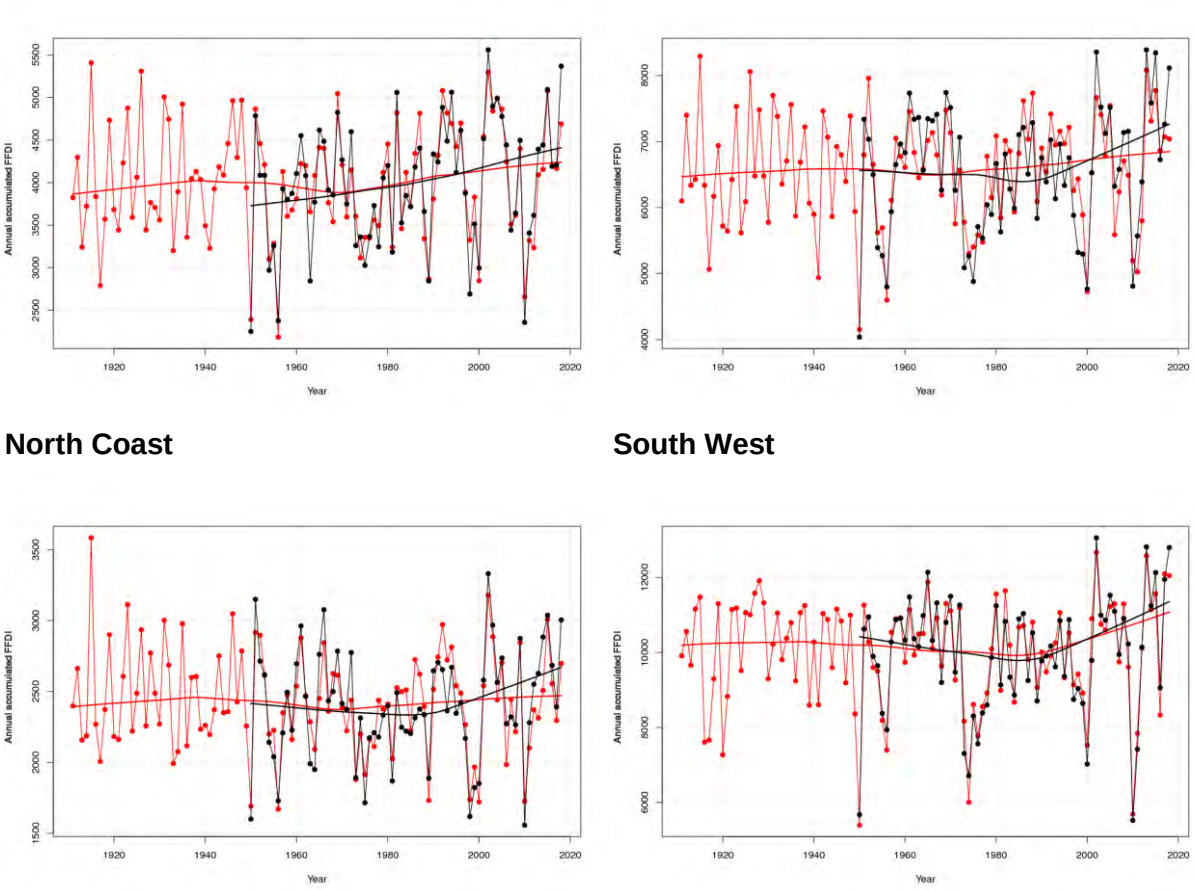

North Coast **South West**

Figure 37: Reconstruction of annual accumulated FFDI across the period 1911 to 2018 for Queensland and the nine subregions (red lines and dots), compared against the observed values across the period 1950 to 2018 (black lines and dots). *Lowess* regressions are superimposed for both time series. The observed data use a span parameter of 0.8, while the reconstructions use a span parameter of 0.8 × 69 / 108 (= 0.511) to match the temporal scale of the modelling to the different lengths of the two time series.

Figure 37 shows reconstructions of the annual accumulated FFDI averaged across Queensland and the nine subregions back to 1911 (red lines and dots), using annual rainfall, annual maximum temperature and annual drought factor as predictors in OLS linear regression models. The original observational data are also shown (black lines and dots). *Lowess* regressions of the two time series are also shown. As mentioned in the Data and Methods section, the span parameter used in the *lowess* modelling of the longer time series has been adjusted downwards to match the temporal implications of the span parameter choice used on the shorter time series.

At the Statewide level, the reconstruction is fairly good, and does not suggest an end effect which would lead to the trend-change to be over-estimated or under-estimated as a consequence of the dataset starting at 1950. The reconstruction suggests that the annual accumulated FFDI in the two decades prior to 1950 was comparable to that of the two decades subsequent to 1950, apart from the strong negative departures brought on by very wet conditions (e.g., in 1950). The reconstruction suggests that the annual accumulated FFDI was very high in 1915, but whether or not it was higher than the highest post-1950 value (that of 2002) remains a matter of conjecture. [1915 was a drought year across much of eastern Queensland, with widespread very-much-below-average (decile 1) rainfall.] Because the reconstructions do not involve the afternoon windspeed, there is an implicit assumption in the reconstruction process that the windspeed has not changed materially as far as the long-term trends in the annual accumulated FFDI is concerned.

In contrast, the *lowess* modellings of the reconstructions for the South East Coast and Wide Bay and Burnett subregions suggest that there is a substantial end effect to be taken into account when interpreting the trend changes in the observed dataset because it begins in 1950. As noted above, 1950 was a very wet year, and the 1950s generally a wet period. From about 1970 onwards, the *lowess* modellings of the reconstructions for these two subregions are in reasonably close agreement. The reconstructions get progressively worse moving up the east coast, with the Cape York Peninsula reconstruction being rather poor, and the North West reconstruction not much better, but the Central South, Central and South West reconstructions match the Statewide reconstruction for fidelity, although with slight concerns about end effects at the start of the data.

It is perhaps not surprising that this method of reconstruction is less successful in the smaller coastal subregions. If adverse fire-weather conditions arise through hot dry winds blowing off the continental interior, then the rainfall and drought factor conditions in upstream parts might be of comparable importance to the local conditions in ensuring a successful reconstruction.

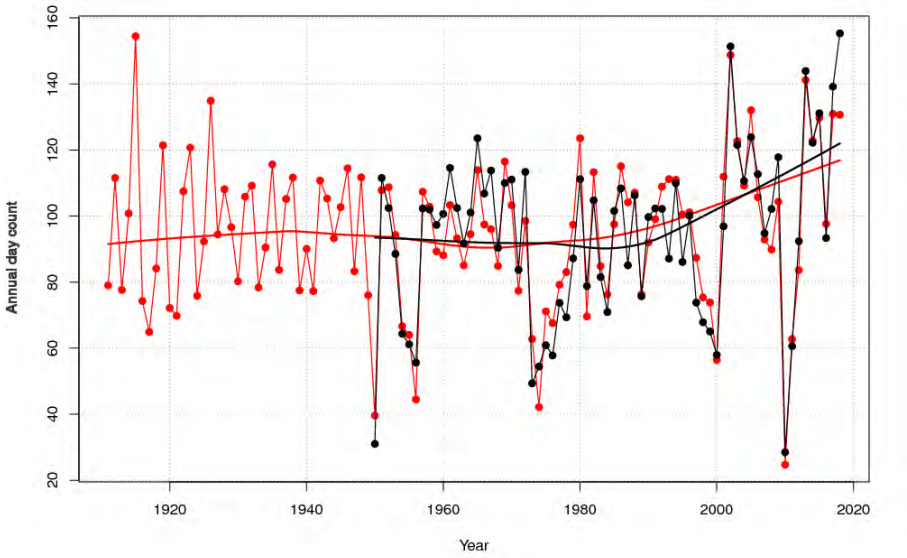

Figure 38: Reconstruction of annual FFDI ≥ 25 days across the period 1911 to 2018 for Queensland (red lines and dots), compared against the observed values across the period 1950 to 2018 (black lines and dots). *Lowess* regressions are superimposed for both time series, as per Figure 37.

Figure 38 shows the analogous reconstruction for annual FFDI ≥ 25 days averaged across Queensland (subregions not shown) for the period 1911 to 2018. As with the annual accumulated FFDI reconstruction above, there is little indication of an end effect in the trend modelling at the start of the observed dataset. Likewise, there is the suggestion that the incidence of FFDI ≥ 25 days in 1915 might have been comparable to the highest values seen in the 21st Century so far, but the reconstruction *does not* suggest a comparable frequency to the occurrence of such extreme years. Analogous reconstructions have not been attempted for the subregions, in part because the method used does not constrain the reconstruction to remain non-negative, something that is important for those subregions where FFDI ≥ 25 days are climatologically infrequent.

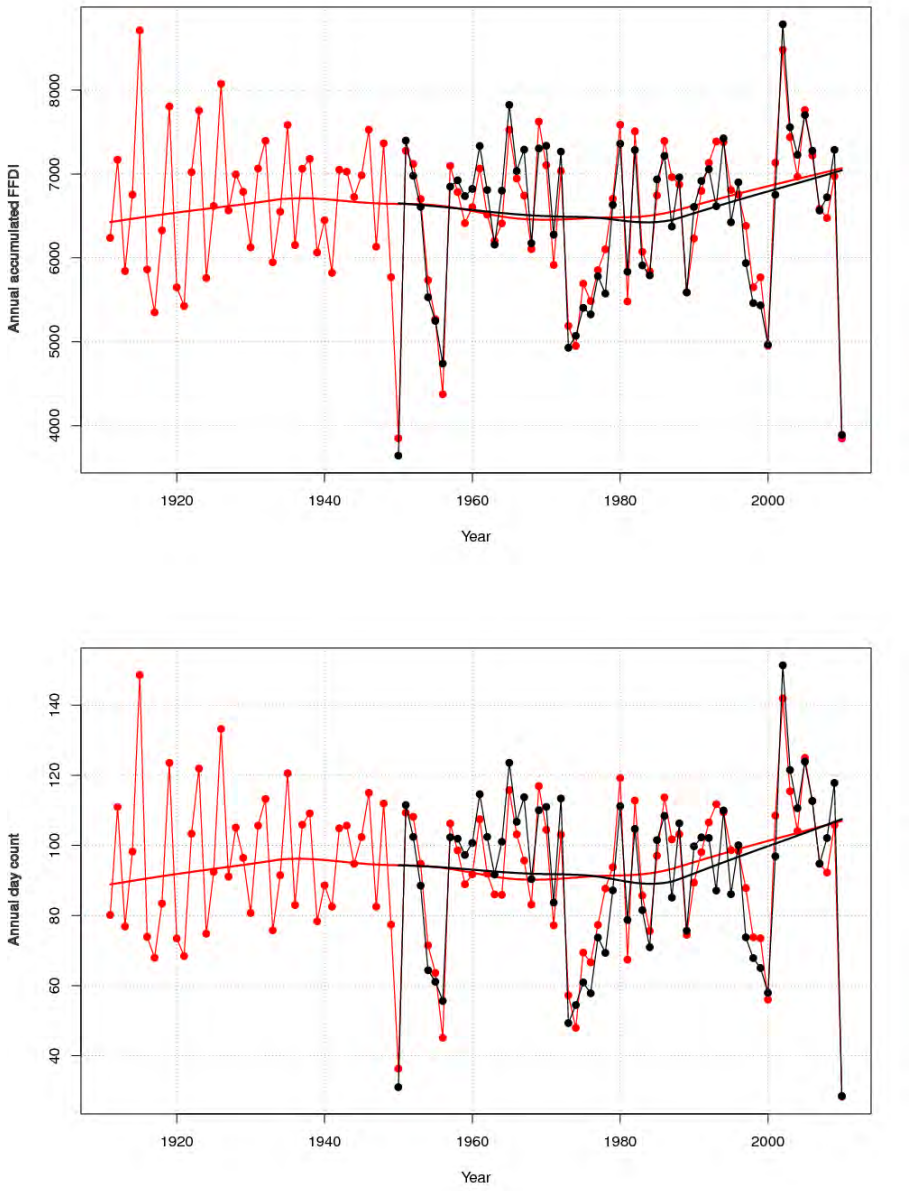

Figure 39: Reconstructions of annual accumulated FFDI (top) and annual FFDI ≥ 25 days (bottom) across the period 1911 to 2010 for Queensland (red lines and dots), compared against the observed values across the period 1950 to 2010 (black lines and dots). *Lowess* regressions are superimposed for both time series, as per Figure 37. These reconstructions additionally use ECMWF Reanalysis afternoon wind speeds.

Two additional reconstructions have been attempted for Statewide annual accumulated FFDI and annual FFDI ≥ 25 days across the period 1911 to 2010 (Figure 39). These

reconstructions differ from those shown above in Figures 37 and 38, in that they use an additional predictor, annually averaged afternoon (0600 UTC) wind speed obtained from the ECMWF 20th Century reanalyses. The reconstructions can however only proceed as far as 2010 because that is the extent of the reanalyses. Apart from the extra predictor (used linearly and potentially in cross terms with the other predictors) and the eight fewer years, the reconstruction methodology is the same as that used above. A minor point to be noted is that the NCEP wind reanalyses have been subjected to a bias-correction procedure (see Dowdy (2018) for details) prior to their use in the construction of the FFDI dataset, where as the ECMWF reanalyses have not been so adjusted, but the lack of such an adjustment will to some extent be taken care of in the reconstruction process. The inclusion of the afternoon wind speed in the reconstructions improves the modelling to a minor extent, as evidenced by the better matching of the *lowess regressions*, but the broad conclusions are not much changed.

Expansion of the Fire-weather Season

In those subregions where there is a clear distinction between the active fire-weather season and in the inactive fire-weather season, a line of enquiry is available to assess the expansion of the fire-weather season (i.e., whether the fire-weather season is expanding or contracting). This approach involves calculating the first and last days of the FFDI being above suitable thresholds somewhere in the region or subregion in every fire-weather season in the study period. By doing so, extensions to the length of the fire-weather season (including advances of the onset), can be tracked. This approach only works for thresholds that are always attained, but more importantly requires a clean break from one fire-weather season to the next. Such a clean break is not obtained in all parts of Queensland: in some parts of the State, the fire-weather season is effectively an all-year-round proposition. In those subregions of Queensland where the length of the fire-weather season can be assessed in this manner, results will be presented in the Regional Fact Sheets section.

Figure 40 shows the time series of the day index of the earliest occurrence of FFDI > 80 somewhere in Queensland for the June to May fire-weather years from 1950/1951 to 2017/2018. The first occurrence of FFDI > 80 somewhere in Queensland is now arriving around 26 days earlier at the end of the study period than at the beginning of the study period. The threshold of 80 FFDI points is chosen for this calculation because this threshold is exceeded somewhere in Queensland in every year of the dataset, whereas the threshold of 90 FFDI points is not so exceeded. The fire-weather year is chosen to start in June for this calculation because of the results shown in Figure 13. Figure 40 shows that only in one year (2002) in the dataset has an FFDI > 80 been observed as early as June. This advancing of the onset of elevated (FFDI > 80) fire-weather conditions somewhere in Queensland should be treated with some caution, as a comparison with Figure J5 reveals that in most years the first occurrence of FFDI > 80 somewhere in Queensland is actually occurring somewhere in the South West subregion, and that the result shown in Figure 40 is mostly reflective of what is happening in the South West subregion because that subregion climatologically speaking has fire weather more extreme than much of the rest of the State. [It should also be noted that the South West subregion does not contain significant amounts of actual forest, although this result is likely to have implications for changes in grass-fire-weather conditions, which have not been studied here.] The interannual variability in this index is not particularly large, although extreme variations are intermittently possible, as in the El Niño year of 2002

(Fawcett and Trewin 2003, Jones 2003) where the first occurrence came very early and in the La Niña year of 2010 (Ganter 2011) where the first occurrence came very late.

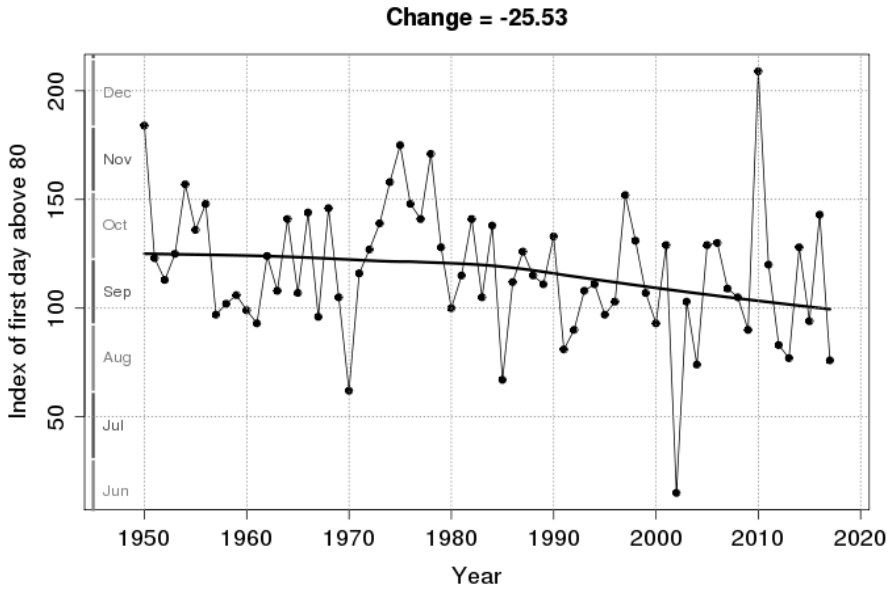

Figure 40: Time series of the index of the earliest FFDI > 80 day for Queensland (June-to-May years 1950/1951-2017/2018). The earliest FFDI > 80 day is now arriving around 26 days earlier. This graph is also shown in the Regional Fact Sheets section as Figure A5.

Figure 41 shows the corresponding calculation for the last FFDI > 80 day somewhere in Queensland for the June-to-May fire-weather year. The last FFDI > 80 day somewhere in Queensland is now arriving around 12 days later. [Together these two results imply an expansion at this level of intensity of the fire-weather season of around 38 days, or more than one month's worth.] Here also, a comparison with Figure J6 indicates that the results shown in Figure 41 are mostly indicative of what is happening in the South West subregion, for the same climatological reason.

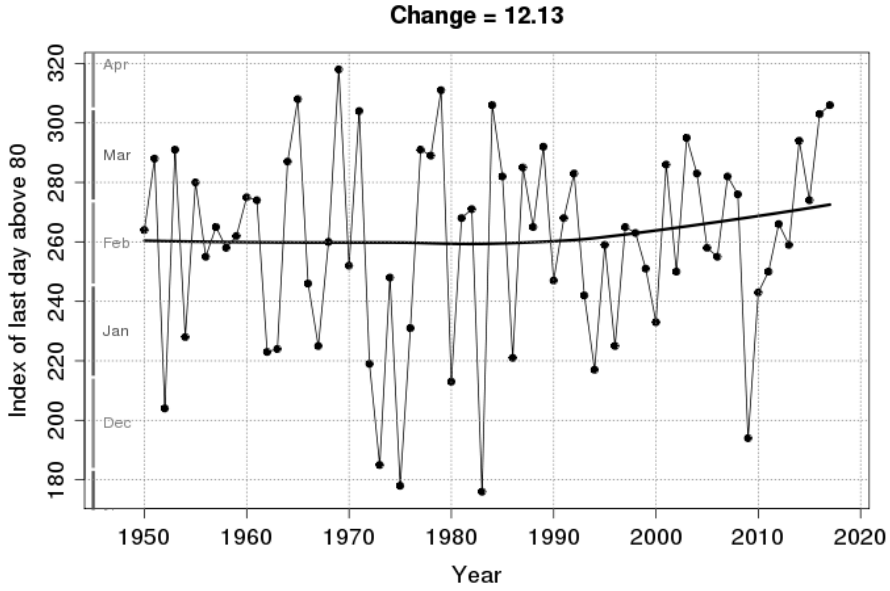

Figure 41: Time series of the index of the latest FFDI > 80 day for Queensland (June-to-May years 1950/1951-2017/2018). The latest FFDI > 80 day is now arriving around 12 days later. This graph is also shown in the Regional Fact Sheets section as Figure A6.

Since this primary approach cannot be used in all nine subregions, nor can it be used across a wide range of FFDI thresholds, a secondary approach is also pursued. Figure 42 shows Hovmöller plots of the monthly FFDI ≥ 25 day counts for each subregion. In these plots, the year is shown on the vertical axis from 1950 (bottom) to 2018 (top), while the month of the year is shown on the horizontal axis (January through to December, with January being repeated after December so as not to truncate the results). In the plots on the left-hand side of the figure, the Hovmöller plots of the actual data are shown. These are typically quite noisy, as fire weather in Queensland is highly variable from year to year. In the plots on the right-hand side of the figure, an OLS linear regression trend is calculated for each of the twelve calendar months of the year separately, and the Hovmöller plot of those linear trends shown, to give a clearer representation of the emerging trends. These linear trends are plotted on the same scale as the raw data.

Queensland

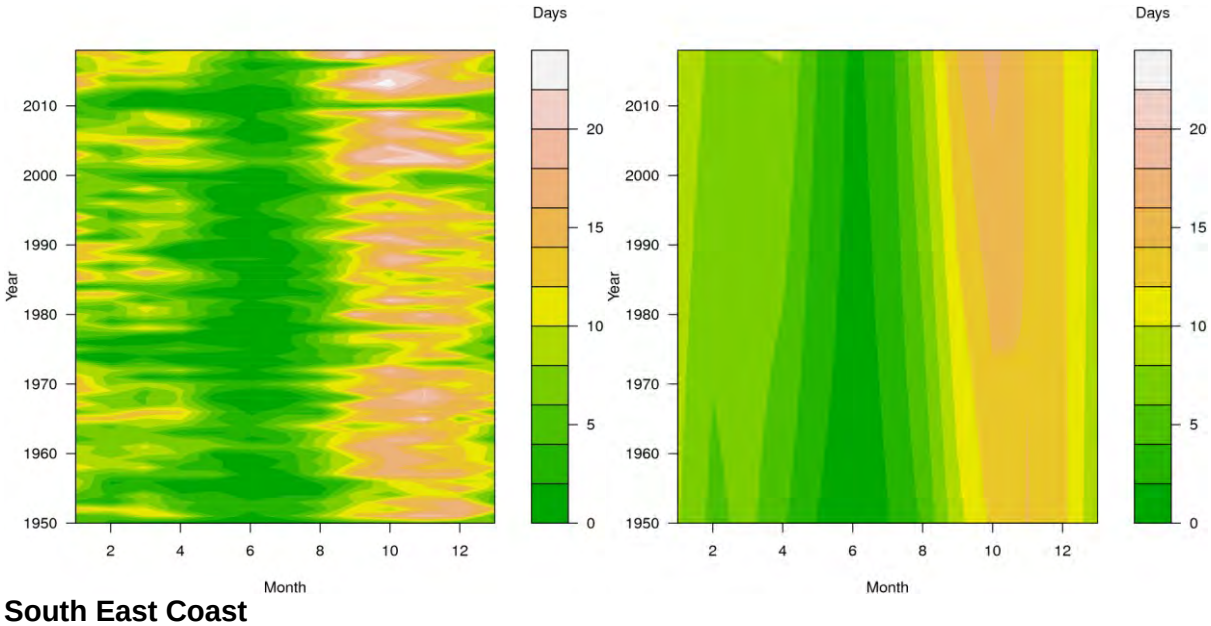

South East Coast

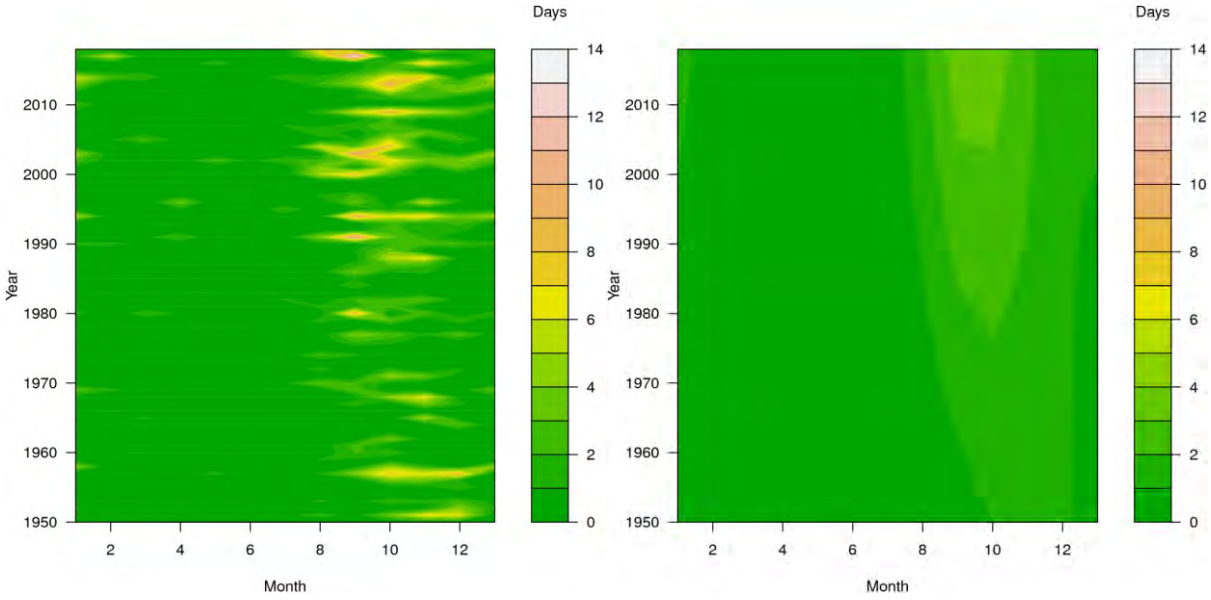

Wide Bay and Burnett

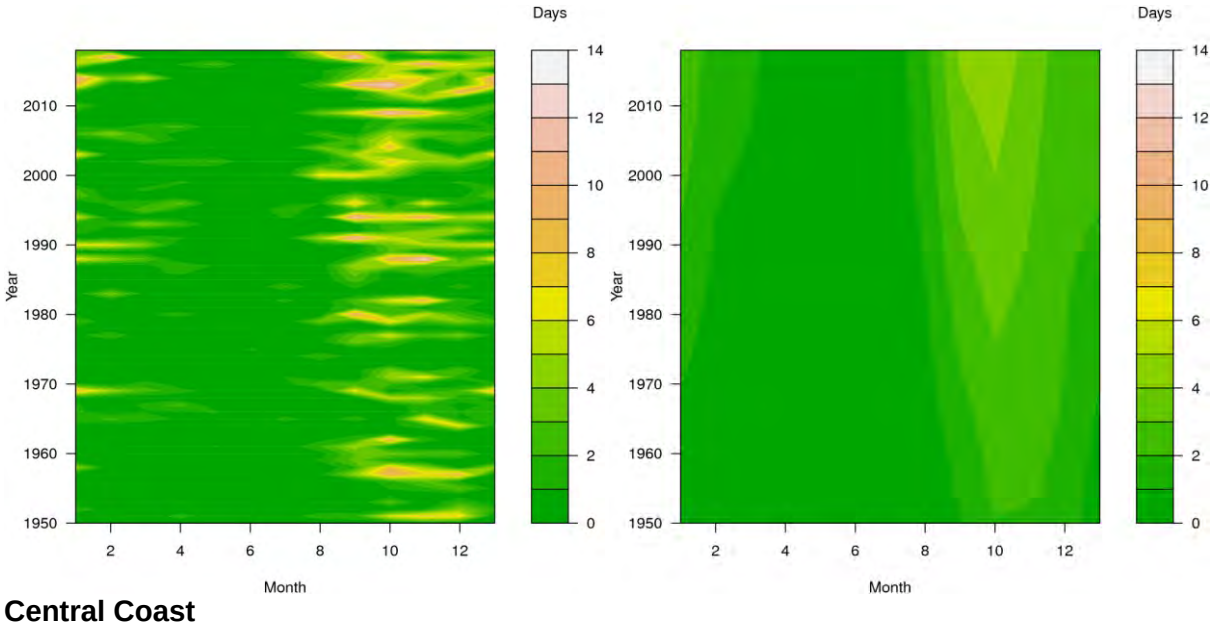

Central Coast

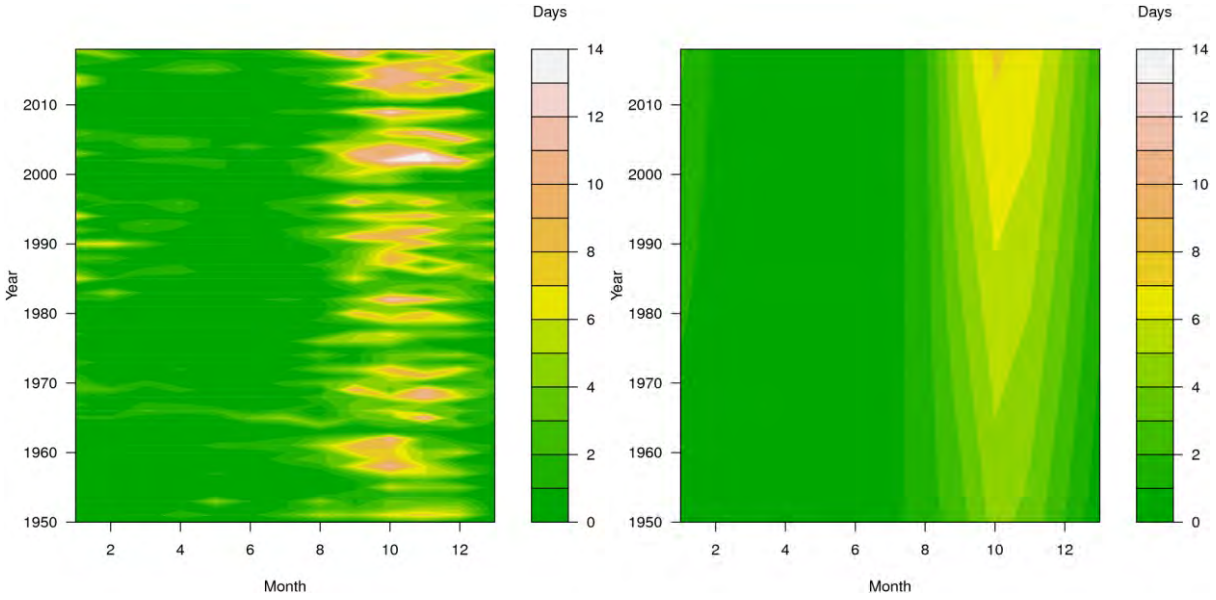

North Coast

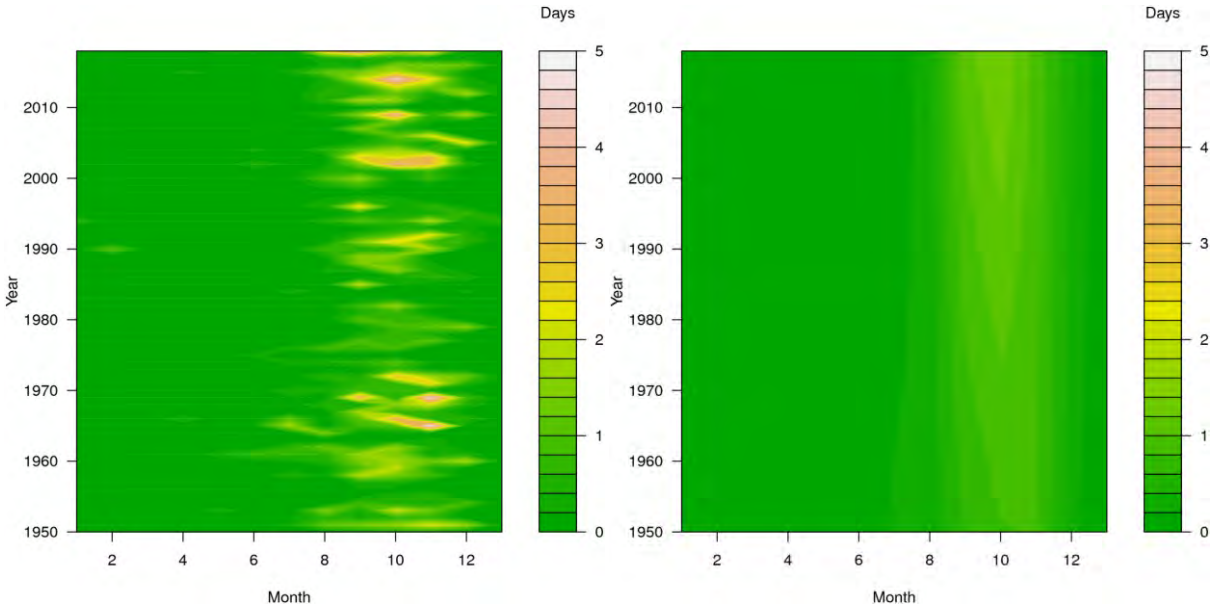

Cape York Peninsula

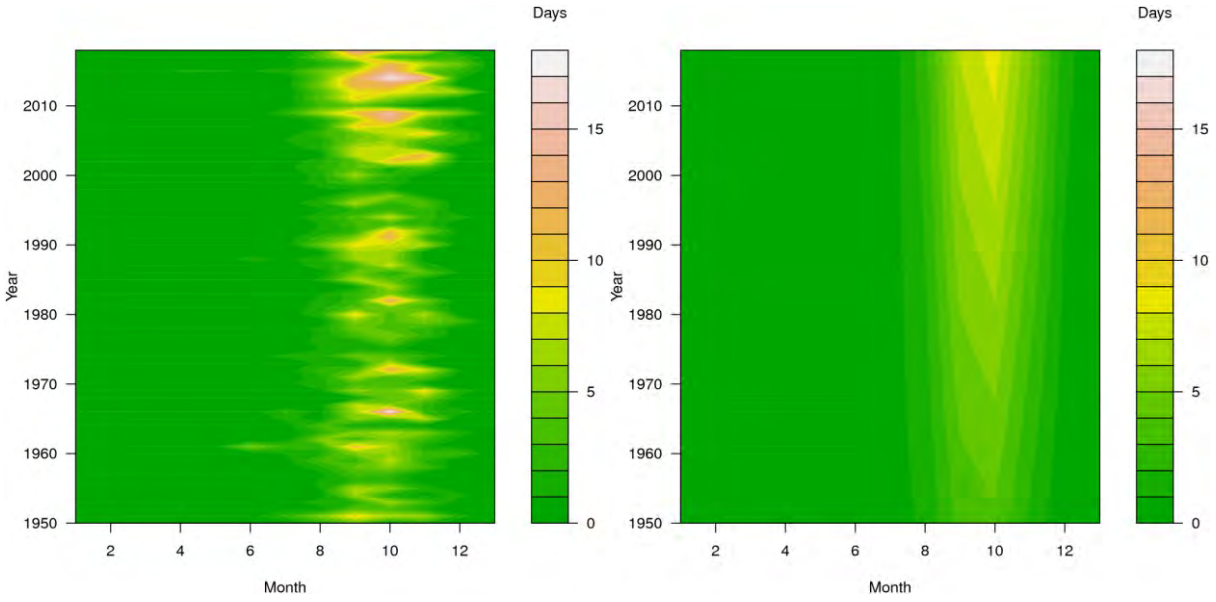

Central South

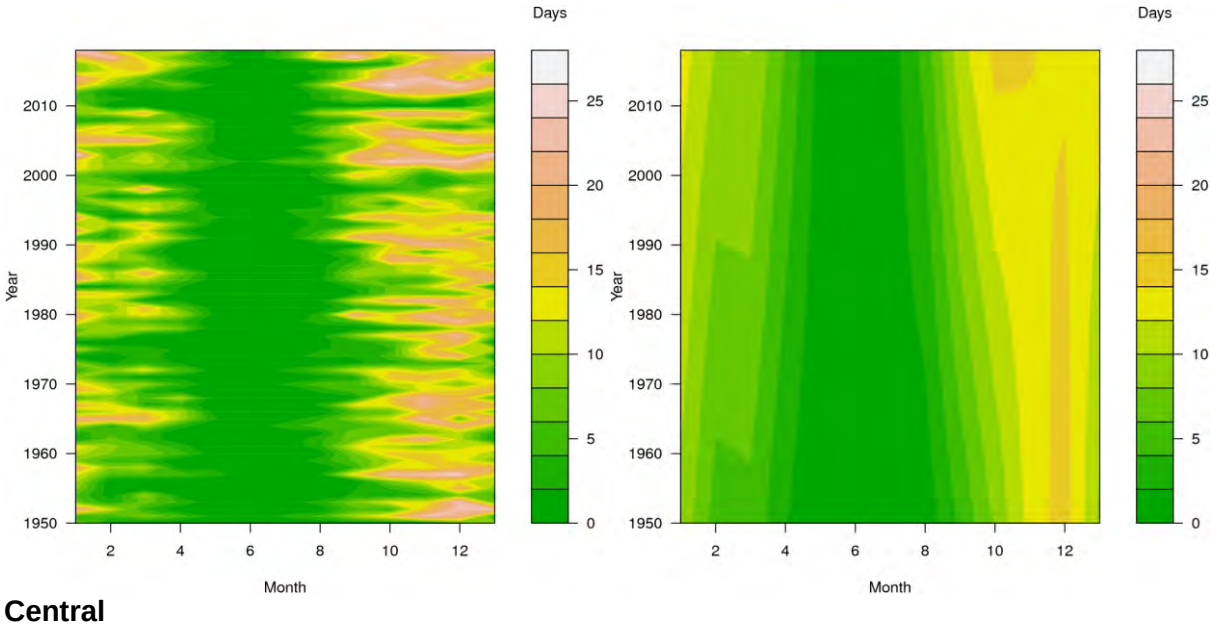

Central

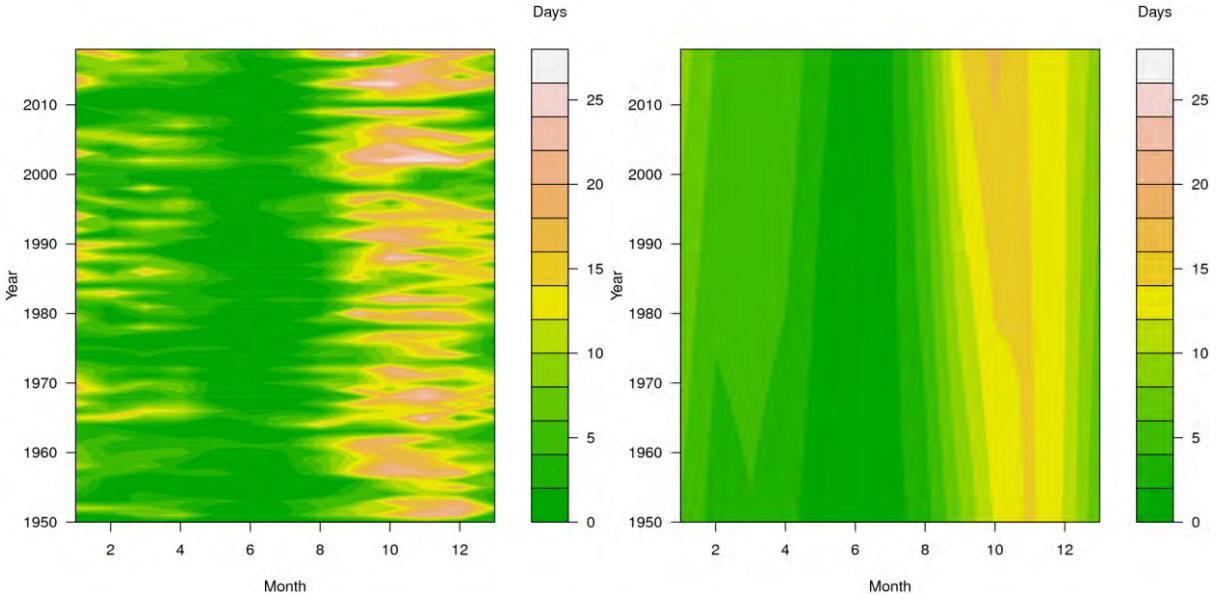

North West

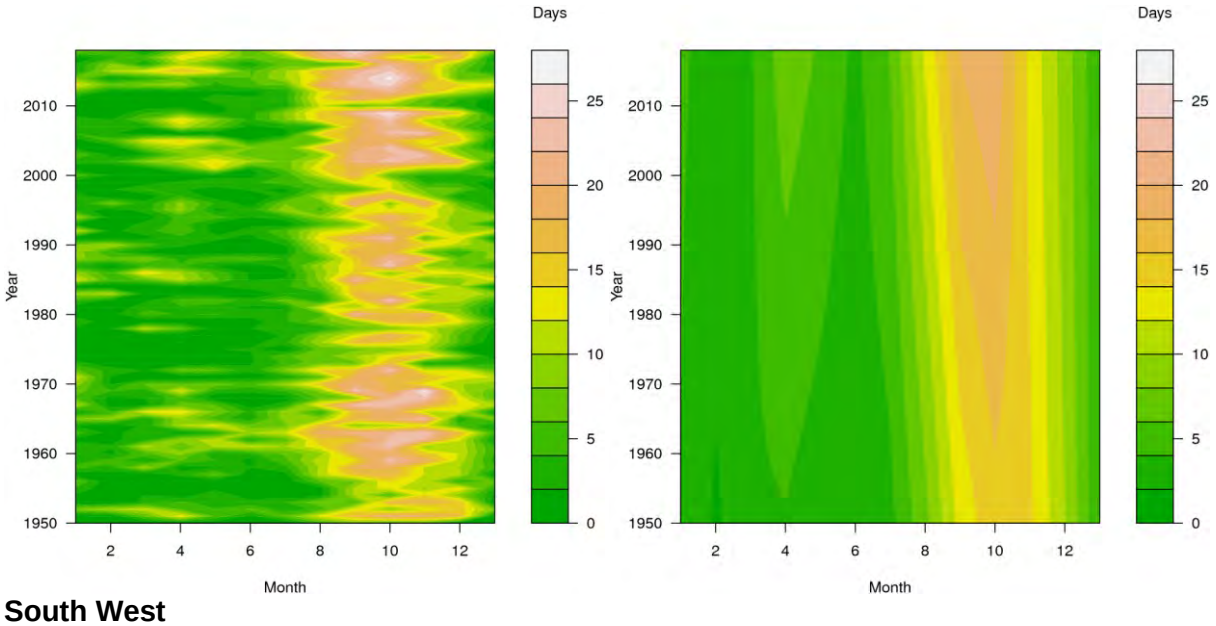

South West

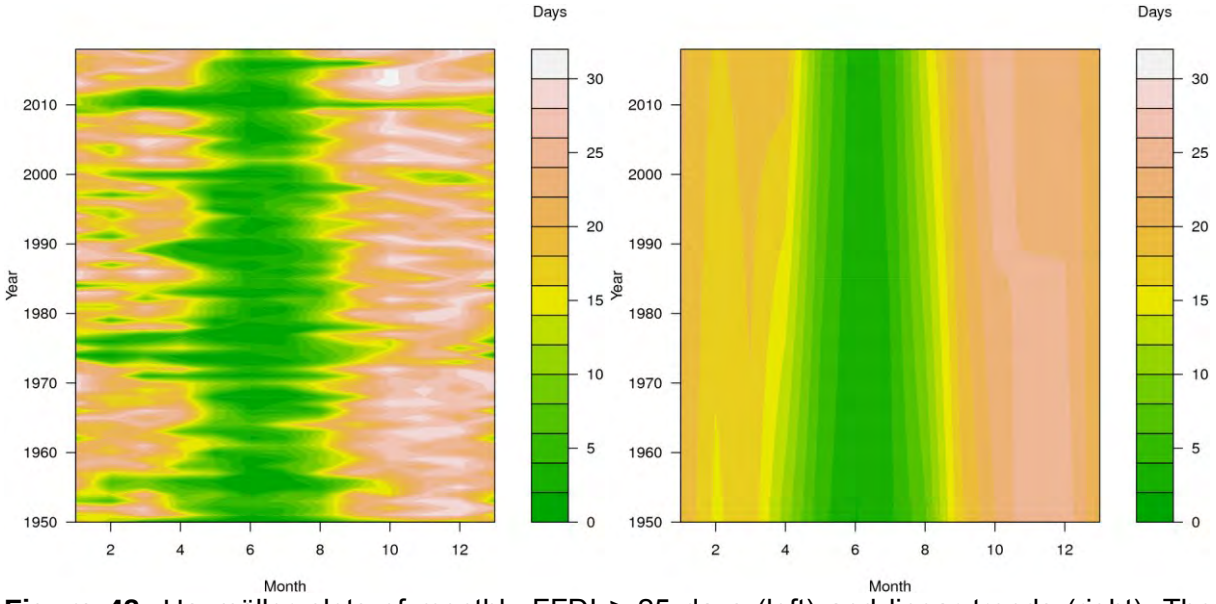

Figure 42: Hovmöller plots of monthly FFDI ≥ 25 days (left) and linear trends (right). The January values are repeated on the right to complete the annual cycle in the plotting. The contouring is of FFDI ≥ 25 days per month. Note that the contouring is specific to each subregion, and varies from subregion to subregion. In two subregions, the South East Coast and Cape York Peninsula subregions, the linear regressions on the monthly time series occasionally go negative. Such negative values are unphysical, and are caused in the linear regressions by the original data having low magnitude. Accordingly, such negative values are set to zero in the Hovmöller plots.

For the State as a whole, the narrowing of the green bands (proceeding from bottom to top) suggests that the length of the inactive part of the fire-weather season (characterised as those months having very few FFDI ≥ 25 days) is shortening, while the widening of the orange/beige bands (again proceeding from bottom to top) suggests that the length of the active part of the fire-weather season (characterised by having the most FFDI ≥ 25 days in the months) is lengthening. Further, the slope of the yellow bands suggests that the lengthening of the active part of the fire-weather season is more due to the onset advancing (arriving earlier) more than changes at the other end of the active part of the season.

In all five east coastal subregions, the occurrence of fire-weather conditions is sporadic, although mainly confined to the second half of the year, and it is difficult to say much more than that the occurrence of FFDI ≥ 25 days has increased over time. In the four western subregions, the picture is a little clearer. The onset of the active part of the fire-weather season is generally advancing (arriving earlier). In the Central South and South West subregions, there are indications that the cessation of the active part of the fire-weather season is delaying (arriving later). In the North West subregion, the picture is complicated by an out-of-season increase in fire-weather activity around April.

Figure 43 shows the analogous results for FFDI ≥ 50 days, for selected subregions. This higher threshold is infrequently seen in the cooler and wetter subregions, and so results are not shown for those subregions. The Statewide results indicate a broadening of the part of the year where FFDI ≥ 50 days occur, with them becoming less concentrated in December over time. A similar broadening can be seen in the Central South subregion. In the Central subregion, it is more that they are arriving earlier.

Queensland

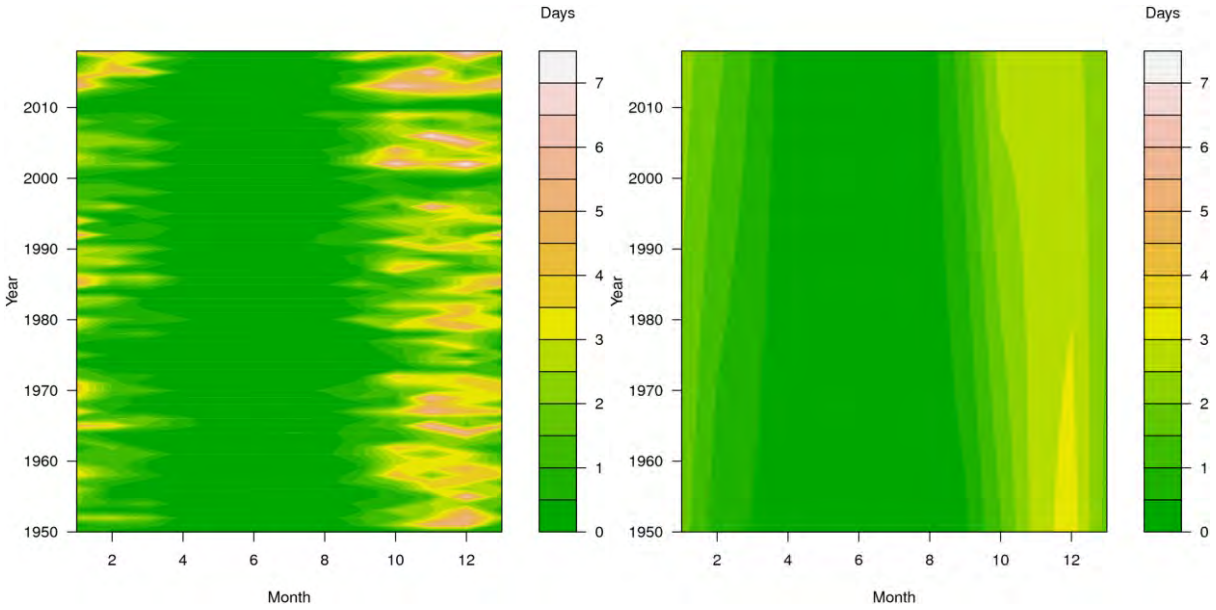

Central South

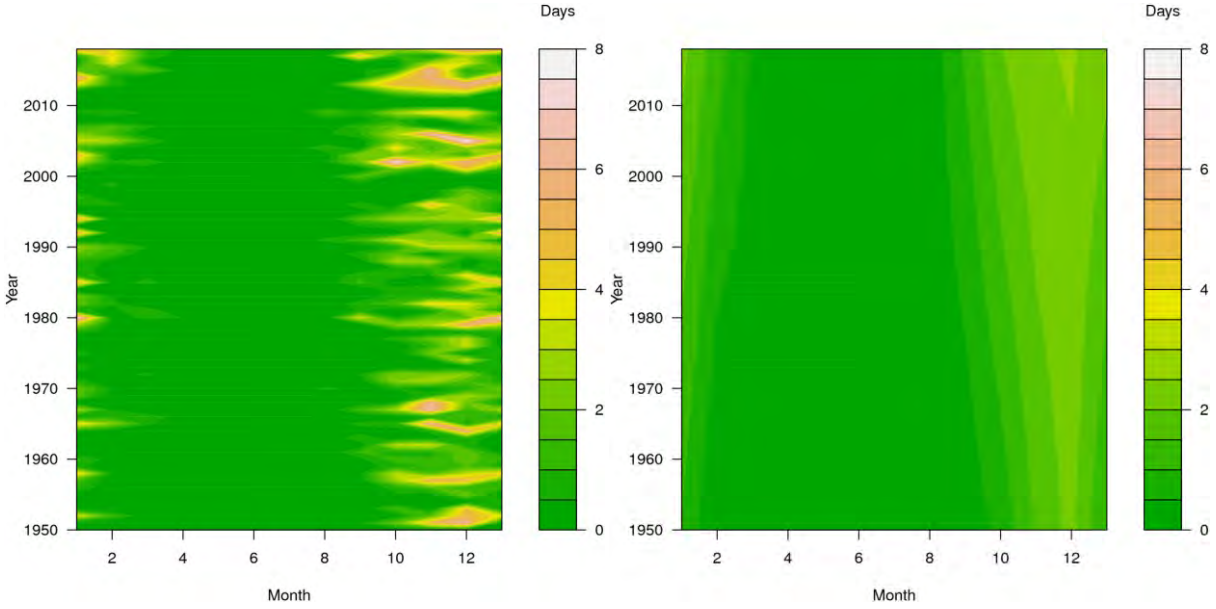

Central

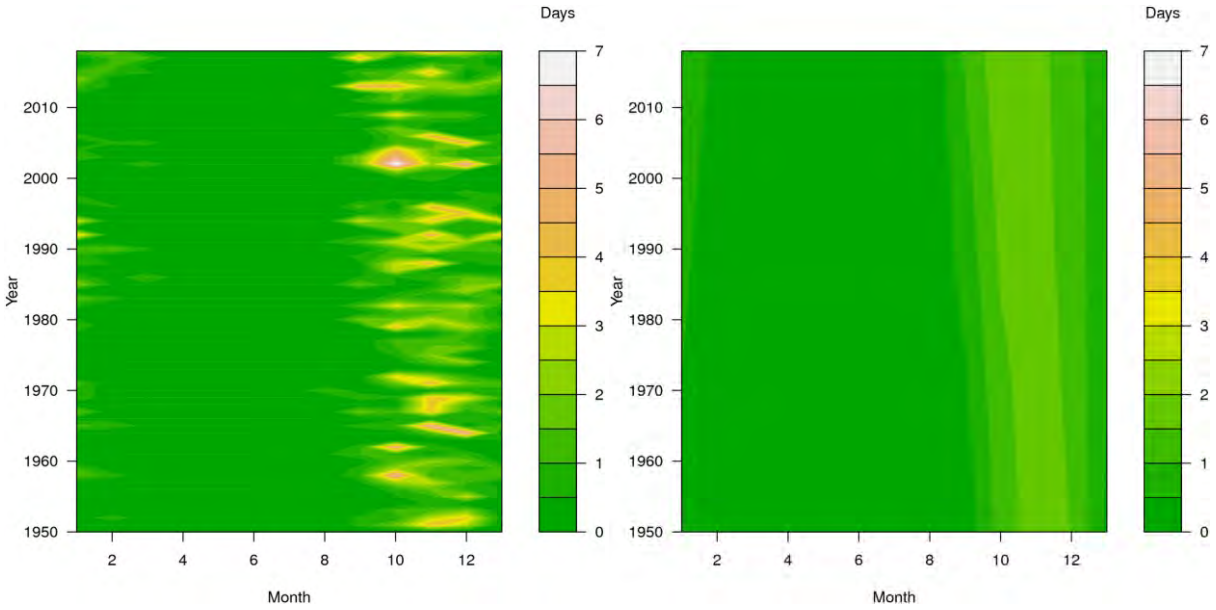

North West

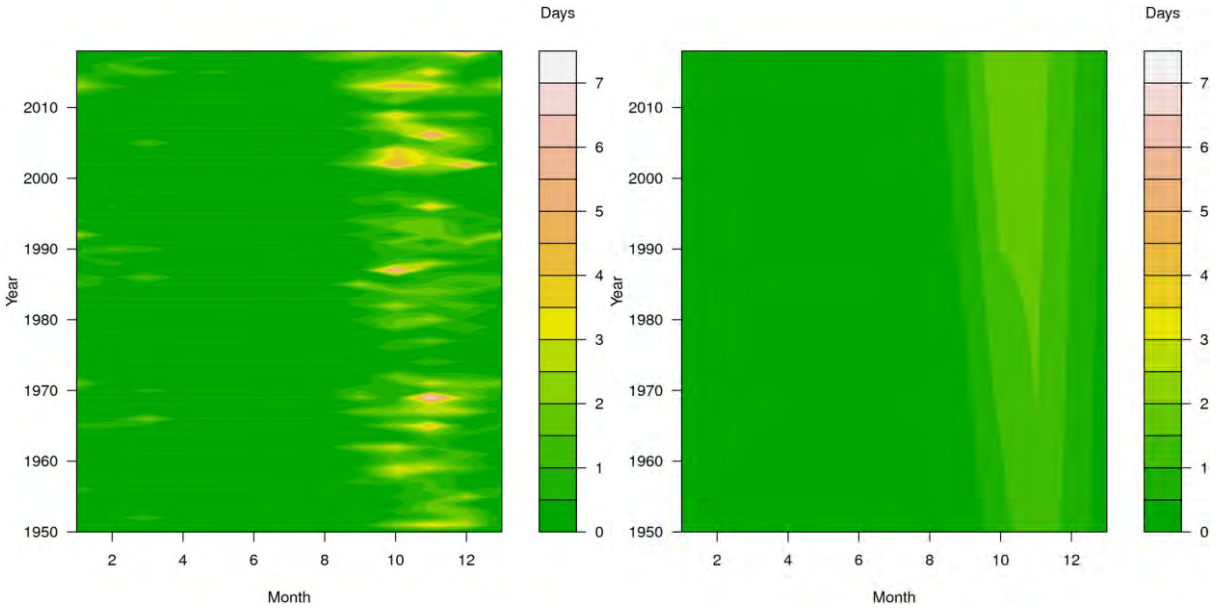

South West

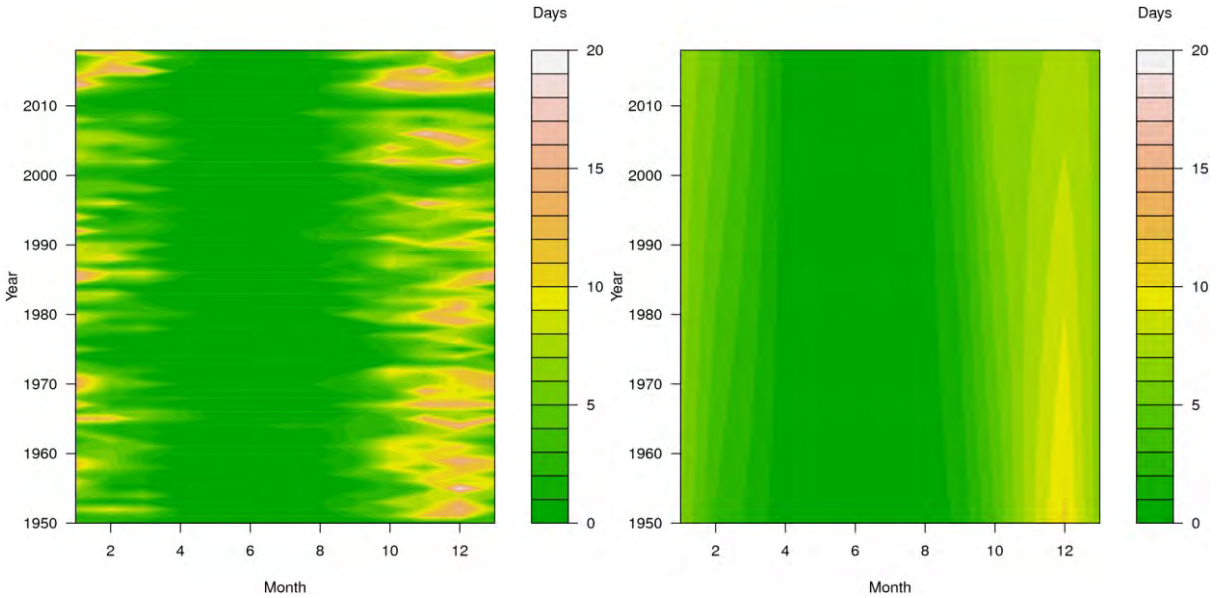

Figure 43: Hovmöller plots of monthly FFDI ≥ 50 days (left) and linear trends (right). The January values are repeated on the right to complete the annual cycle in the plotting. The contouring is of FFDI ≥ 50 days per month. Note that the contouring is specific to each subregion, and varies from subregion to subregion. In three subregions, the Central South, Central and North West subregions, the linear regressions on the monthly time series occasionally go negative. Such negative values are unphysical, and are caused in the linear regressions by the original data having low magnitude. Accordingly, such negative values are set to zero in the Hovmöller plots.

This approach to looking at the data can be applied to the ingredients in the FFDI calculation. Figure 44 shows Hovmöller plots of monthly averages of the daily afternoon windspeeds used in the FFDI calculation, together with the linear trends in those monthly averages. At the Statewide level, peak windiness occurs during the Spring months, with a decline in the Spring intensity across the study period. A decline is also seen in the Winter intensity. In the South East Coast subregion, Winter afternoon wind speed has decreased over time, but Spring afternoon wind speed has increased. The decline in Winter afternoon wind speed is also seen in the Wide Bay and Burnett subregion. In the North Coast, Central South and Central subregions, Spring afternoon wind speed has decreased.

Queensland

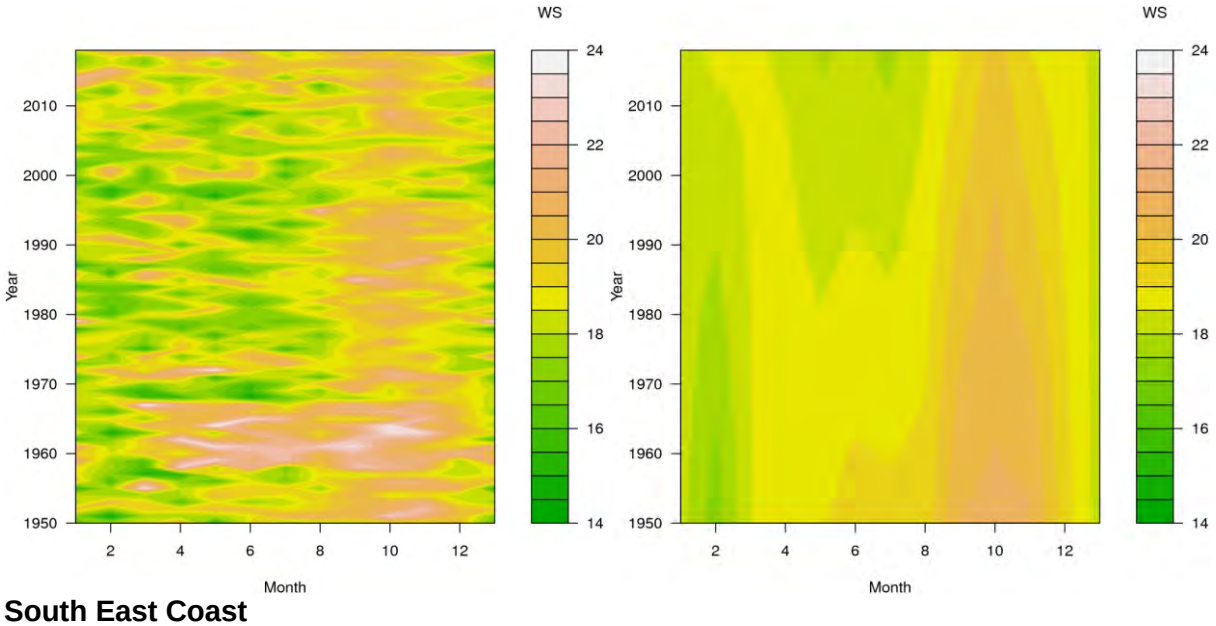

South East Coast

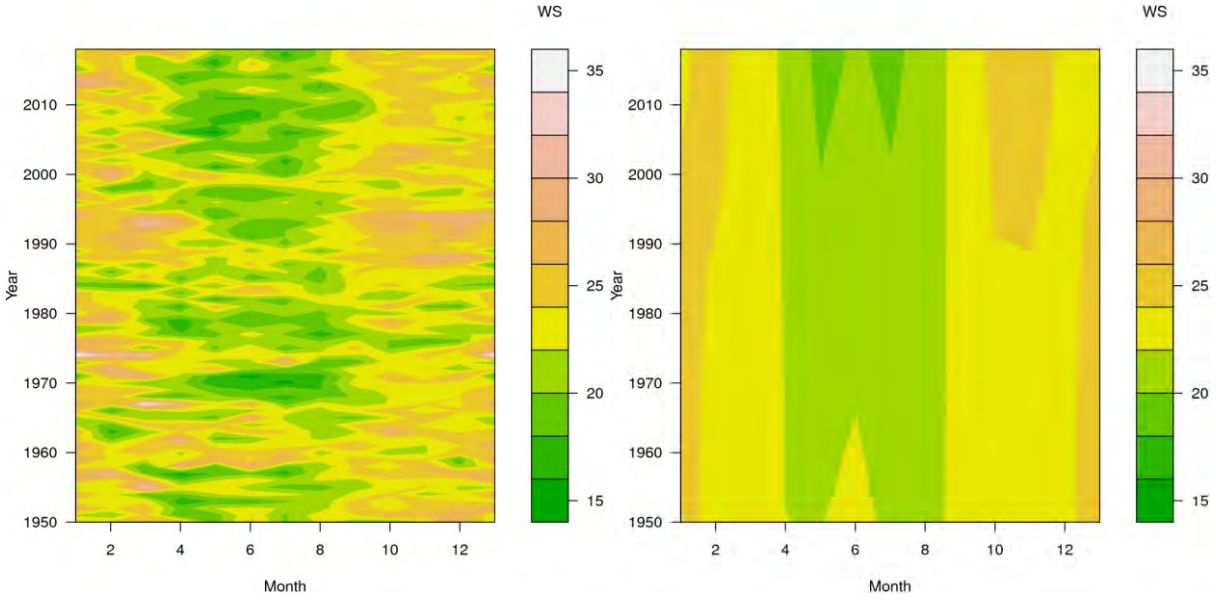

Wide Bay and Burnett

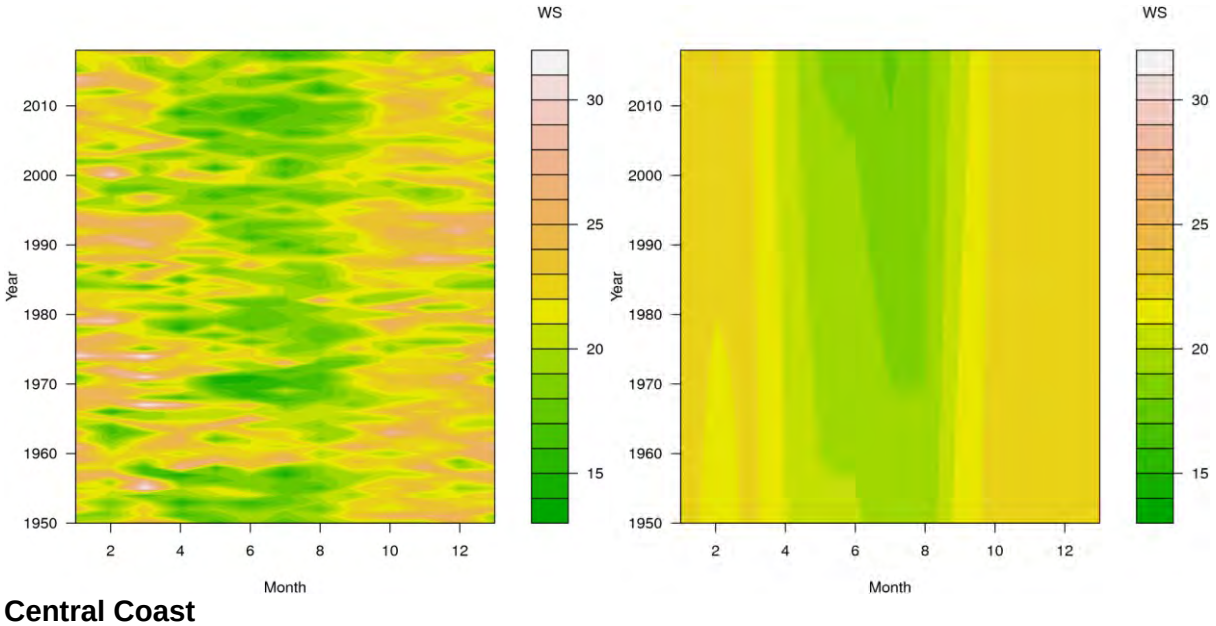

Central Coast

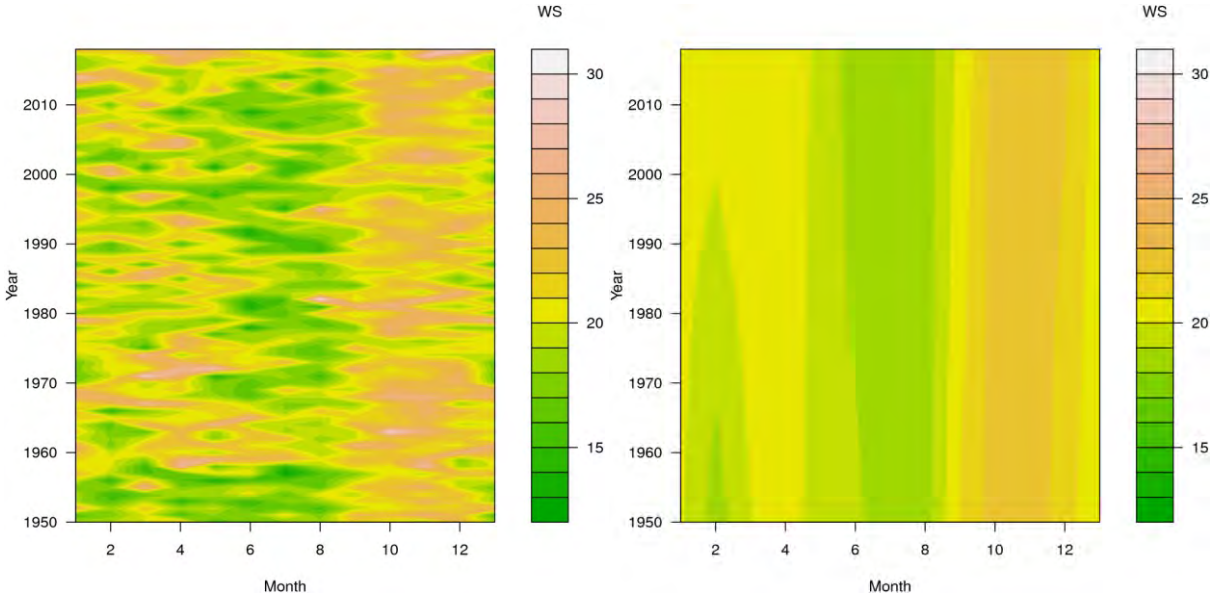

North Coast

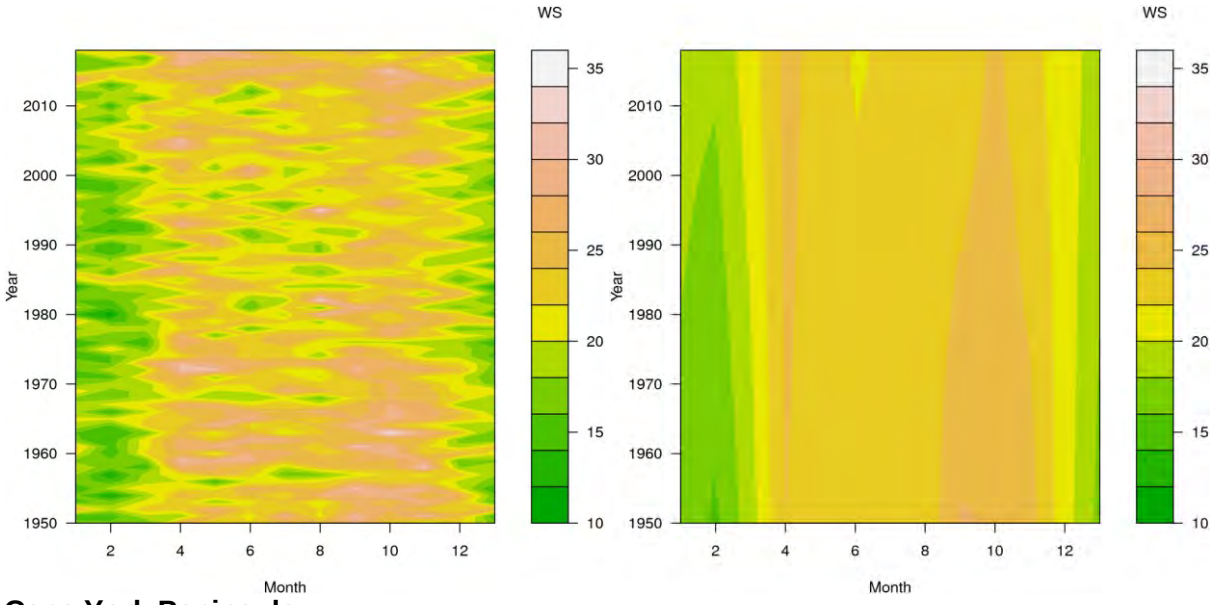

Cape York Peninsula

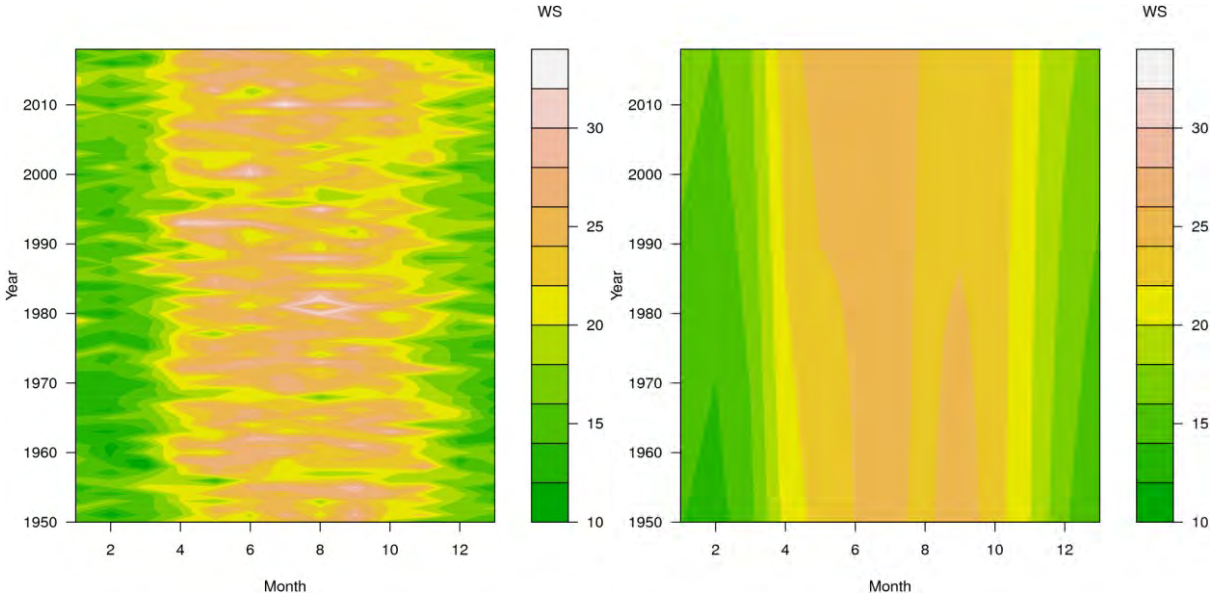

Central South

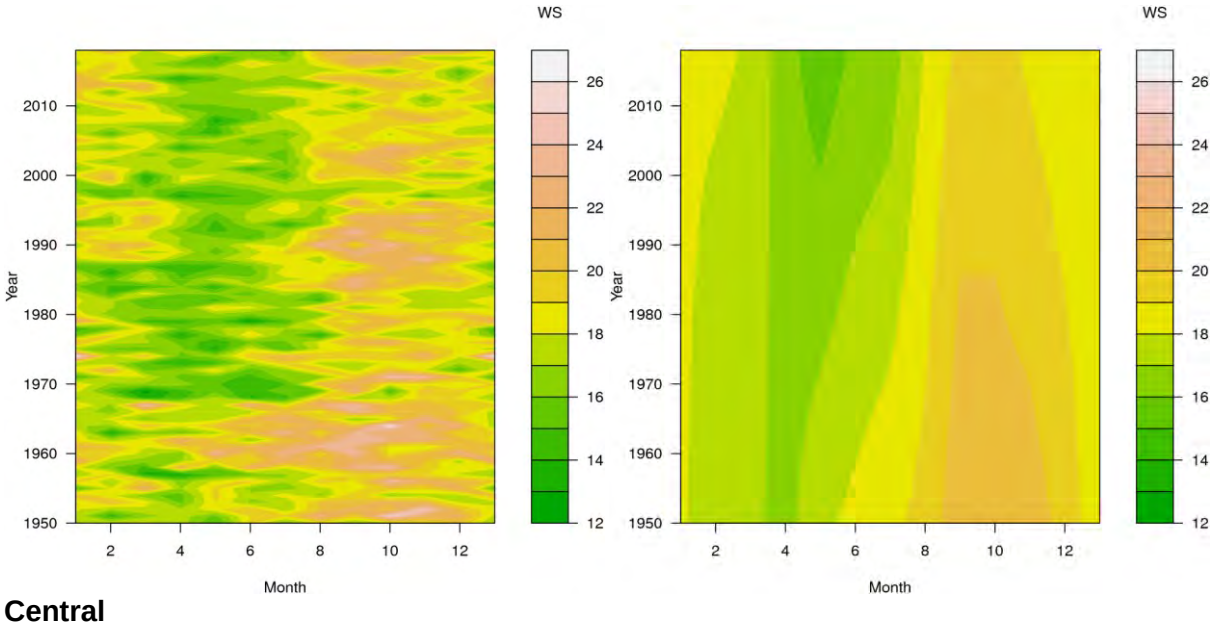

Central

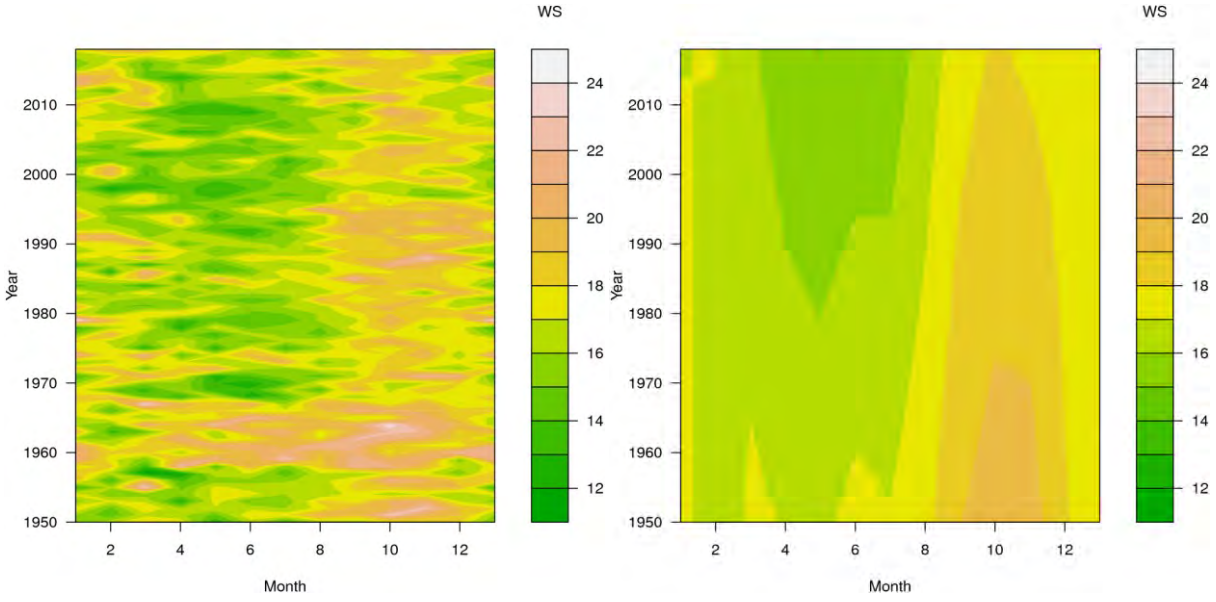

North West

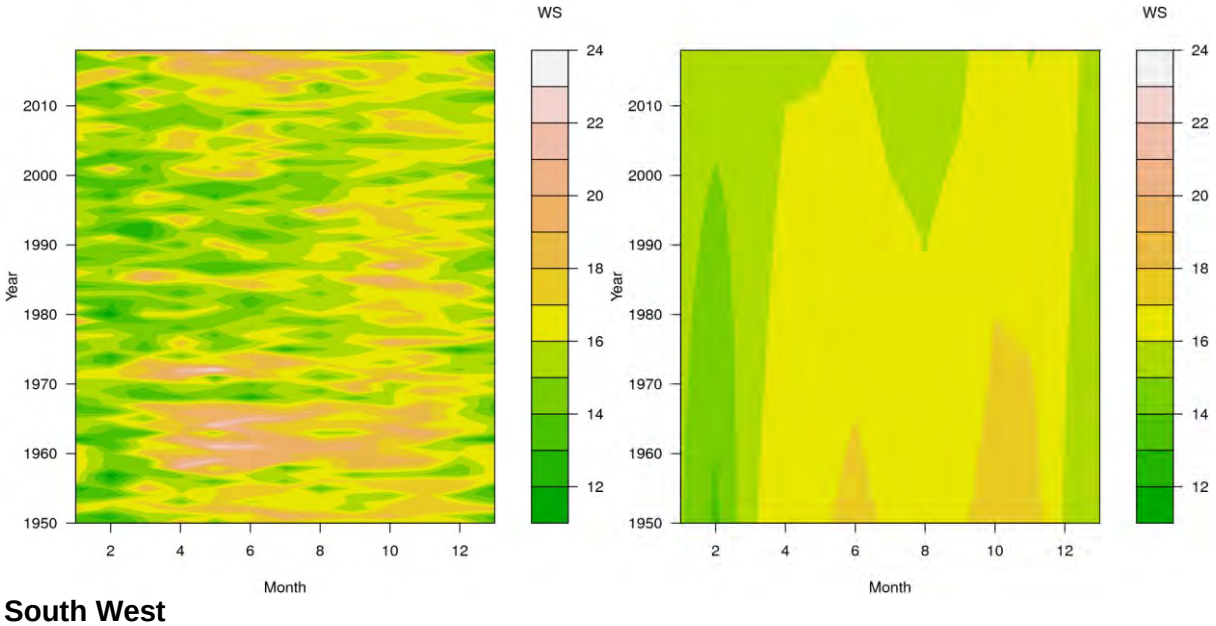

South West

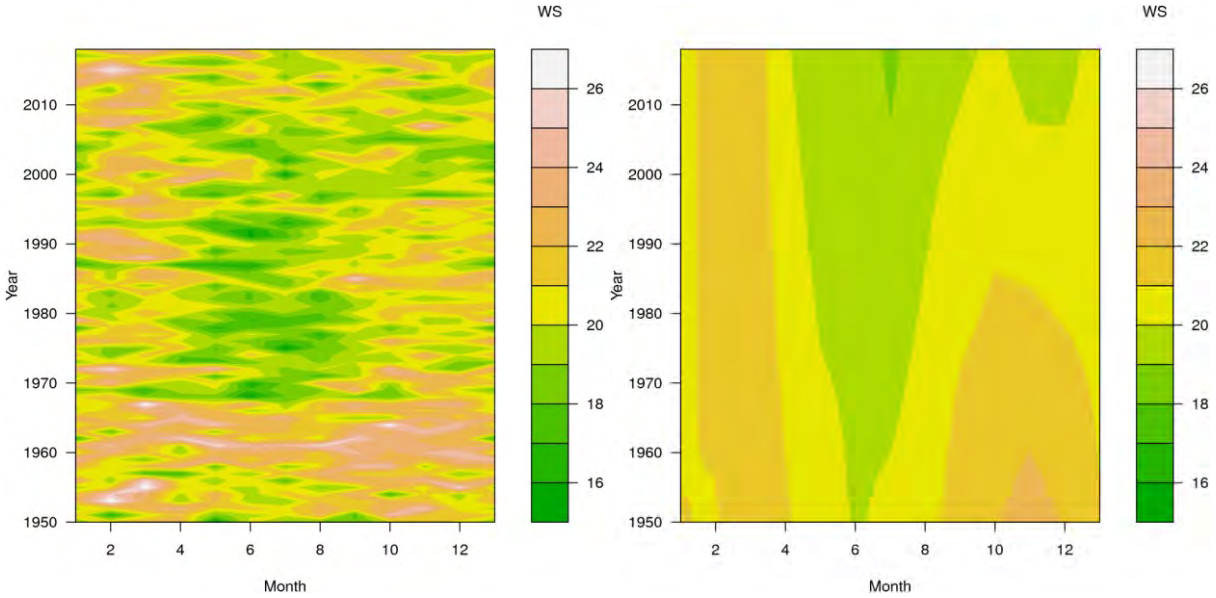

Figure 44: Hovmöller plots of monthly afternoon windspeeds (in km/h) (left) and linear trends (right). The January values are repeated on the right to complete the annual cycle in the plotting. Note that the contouring is specific to each subregion, and varies from subregion to subregion.

Figure 45 shows Hovmöller plots of monthly averages of the daily afternoon relative humidity used in the FFDI calculation, together with linear trends in those monthly averages. At the State level, the afternoon relative humidity is lowest in the Spring months, and the trend has been towards lower Spring afternoon relative humidity. A similar trend is seen in all the east-coast subregions, apart from it being slightly earlier (August - October, rather than

September - November) in some of them. In the Central South and South West subregions, the decline in June afternoon relative humidity is particularly evident.

Queensland

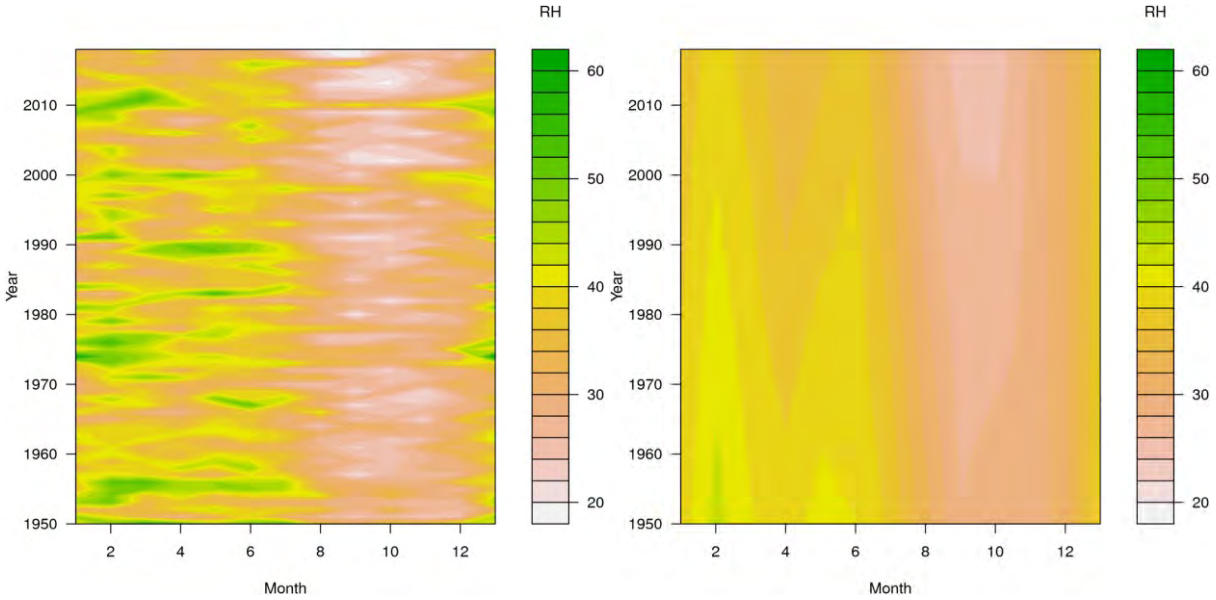

South East Coast

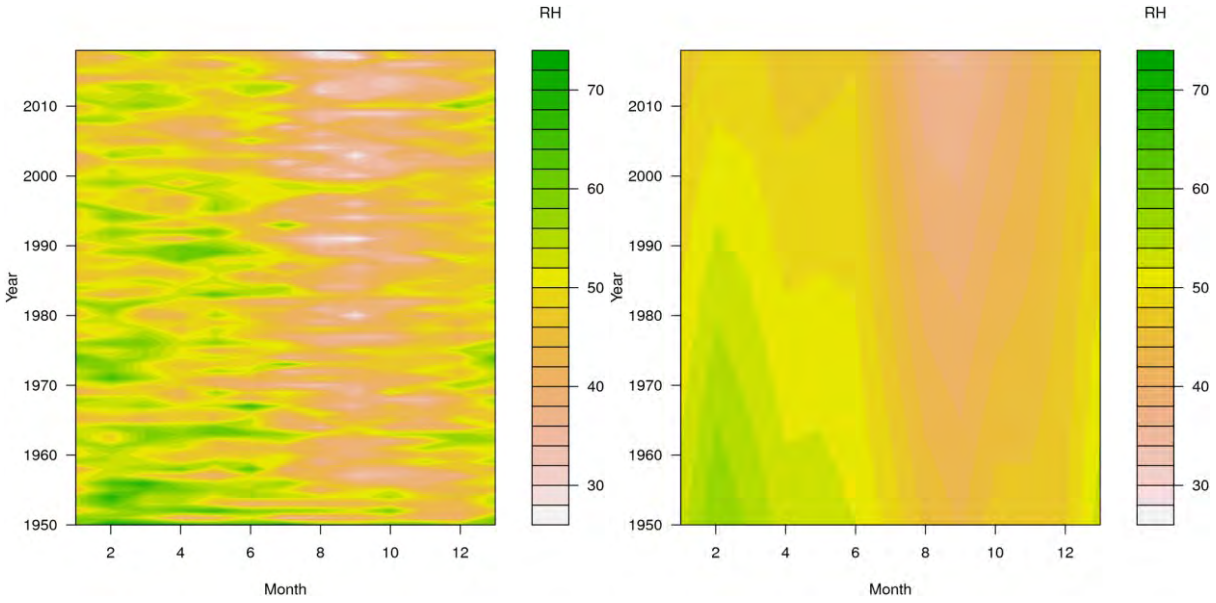

Wide Bay and Burnett

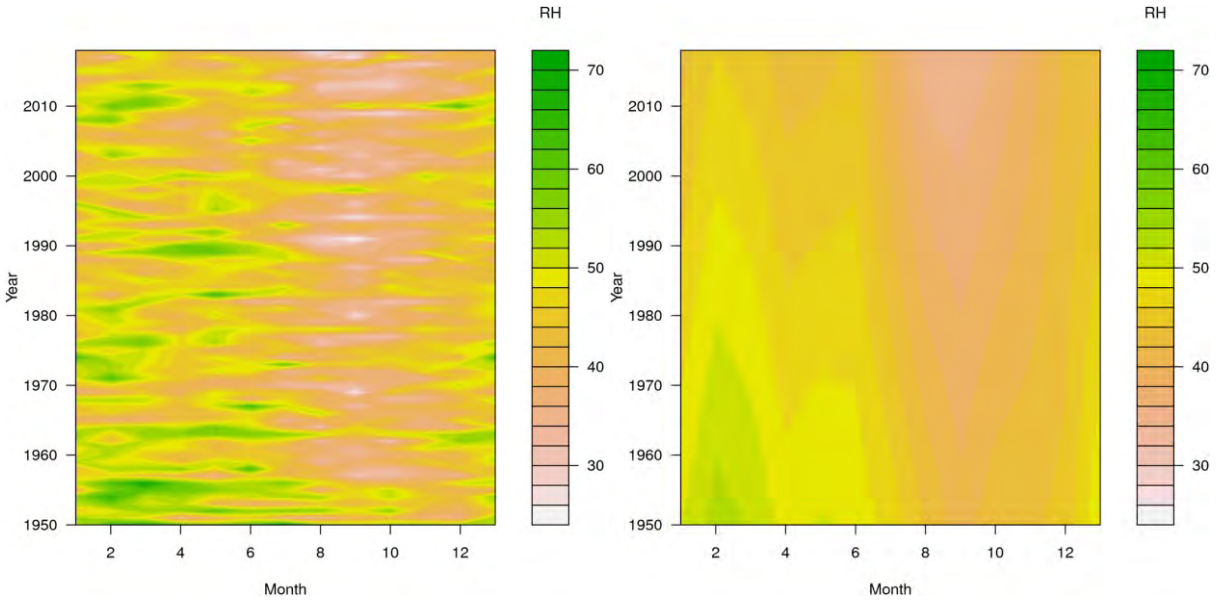

Central Coast

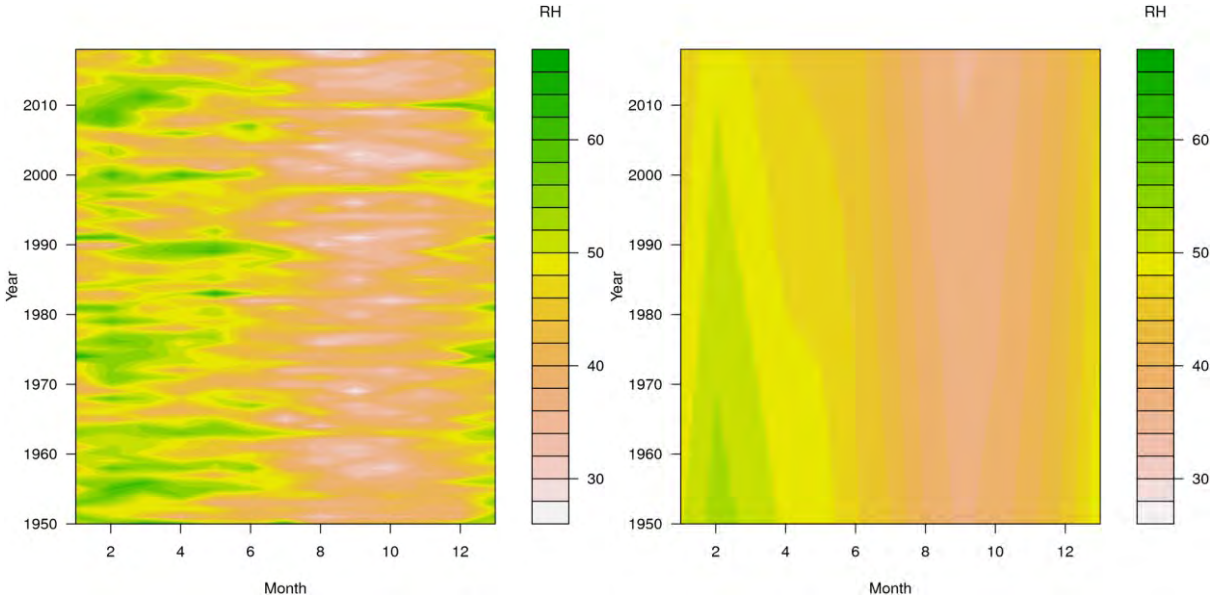

North Coast

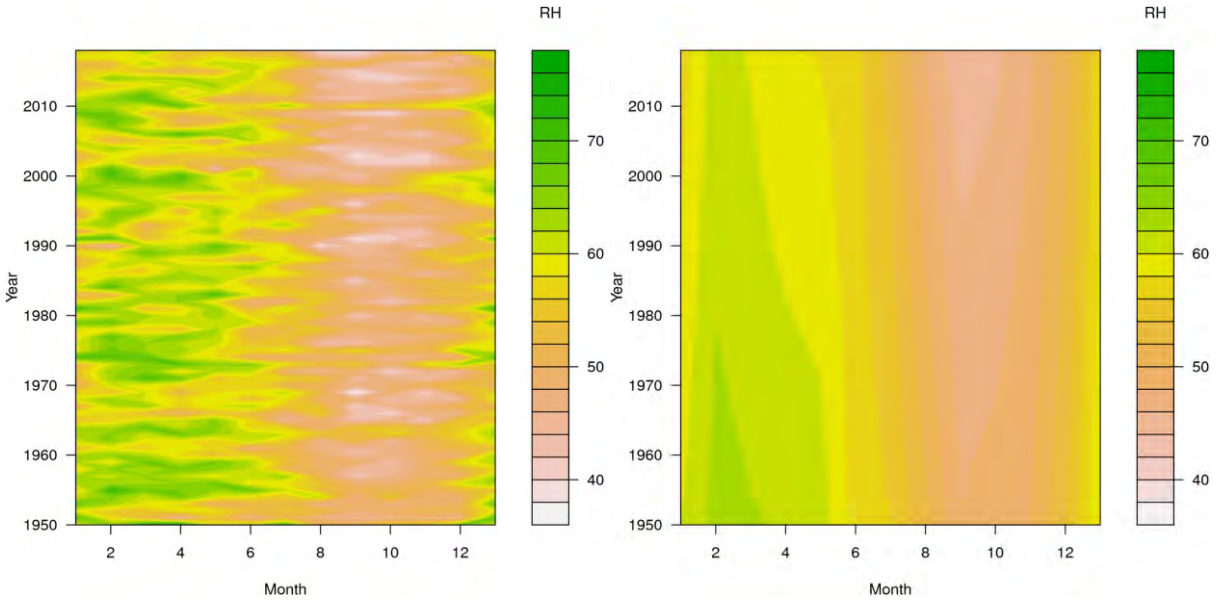

Cape York Peninsula

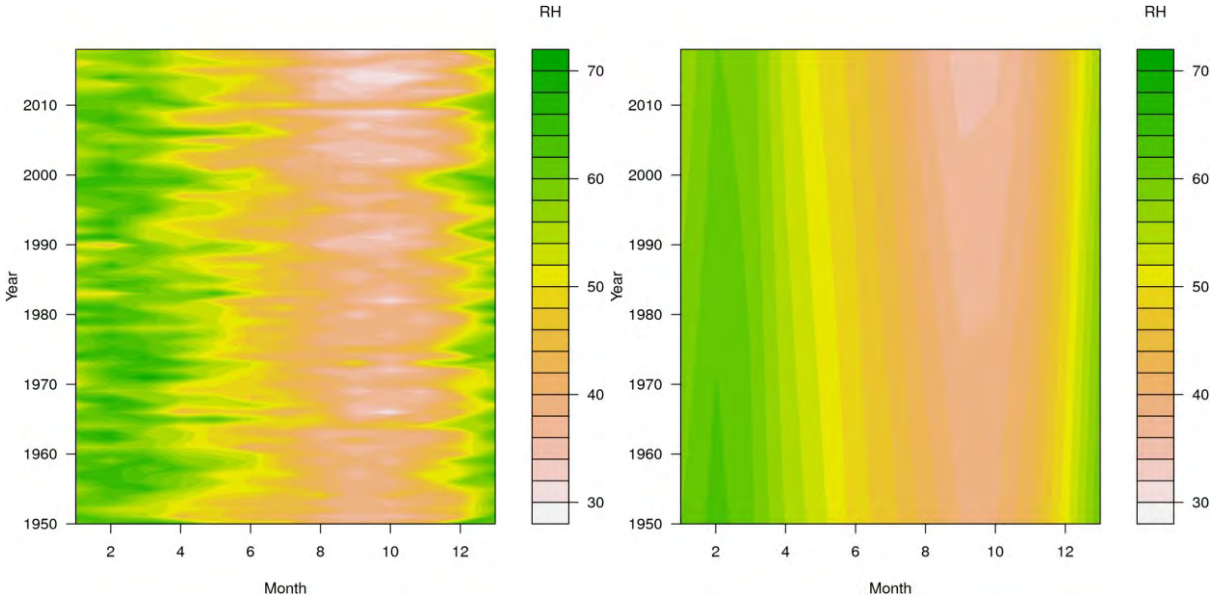

Central South

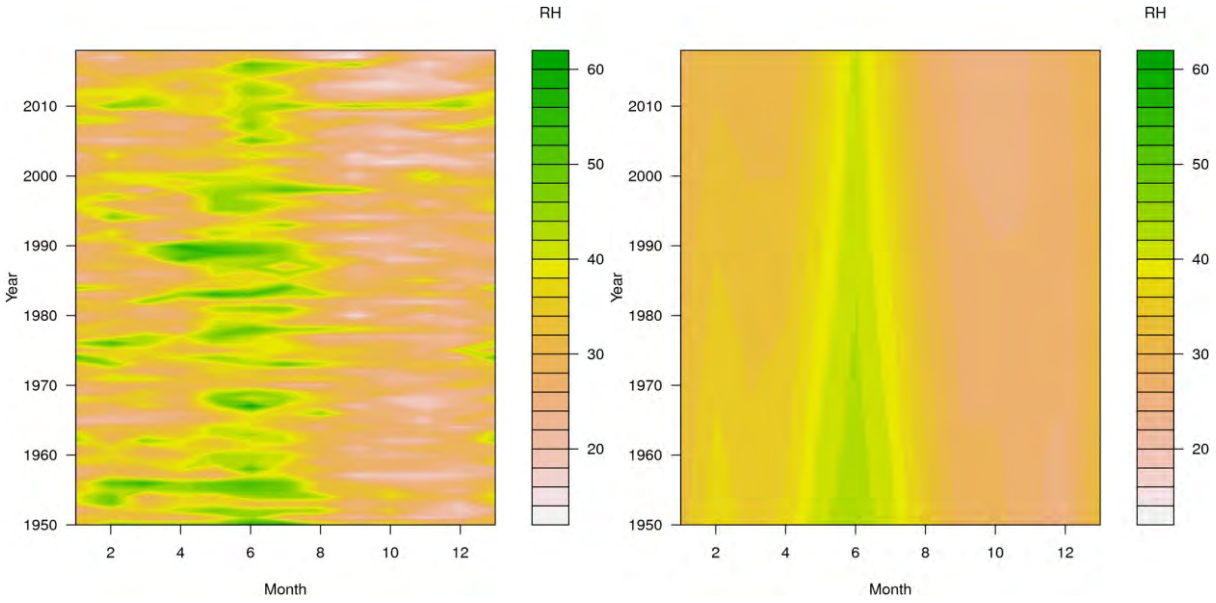

Central

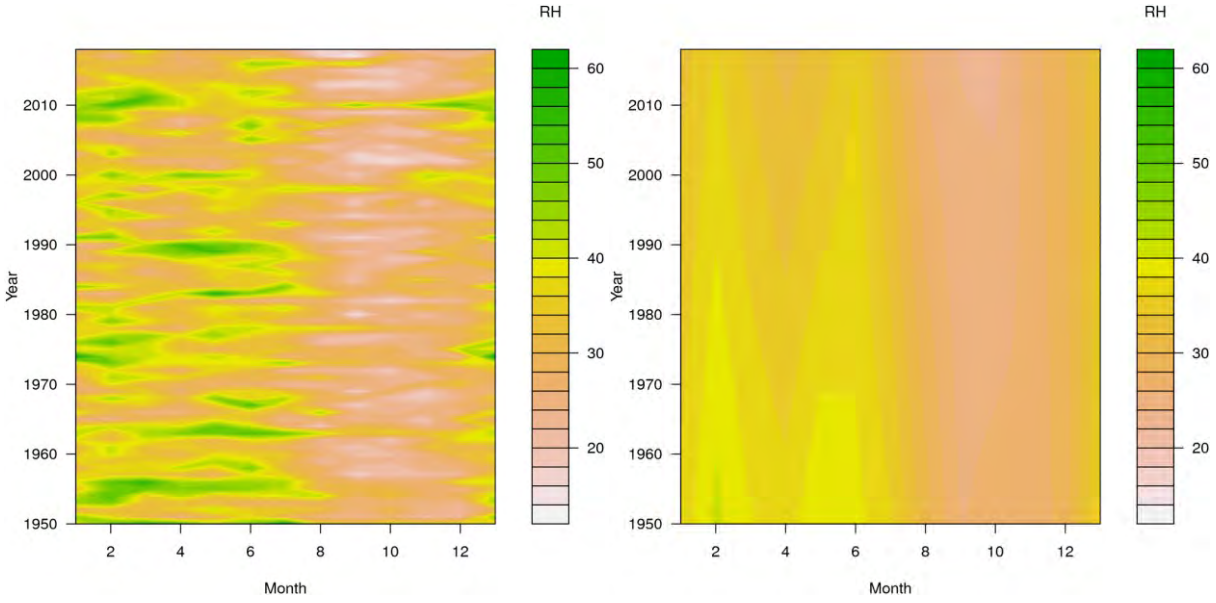

North West

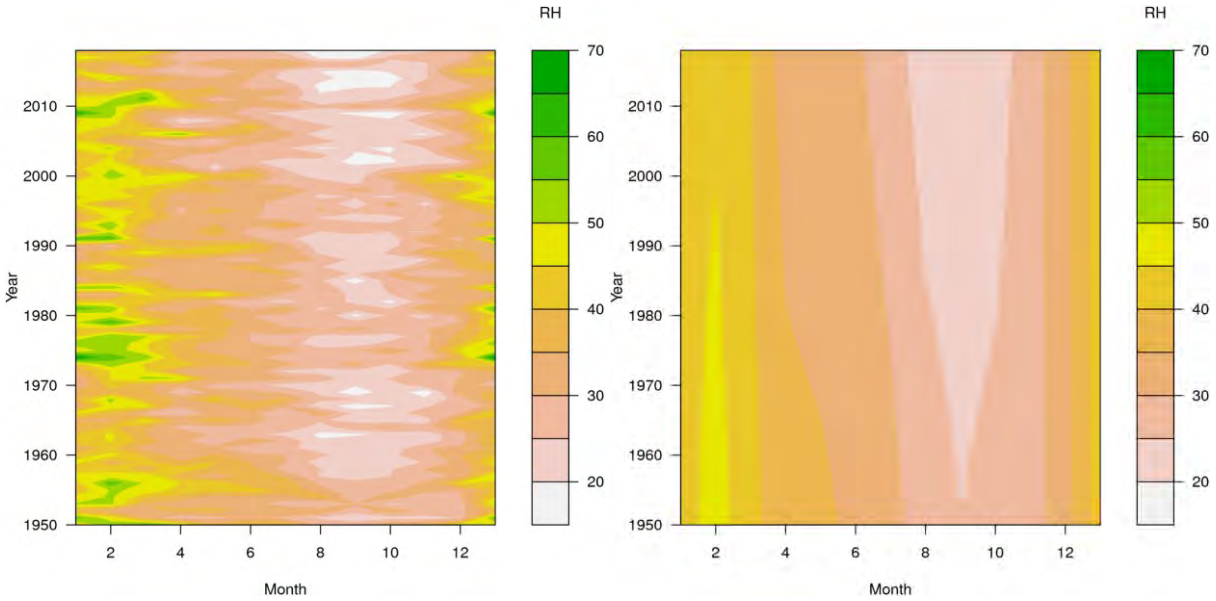

South West

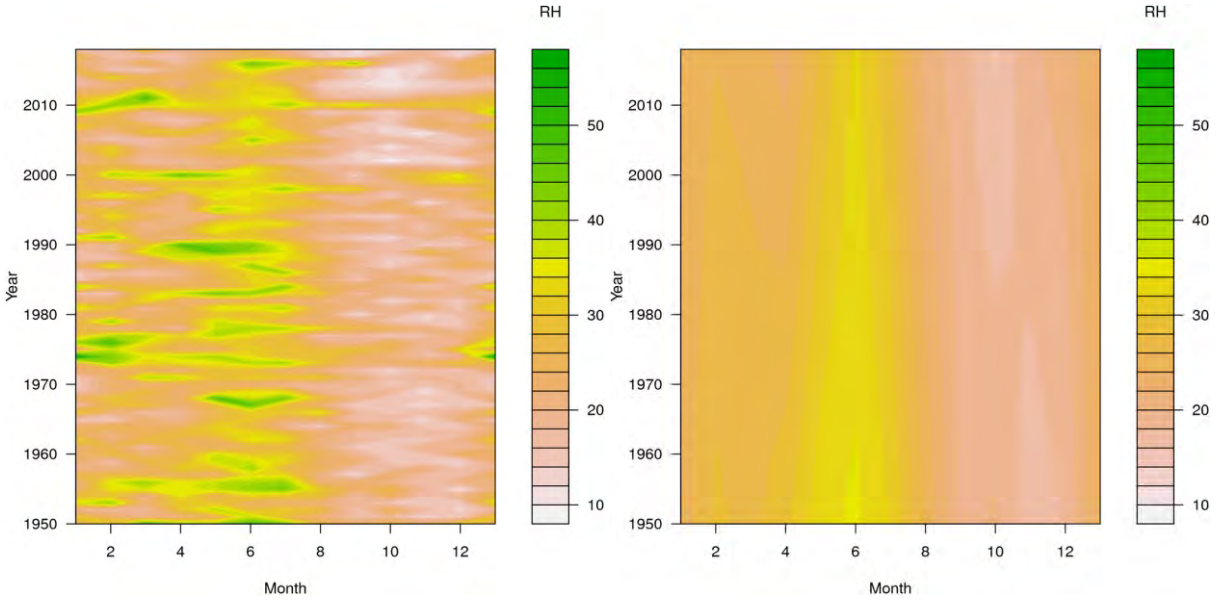

Figure 45: Hovmöller plots of monthly afternoon relative humidity (left) and linear trends (right). The January values are repeated on the right to complete the annual cycle in the plotting. Note that the contouring is specific to each subregion, and varies from subregion to subregion.

Regional Fact Sheets

Observed changes are now presented for the State and the nine subregions individually, in a sequence of fact sheets, one for each region or subregion. Each fact sheet shows a map of the subregion relative to the State of Queensland. [In the first (State) fact sheet, the map shows all nine subregions.] The fact sheets contain the following elements.

- A time series plot of annual accumulated FFDI is shown for the period 1950-2018, together with the *lowess* regression. The total change in FFDI units is shown above the graph, together with the percentage change. The total change is calculated as {last point on the regression line} − {first point on the regression line}. The percentage change is calculated as {last point on the regression line} relative to {first point on the regression line}.
- A time series plot of the annual number of FFDI ≥ 25 days averaged across the region or subregion for the period 1950-2018, together with the *lowess* regression. The total change in days is shown above the graph, together with the percentage change.
- An analogous plot for the annual number of FFDI ≥ 50 days averaged across the region or subregion.
- A plot of the time series of the day index of the earliest day in the fire-weather season with FFDI above the highest threshold (as rounded) which is achieved *somewhere* in the subregion in *all* years of the dataset. The choice of fire-weather season is specific to the subregion, and varies from subregion to subregion. Due to the characteristics of the fire-weather season, this plot cannot be calculated for all subregions, as it requires the most intense part of the fire-weather season to be statistically isolated to a particular part of the year, and to not be an all-year-round proposition.
- The analogous plot for the latest day in the fire-weather season.
- For the South East Coast subregion and the Wide Bay and Burnett subregion, rather than the indices of the first and last occurrence of FFDI above 25 somewhere in the subregion, the first-quarter-point and third-quarter-point indices are shown. These points mark out the *middle half* (also known as the interquartile range) within each fire-weather season of the occurrences of FFDI above 25 somewhere in the subregion. These quantile points are more likely to be statistically isolated in the required manner than the first and last occurrences. An expansion of the interquartile range within the fire-weather season will be *an* indicator that the total fire-weather season is changing adversely. [An expansion of the interquartile range of a distribution does not directly or necessarily imply the expansion of the range of the distribution, although for the interquartile range to expand

without the range expanding would imply a change in the shape of the distribution which might be ruled out by other considerations.]

- A time series plot of daily FFDI averaged across the region or subregion for the period January 1950 to December 2018.

Queensland

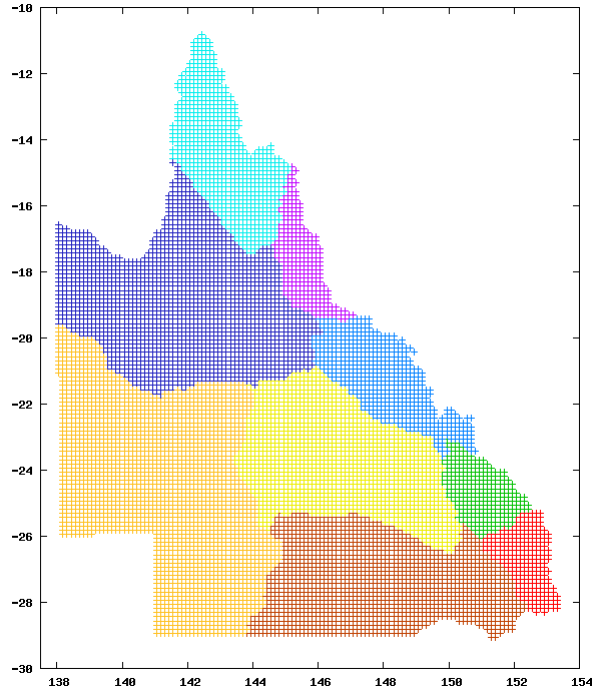

Figure A1: The subregions used in this study.

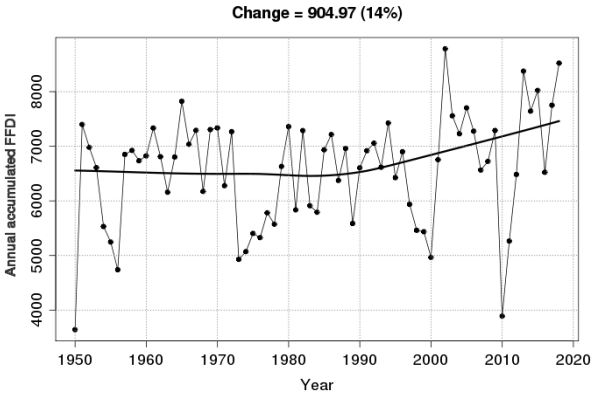

Figure A2: Time series of annual accumulated FFDI across Queensland (1950-2018). Annual accumulated FFDI has increased by 14%.

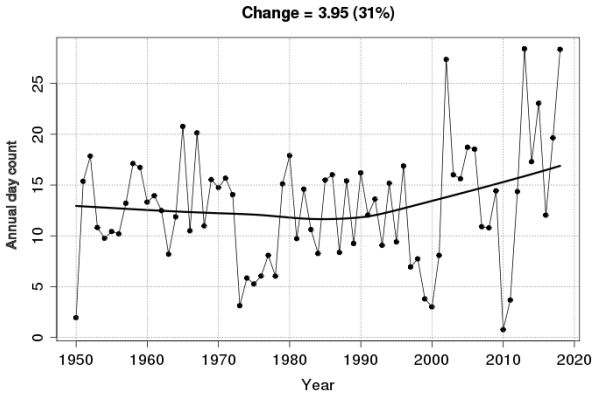

Figure A4: Time series of annual FFDI ≥ 50 days across Queensland (1950-2018). The average annual occurrence of FFDI ≥ 50 days has increased by 31%.

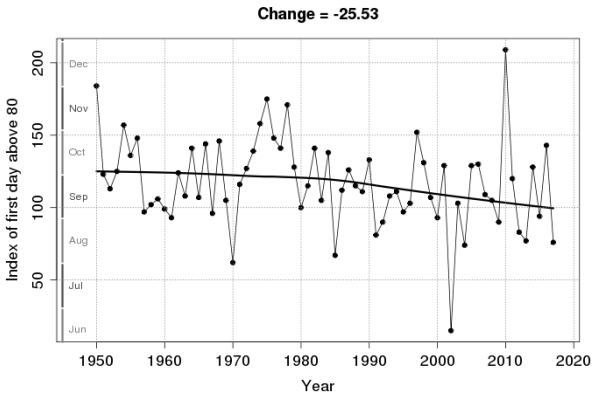

Figure A5: Time series of the index of the earliest FFDI > 80 day for Queensland (June-to-May years 1950/1951- 2017/2018). The earliest FFDI > 80 day is now arriving around 26 days earlier. In most years, the first occurrence of an FFDI > 80 somewhere in Queensland actually occurs in the South West region, so in consequence Figure A5 resembles Figure J5 fairly closely**.**

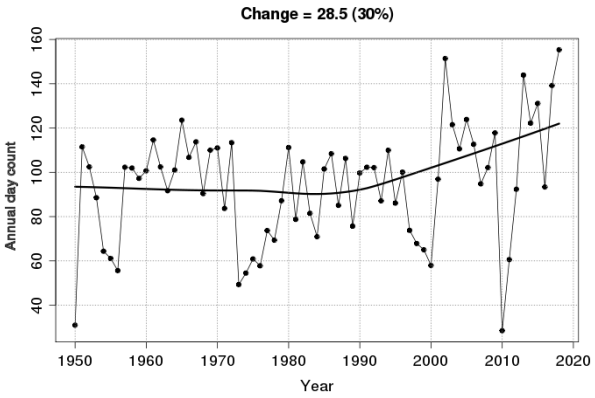

Figure A3: Time series of annual FFDI ≥ 25 days across Queensland (1950-2018). The average annual occurrence of FFDI ≥ 25 days has increased by 30%.

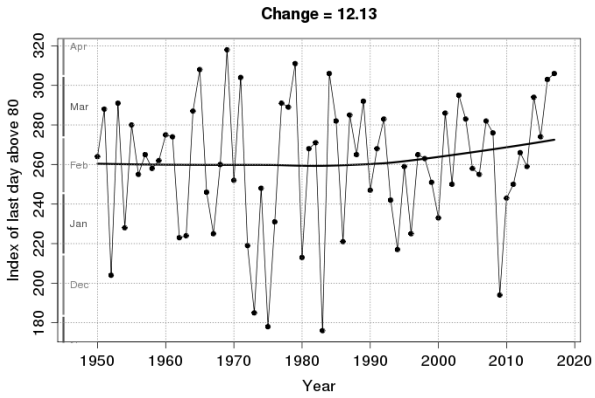

Figure A6: Time series of the index of the latest FFDI > 80 day for Queensland subregion (June-to-May years 1950/1951-2017/2018). The latest FFDI > 80 day is now arriving around 12 days later.

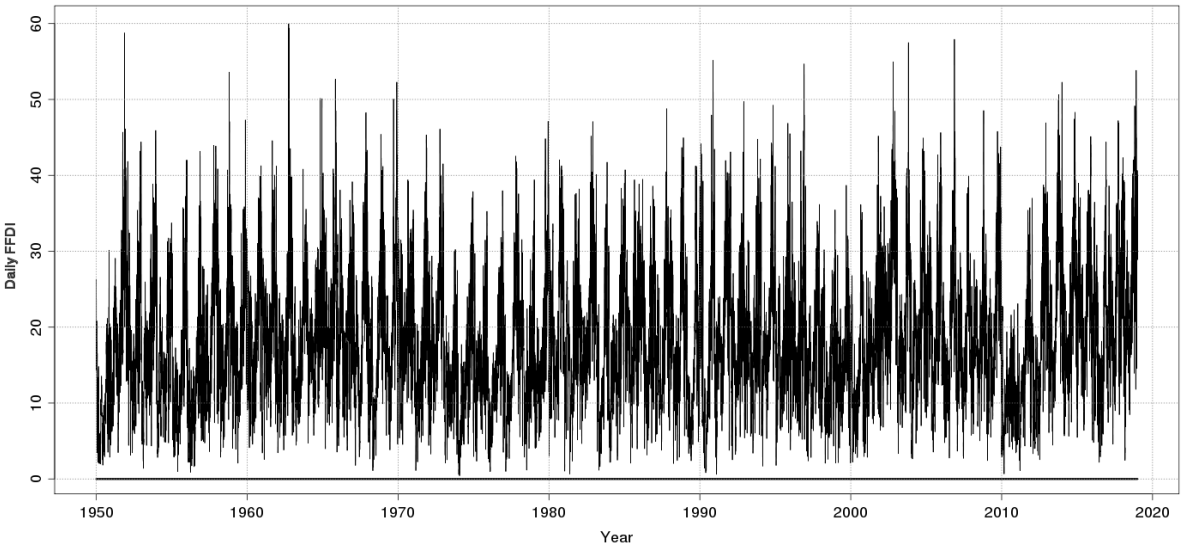

Figure A7: Time series of daily FFDI averaged across Queensland (1950-2018). The day with the highest spatial average for the State was 2 October 1962.

South East Coast

The South East Coast subregion comprises rainfall district 40. Representative locations include Amberley, Brisbane, Caloundra, Coolangatta, Gatton, Gympie, Maryborough and Nambour.

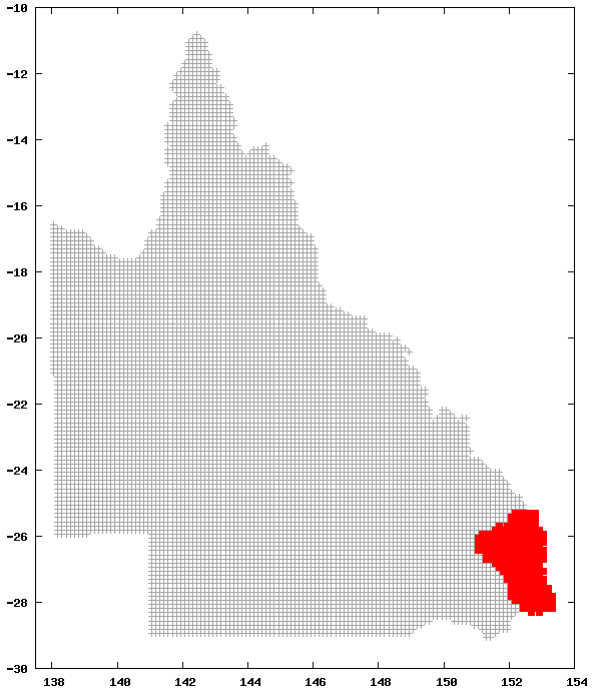

Figure B1: The South East Coast subregion.

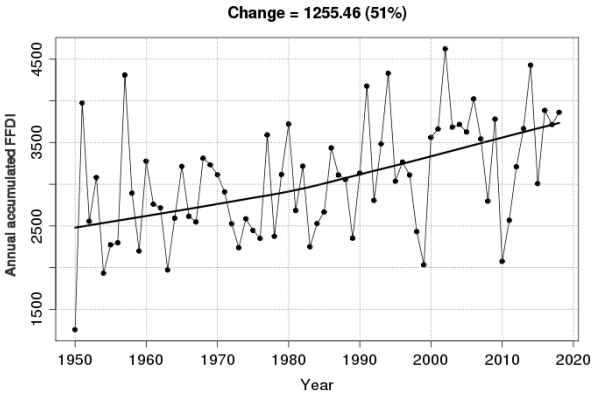

Figure B2: Time series of annual accumulated FFDI across the South East Coast subregion (1950-2018). Annual accumulated FFDI has increased by 51%.

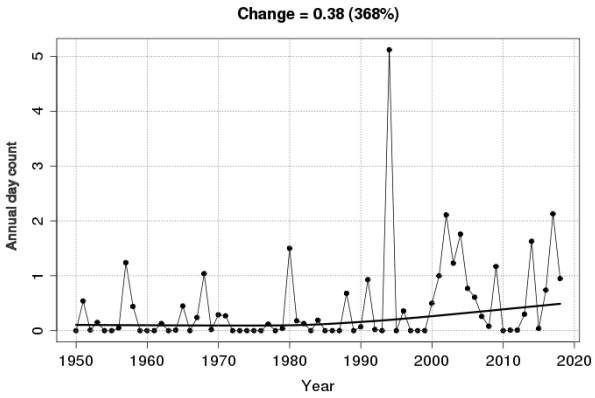

Figure B4: Time series of annual FFDI ≥ 50 days across the South East Coast subregion (1950-2018). The average annual occurrence of FFDI ≥ 50 days has increased by 368%. The percentage change should be treated with considerable caution, as the underlying numbers remain small.

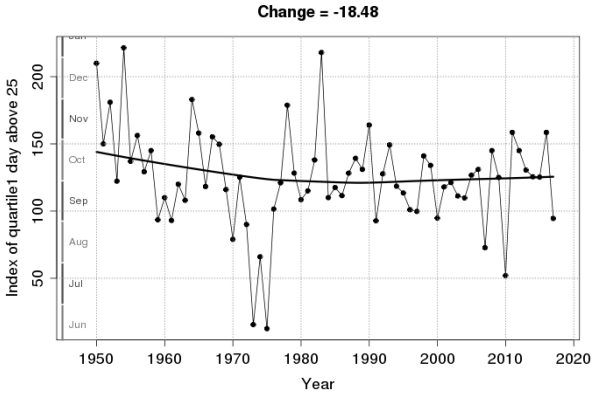

Figure B5: Time series of the index of the first-quarter-point FFDI > 25 day for the South East Coast subregion (June-to-May years 1950/1951- 2017/2018). The first-quarter-point FFDI > 25 day is now arriving around 18 days earlier. In the 2010/2011 fire-weather season, there was only one occurrence (in July 2010) of the FFDI exceeding the 25-point threshold, although

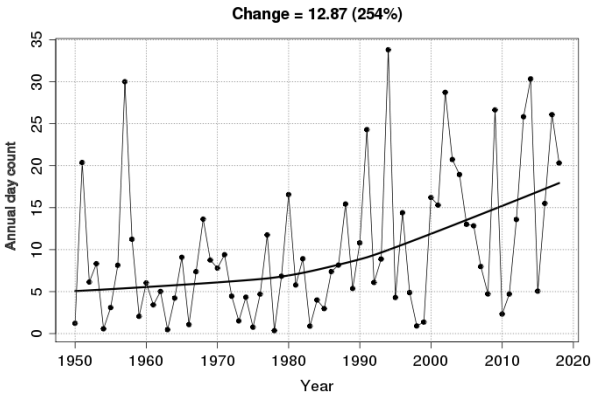

Figure B3: Time series of annual FFDI ≥ 25 days across the South East Coast subregion (1950-2018). The average annual occurrence of FFDI ≥ 25 days has increased by 254%.

there several additional near misses (see also Figure B6).

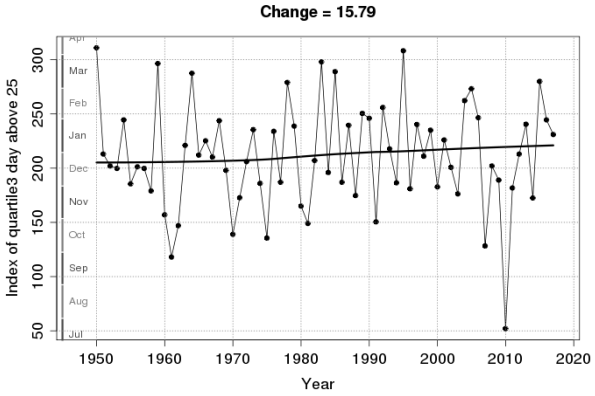

Figure B6: Time series of the index of the third-quarter-point FFDI > 25 day for the South East Coast subregion (June-to-May years 1950/1951- 2017/2018). The third-quarter-point FFDI > 25 day is now arriving around 16 days later.

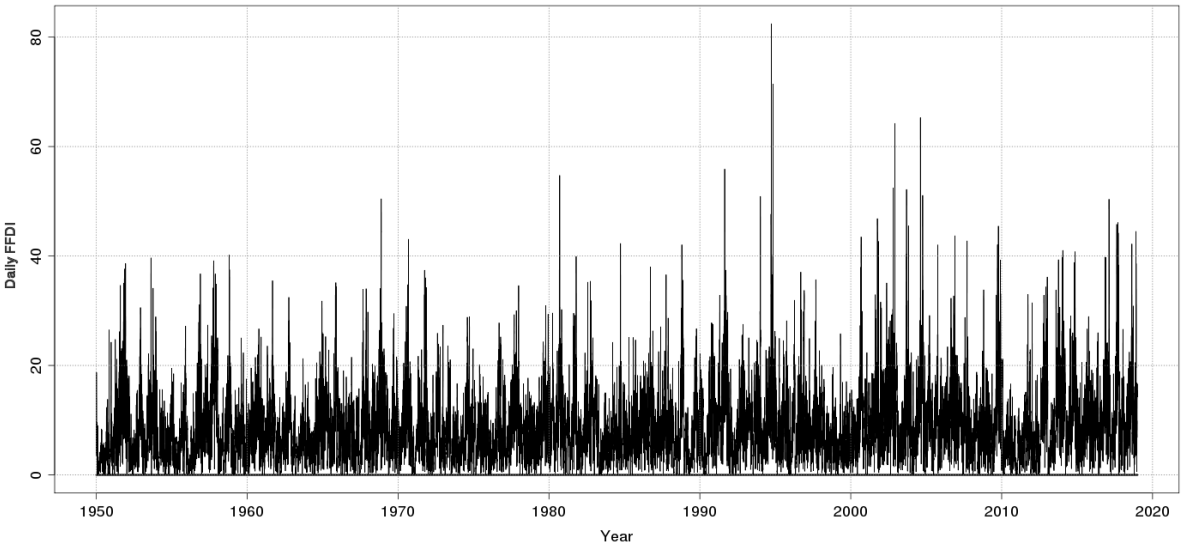

Figure B7: Time series of daily FFDI averaged across the South East Coast subregion (1950-2018). The day with the highest spatial average for the subregion was 27 September 1994. Three serious wildfires burnt through 4800 ha of exotic pine plantations near Beerburrum on 27-28 September and 6-7 November 1994 (Hunt et al. 1995).

Wide Bay and Burnett

The Wide Bay and Burnett subregion comprises rainfall district 39. Representative locations include Bundaberg, Gayndah, Gladstone and Rockhampton.

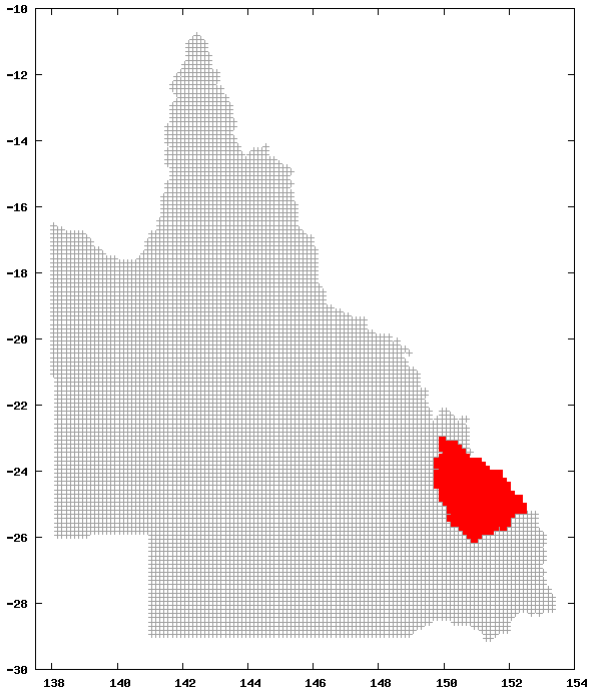

Figure C1: The Wide Bay and Burnett subregion.

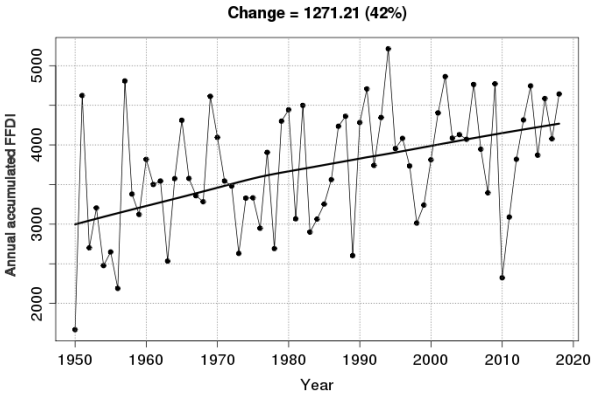

Figure C2: Time series of annual accumulated FFDI across the Wide Bay and Burnett subregion (1950-2018). Annual accumulated FFDI has increased by 42%.

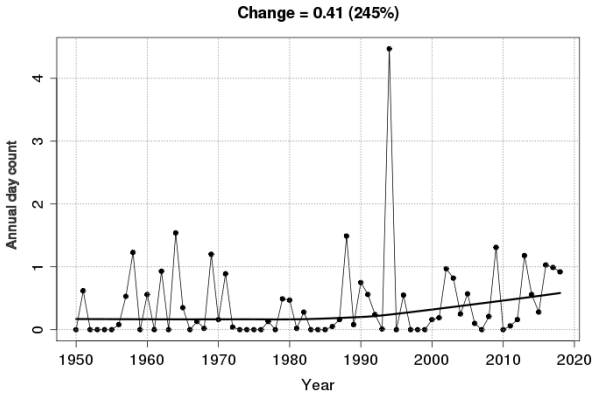

Figure C4: Time series of annual FFDI ≥ 50 days across the Wide Bay and Burnett subregion (1950-2018). The average annual occurrence of FFDI ≥ 50 days has increased by 245%. The percentage change should be treated with considerable caution, as the underlying numbers remain small.

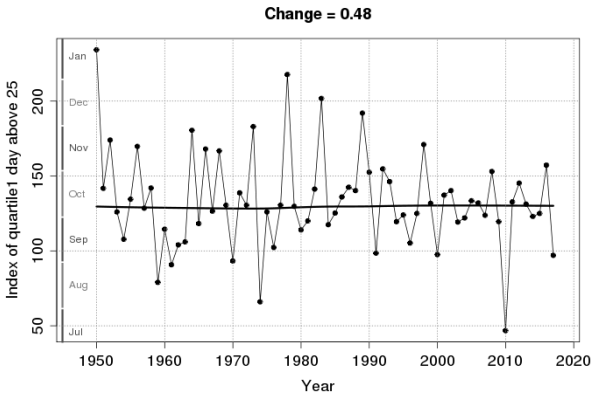

Figure C5: Time series of the index of the first-quarter-point FFDI > 25 day for the Wide Bay and Burnett subregion (June-to-May years 1950/1951- 2017/2018). There is effectively no change in this component of the fire-weather season (the diagnosed change is less than one day).

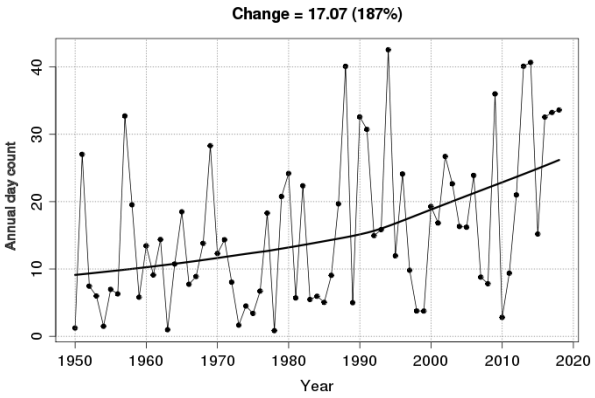

Figure C3: Time series of annual FFDI ≥ 25 days across the Wide Bay and Burnett subregion (1950-2018). The average annual occurrence of FFDI ≥ 25 days has increased by 187%.

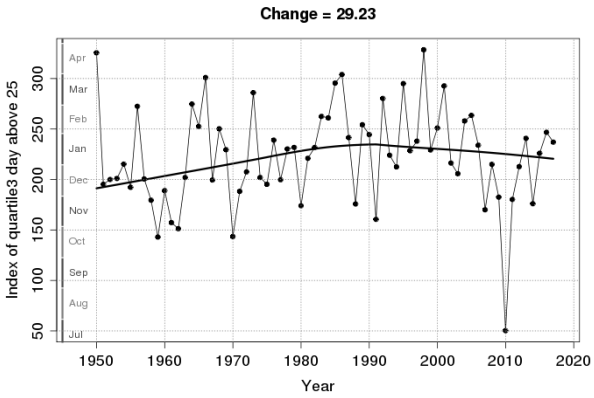

Figure C6: Time series of the index of the third-quarter-point FFDI > 25 day for the Wide Bay and Burnett subregion (June-to-May years 1950/1951- 2017/2018). The third-quarter-point FFDI > 25 day is now arriving around 29 days later.

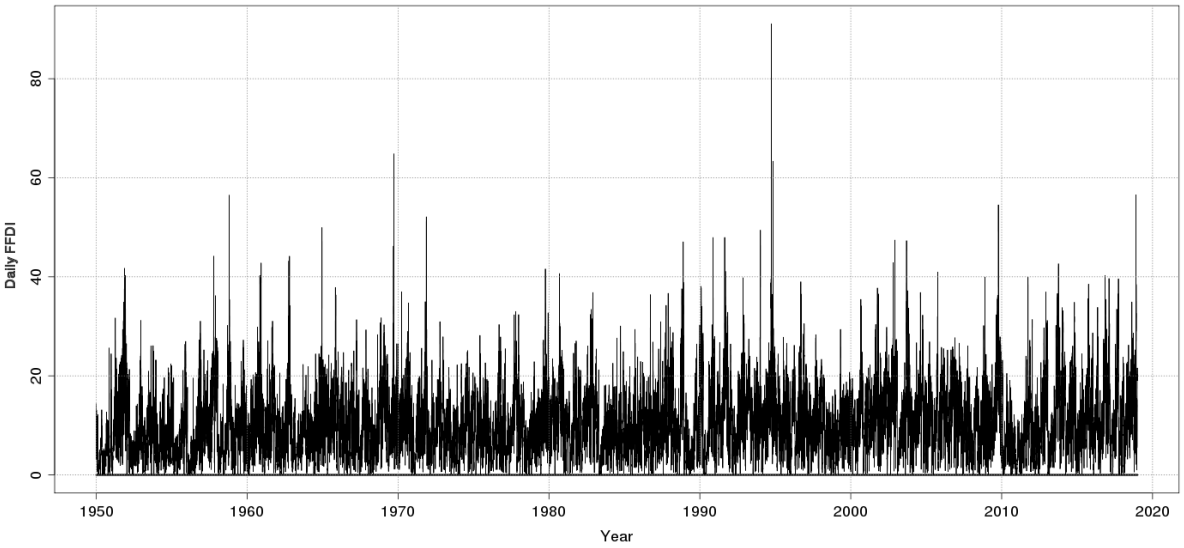

Figure C7: Time series of daily FFDI averaged across the Wide Bay and Burnett subregion (1950-2018). The day with the highest spatial average for the subregion was 27 September 1994.

Central Coast

The Central Coast subregion comprises rainfall districts 33 and 34. Representative locations include Ayr, Bowen, Mackay, Moranbah, Proserpine and Yeppoon.

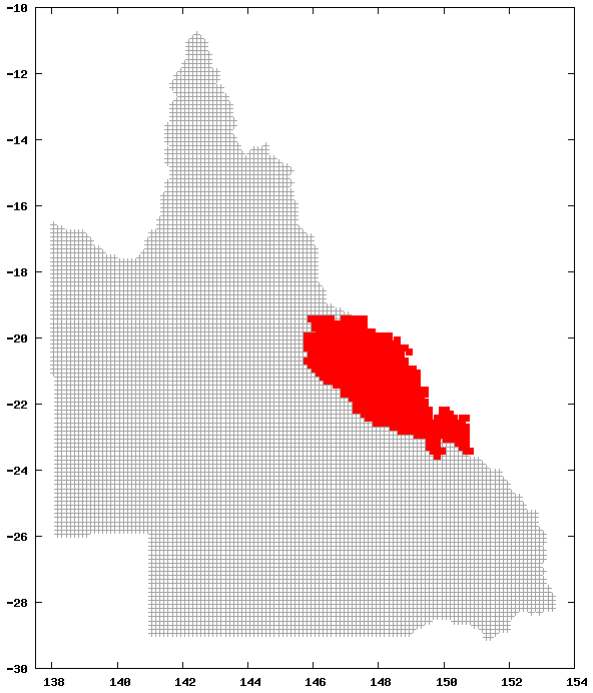

Figure D1: The Central Coast subregion.

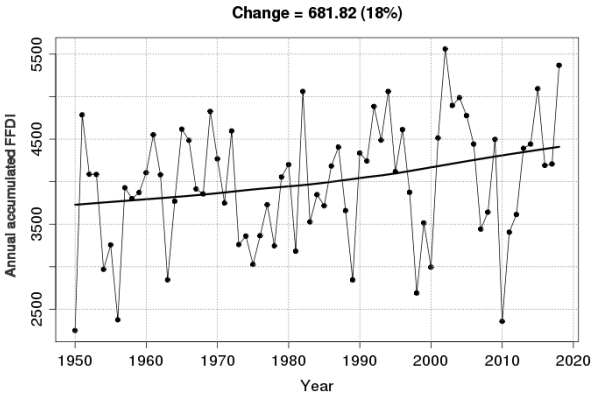

Figure D2: Time series of annual accumulated FFDI across the Central Coast subregion (1950-2018). Annual accumulated FFDI has increased by 18%.

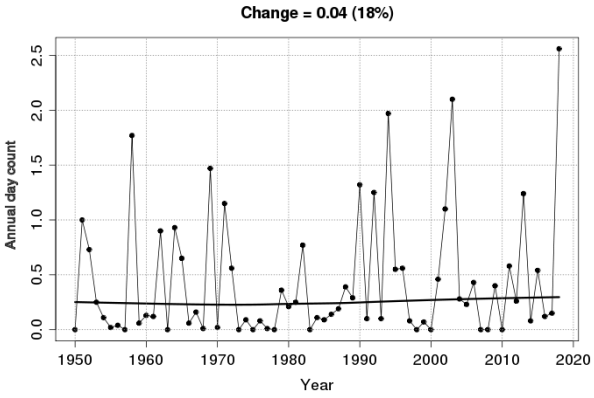

Figure D4: Time series of annual FFDI ≥ 50 days across the Central Coast subregion (1950-2018). The average annual occurrence of FFDI ≥ 50 days has increased by 18%.

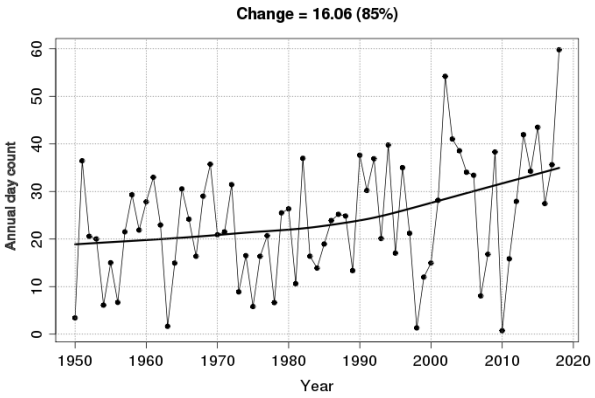

Figure D3: Time series of annual FFDI ≥ 25 days across the Central Coast subregion (1950-2018). The average annual occurrence of FFDI ≥ 25 days has increased by 85%.

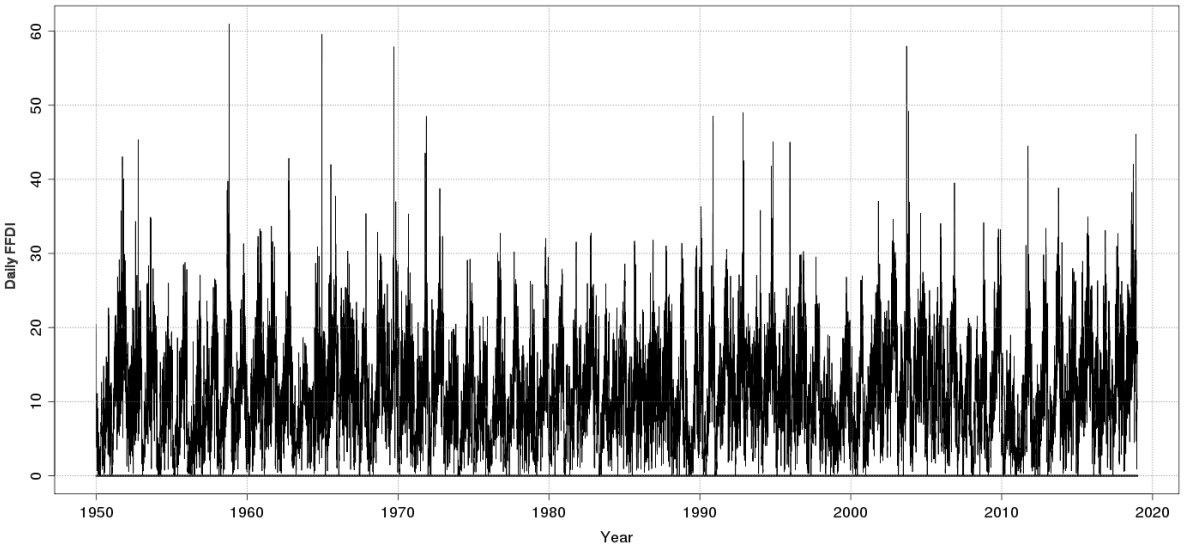

Figure D7: Time series of daily FFDI averaged across the Central Coast subregion (1950-2018). The day with the highest spatial average for the subregion was 25 October 1958.

North Coast

The North Coast subregion comprises rainfall districts 31 and 32. Representative locations include Cairns, Cooktown, Ingham, Innisfail and Townsville.

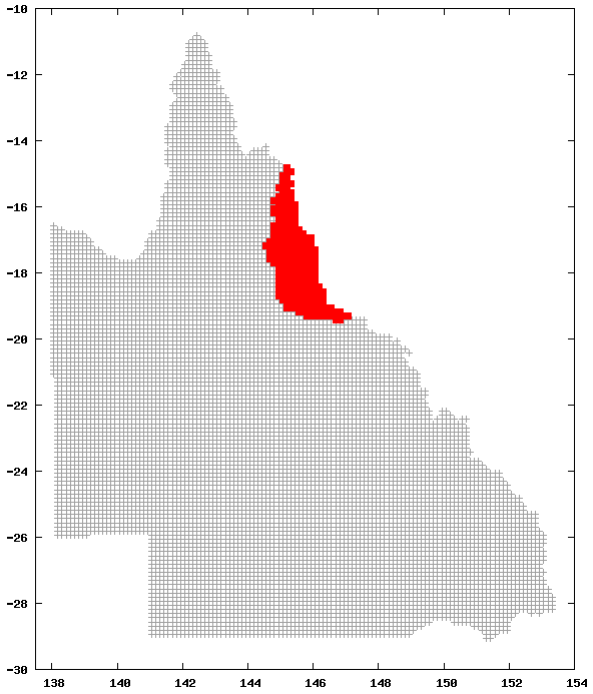

Figure E1: The North Coast subregion.

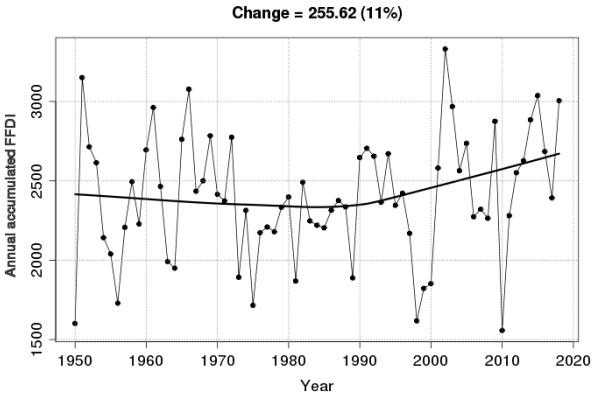

Figure E2: Time series of annual accumulated FFDI across the North Coast subregion (1950-2018). Annual accumulated FFDI has increased by 11%.

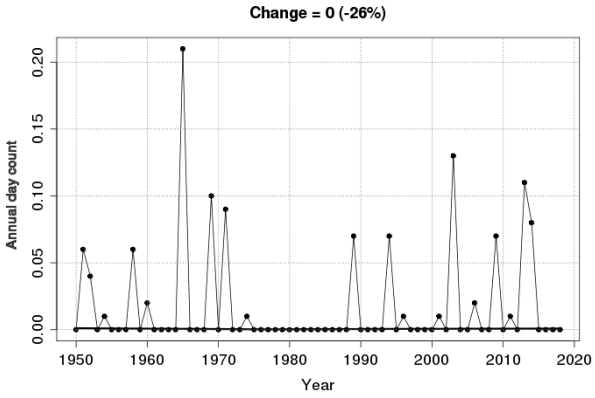

Figure E4: Time series of annual FFDI ≥ 50 days across the North Coast subregion (1950-2018). The average annual occurrence of FFDI ≥ 50 days has decreased by 26%. The percentage change should be treated with considerable caution, as the underlying numbers remain very small.

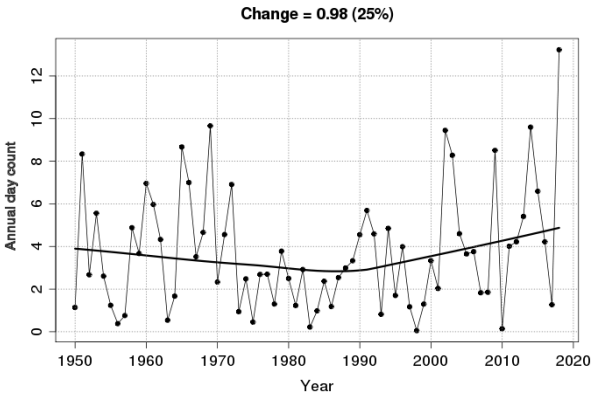

Figure E3: Time series of annual FFDI ≥ 25 days across the North Coast subregion (1950-2018). The average annual occurrence of FFDI ≥ 25 days has increased by 25%. In 2018 the subregion averaged more than 12 FFDI ≥ 25 days. It had not previously averaged more than 10 days.

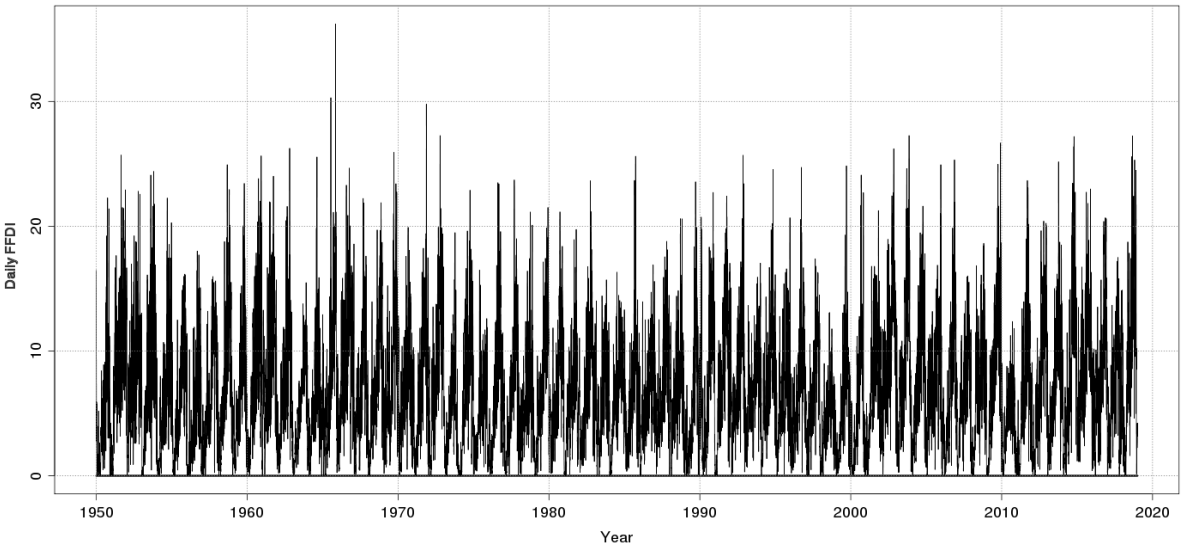

Figure E7: Time series of daily FFDI averaged across the North Coast subregion (1950-2018). The day with the highest spatial average for the subregion was 12 November 1965.

Cape York Peninsula

The Cape York Peninsula subregion comprises rainfall districts 27 and 28. Representative locations include Coen, Palmerville and Weipa.

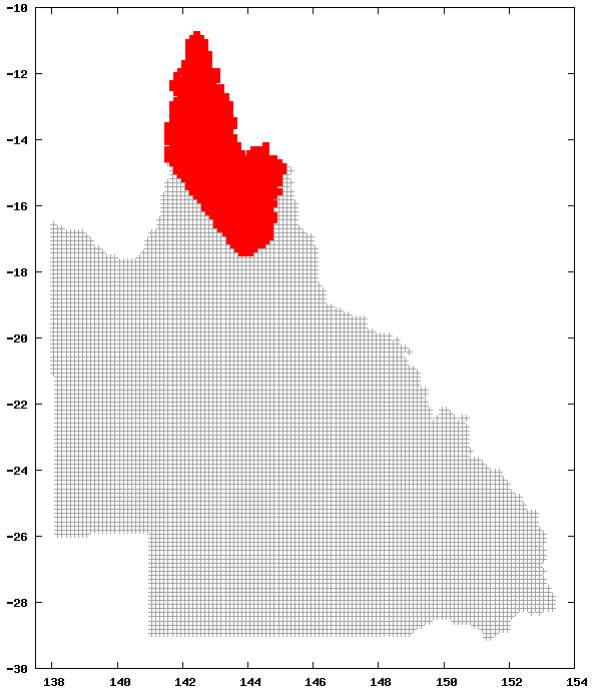

Figure F1: The Cape York Peninsula subregion.

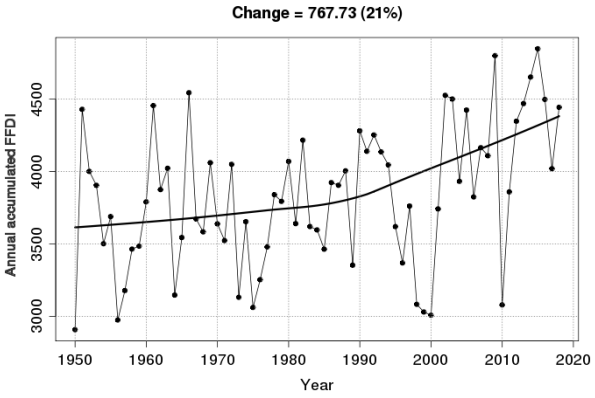

Figure F2: Time series of annual accumulated FFDI across the Cape York Peninsula subregion (1950-2018). Annual accumulated FFDI has increased by 21%.

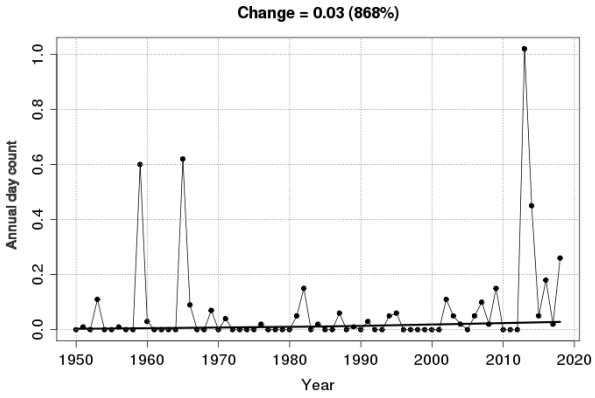

Figure F4: Time series of annual FFDI ≥ 50 days across the Cape York Peninsula subregion (1950-2018). The average annual occurrence of FFDI ≥ 50 days has increased by 868%. The percentage change should be treated with considerable caution, as the underlying numbers remain very small.

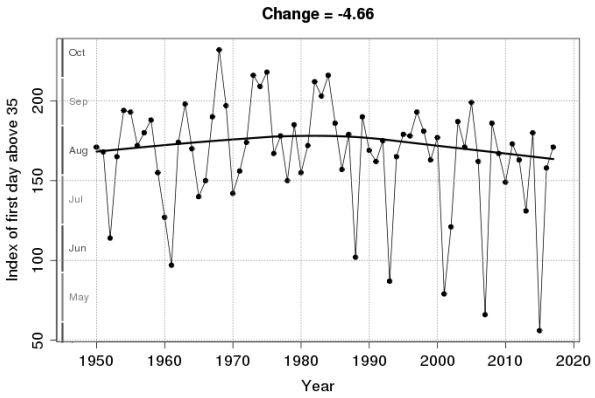

Figure F5: Time series of the index of the earliest FFDI ≥ 35 day for the Cape York Peninsula subregion (March-to-February years 1950/1951-2017/2018). The earliest FFDI > 35 day is now arriving around 5 days earlier.

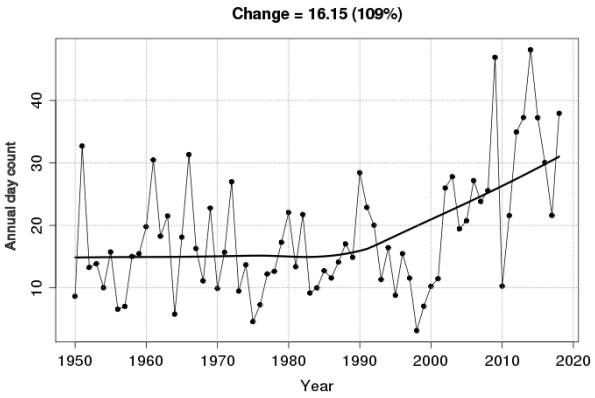

Figure F3: Time series of annual FFDI ≥ 25 days across the Cape York Peninsula subregion (1950-2018). The average annual occurrence of FFDI ≥ 25 days has increased by 109%.

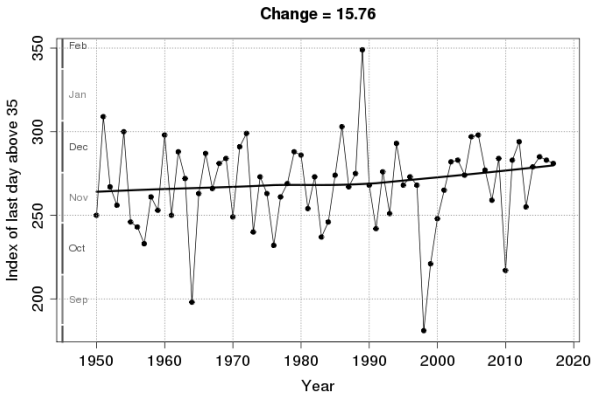

Figure F6: Time series of the index of the latest FFDI ≥ 35 day for the Cape York Peninsula subregion (March-to-February years 1950/1951-2017/2018). The latest FFDI > 35 day is now arriving around 16 days later.

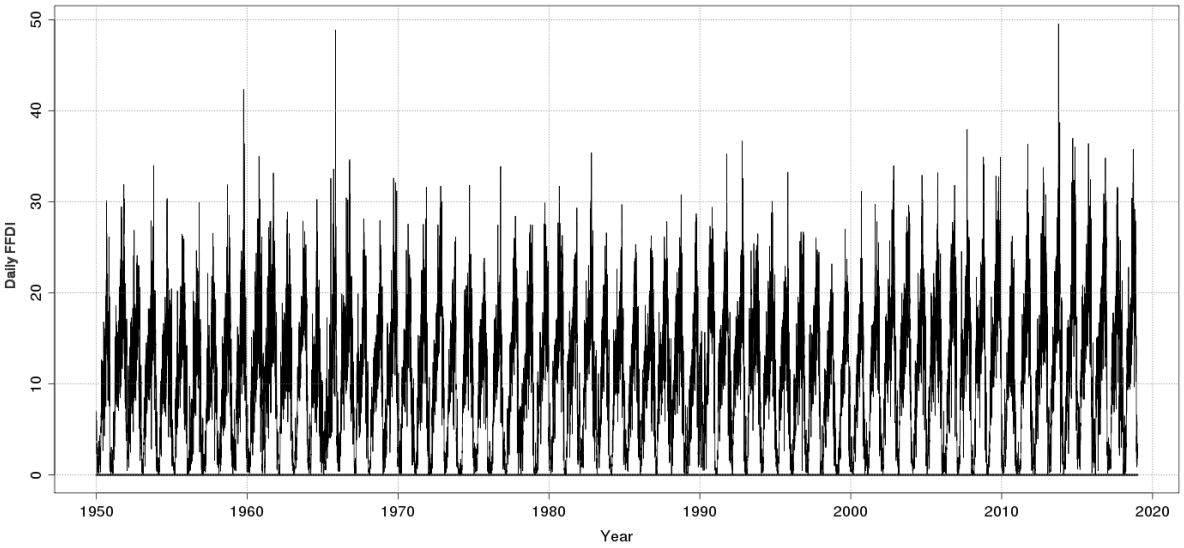

Figure F7: Time series of daily FFDI averaged across the Cape York Peninsula subregion (1950-2018). The day with the highest spatial average for the subregion was 9 October 2013.

Central South

The Central South subregion comprises rainfall districts 41, 42, 43 and 44. It includes the Darling Downs, Maranoa and Warrego regions. Representative locations include Bollon, Charleville, Dalby, Injune, Miles, Mitchell, Roma, Toowoomba, Stanthorpe and Warwick.

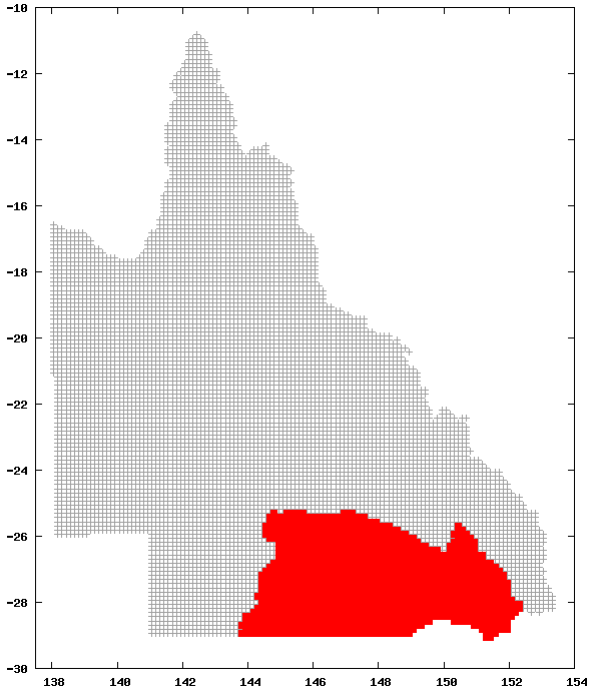

Figure G1: The Central South subregion.

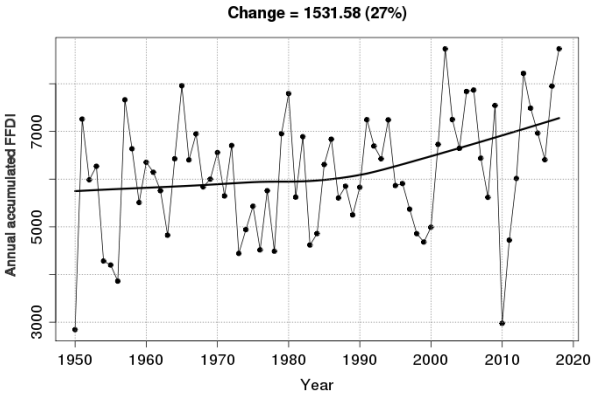

Figure G2: Time series of annual accumulated FFDI across the Central South subregion (1950-2018). Annual accumulated FFDI has increased by 27%.

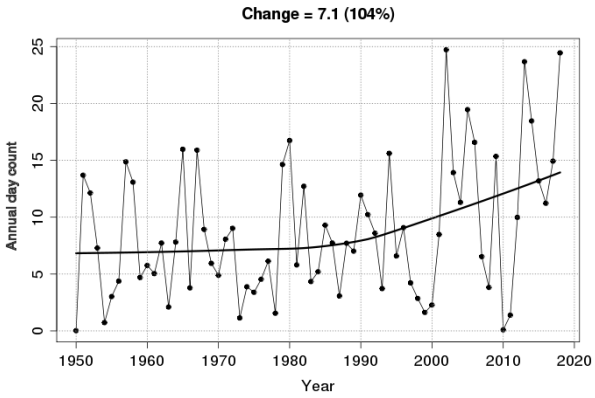

Figure G4: Time series of annual FFDI ≥ 50 days across the Central South subregion (1950-2018). The average annual occurrence of FFDI ≥ 50 days has increased by 104%.

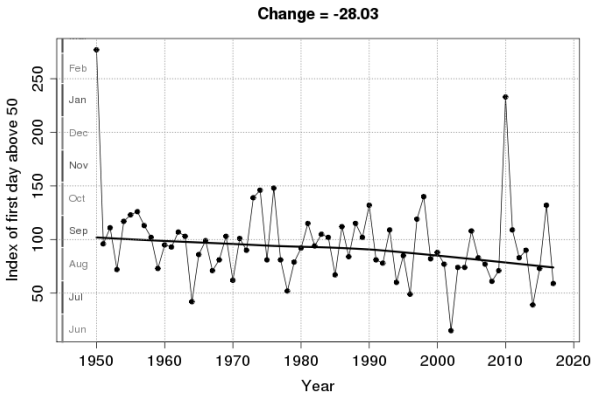

Figure G5: Time series of the index of the earliest FFDI > 50 day for the Central South subregion (June-to-May years 1950/1951-2017/2018). The earliest FFDI > 50 day is now arriving around 28 days earlier.

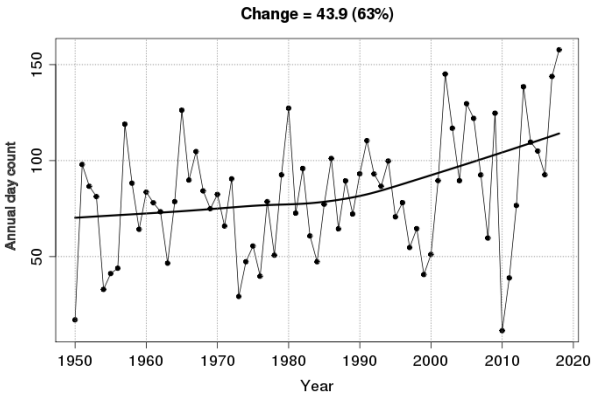

Figure G3: Time series of annual FFDI ≥ 25 days across the Central South subregion (1950-2018). The average annual occurrence of FFDI ≥ 25 days has increased by 63%.

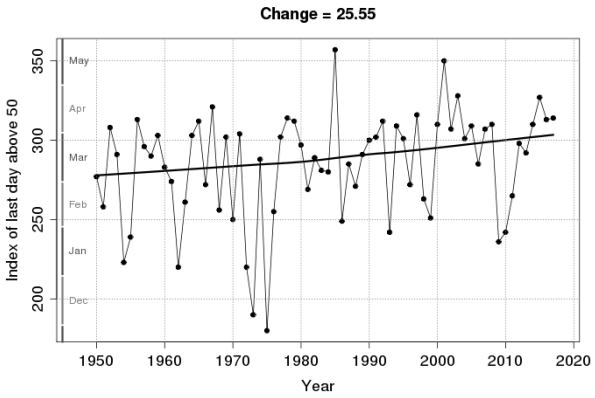

Figure G6: Time series of the index of the latest FFDI > 50 day for the Central South subregion (June-to-May years 1950/1951-2017/2018). The latest FFDI > 50 day is now arriving around 26 days later.

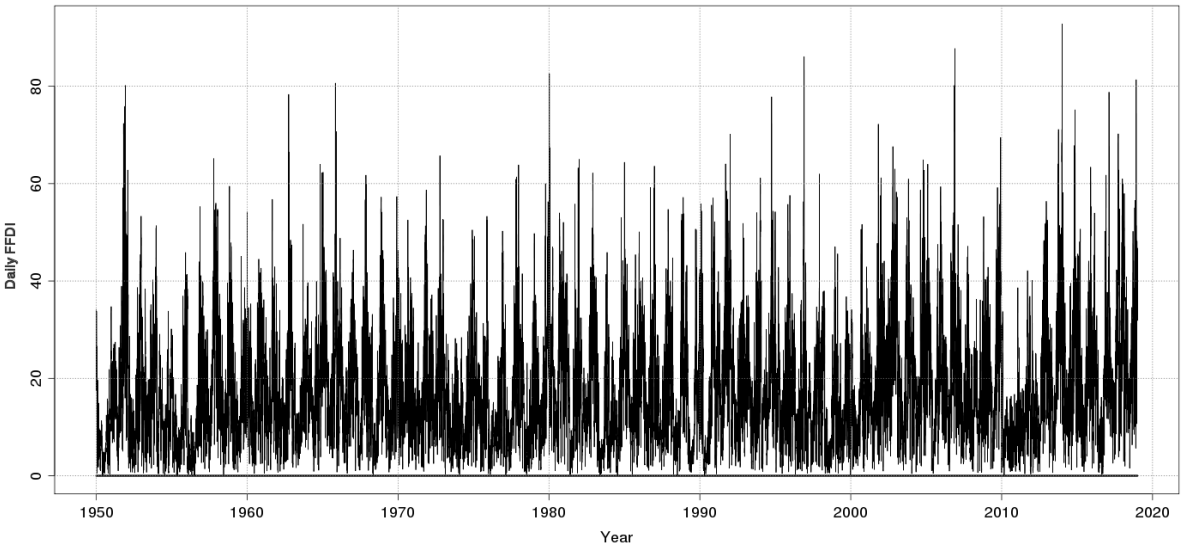

Figure G7: Time series of daily FFDI averaged across the Central South subregion (1950-2018). The day with the highest spatial average for the subregion was 3 January 2014.

Central

The Central subregion comprises rainfall districts 35 and 36. Representative locations include Alpha, Barcaldine, Clermont, Emerald, Longreach, Tambo and Taroom.

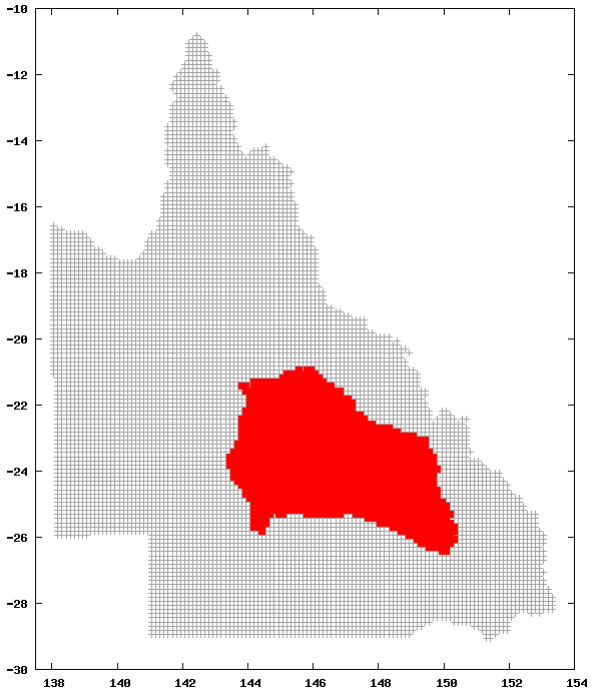

Figure H1: The Central subregion.

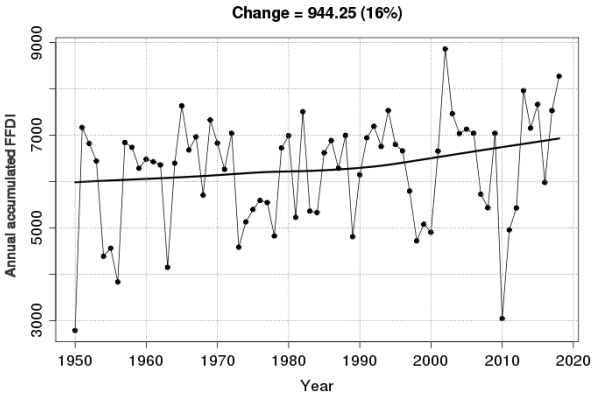

Figure H2: Time series of annual accumulated FFDI across the Central subregion (1950-2018). Annual accumulated FFDI has increased by 16%.

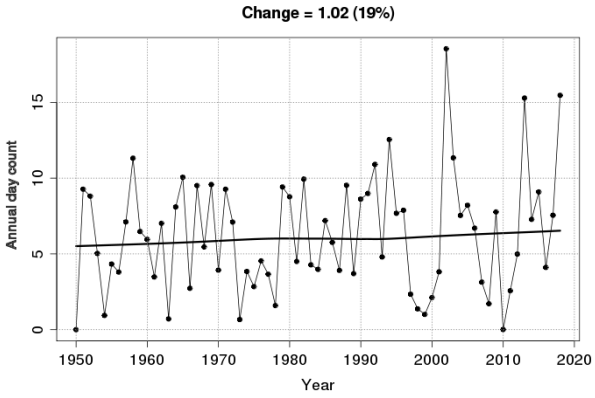

Figure H4: Time series of annual FFDI ≥ 50 days across the Central subregion (1950-2018). The average annual occurrence of FFDI ≥ 50 days has increased by 19%.

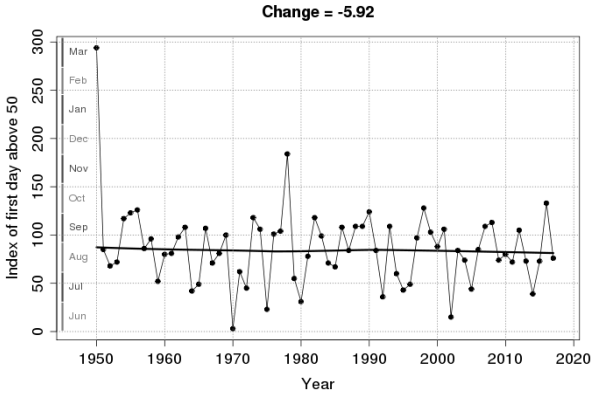

Figure H5: Time series of the index of the earliest FFDI > 50 day for the Central subregion (June-to-May years 1950/1951-2017/2018). The earliest FFDI > 50 day is now arriving around 6 days earlier.

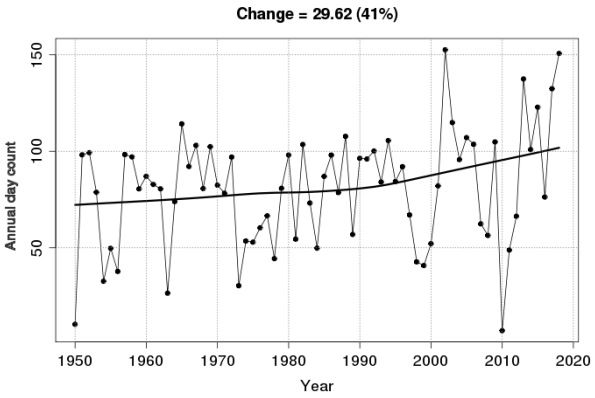

Figure H3: Time series of annual FFDI ≥ 25 days across the Central subregion (1950-2018). The average annual occurrence of FFDI ≥ 25 days has increased by 41%.

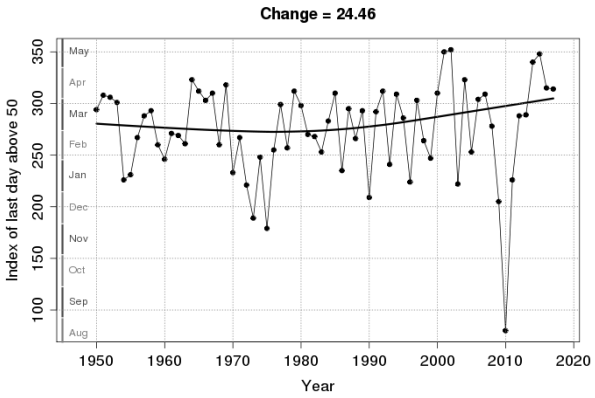

Figure H6: Time series of the index of the latest FFDI > 50 day for the Central subregion (June-to-May years 1950/1951-2017/2018). The latest FFDI > 50 day is now arriving around 24 days later.

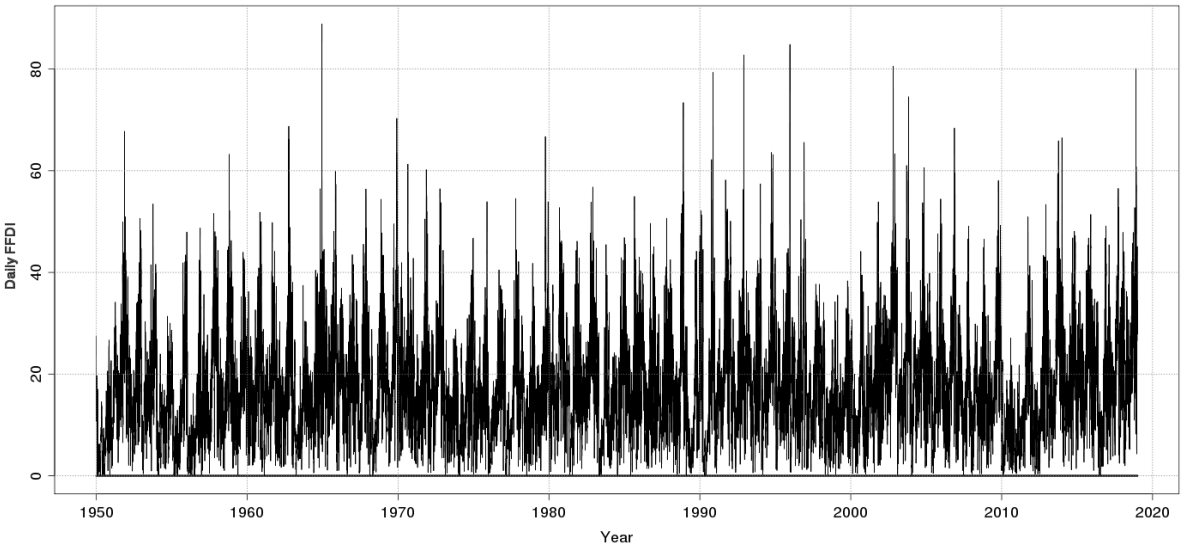

Figure H7: Time series of daily FFDI averaged across the Central subregion (1950-2018). The day with the highest spatial average for the subregion was 16 December 1964.

North West

The North West subregion comprises rainfall districts 29 and 30. Representative locations include Burketown, Hughenden, Kowanyama, Mount Isa and Richmond.

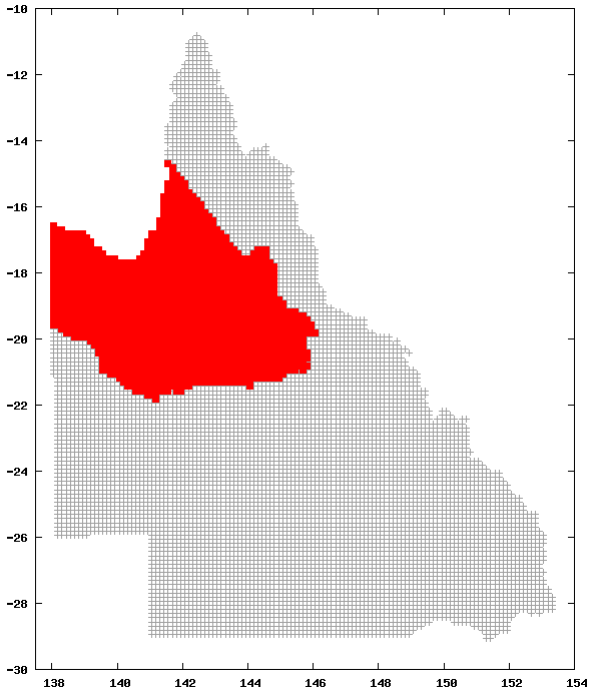

Figure I1: The North West subregion.

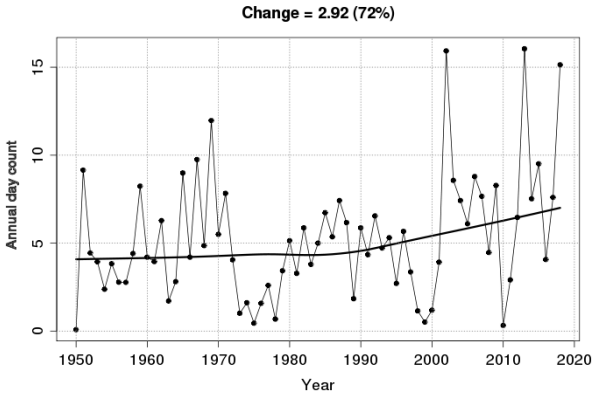

Figure I4: Time series of annual FFDI ≥ 50 days across the North West subregion (1950-2018). The average annual occurrence of FFDI ≥ 50 days has increased by 11%.

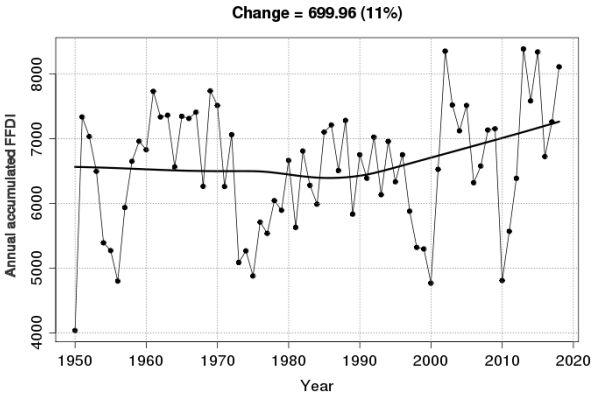

Figure I2: Time series of annual accumulated FFDI across the North West subregion (1950-2018). Annual accumulated FFDI has increased by 11%.

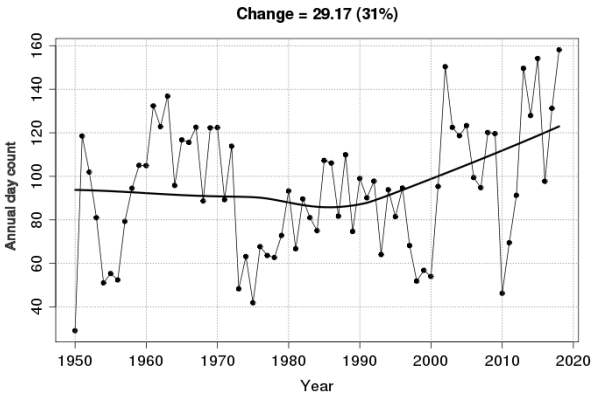

Figure I3: Time series of annual FFDI ≥ 25 days across the North West subregion (1950-2018). The average annual occurrence of FFDI ≥ 25 days has increased by 31%.

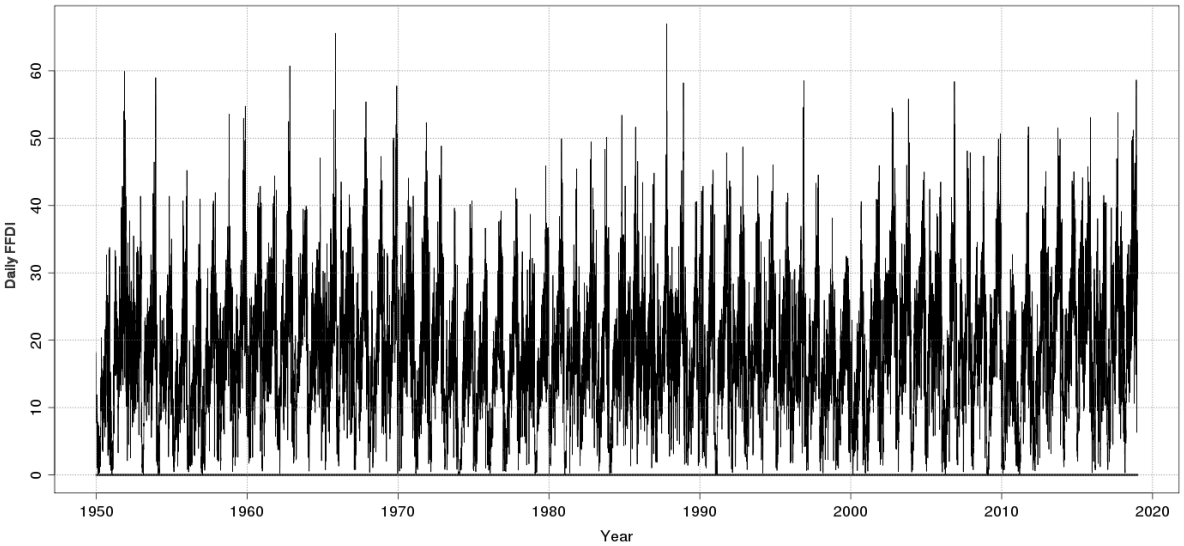

Figure I7: Time series of daily FFDI averaged across the North West subregion (1950-2018). The day with the highest spatial average for the subregion was 23 October 1987.

South West

The South West subregion comprises rainfall districts 37, 38 and 45. Representative locations include Birdsville, Boulia, Camooweal, Thargomindah and Winton.

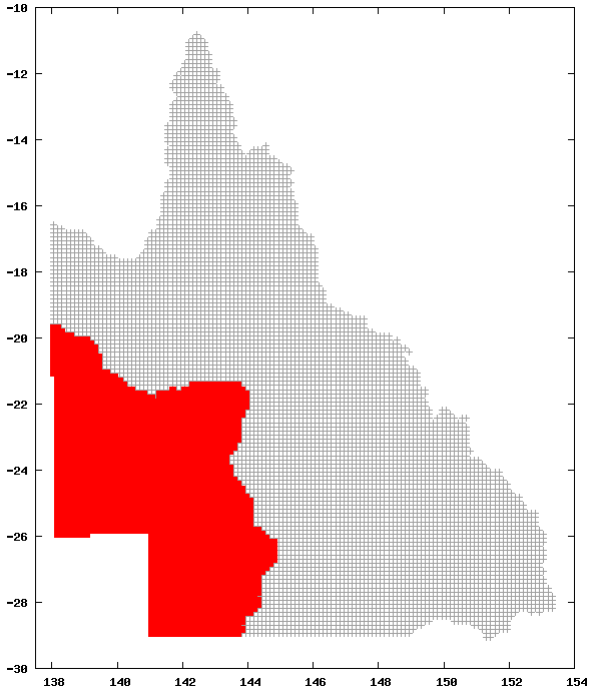

Figure J1: The South West subregion.

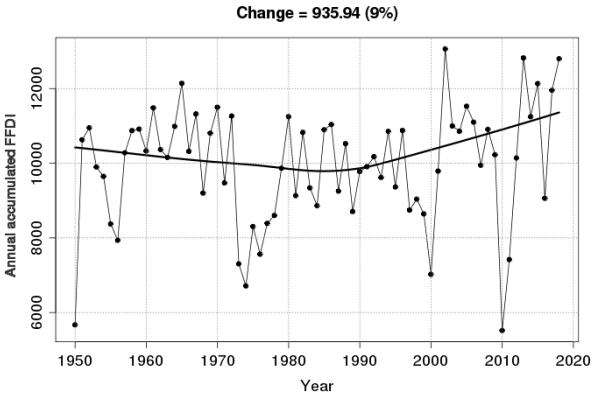

Figure J2: Time series of annual accumulated FFDI across the South West subregion (1950-2018). Annual accumulated FFDI has increased by 9%.

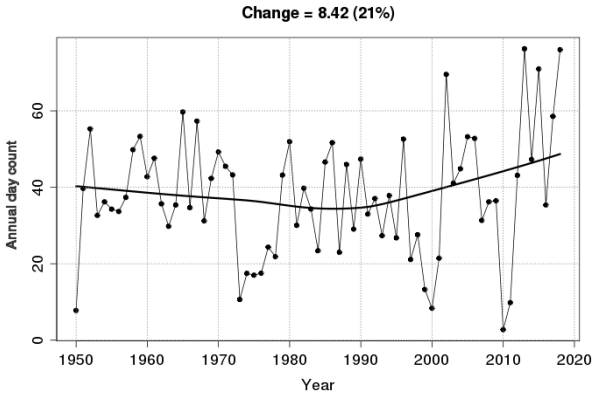

Figure J4: Time series of annual FFDI ≥ 50 days across the South West subregion (1950-2018). The average annual occurrence of FFDI ≥ 50 days has increased by 21%.

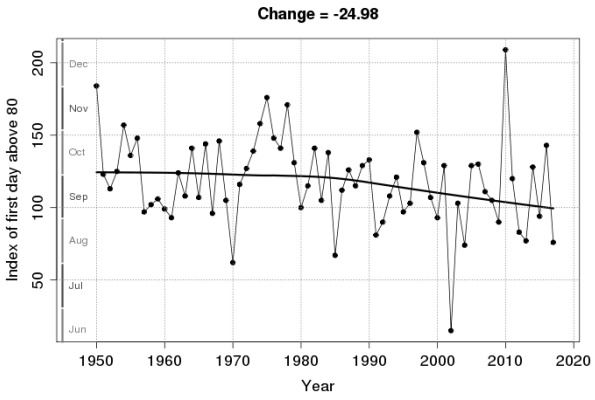

Figure J5: Time series of the index of the earliest FFDI > 80 day for the South West subregion (June-to-May years 1950/1951-2017/2018). The earliest FFDI > 80 day is now arriving around 25 days earlier.

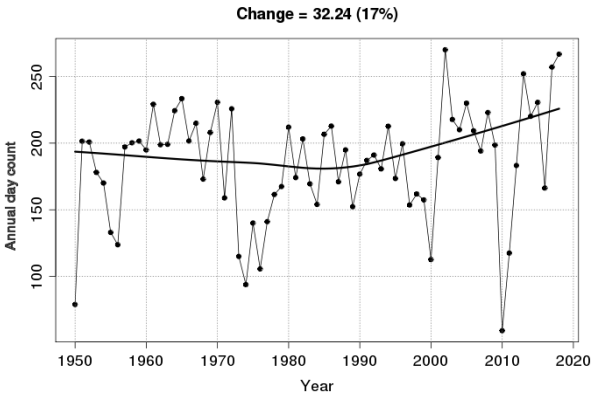

Figure J3: Time series of annual FFDI ≥ 25 days across the South West subregion (1950-2018). The average annual occurrence of FFDI ≥ 25 days has increased by 17%.

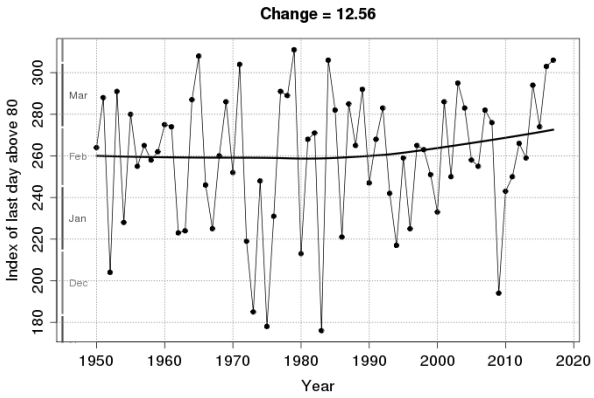

Figure J6: Time series of the index of the latest FFDI > 80 day for the South West subregion (June-to-May years 1950/1951-2017/2018). The latest FFDI > 80 day is now arriving around 13 days later.

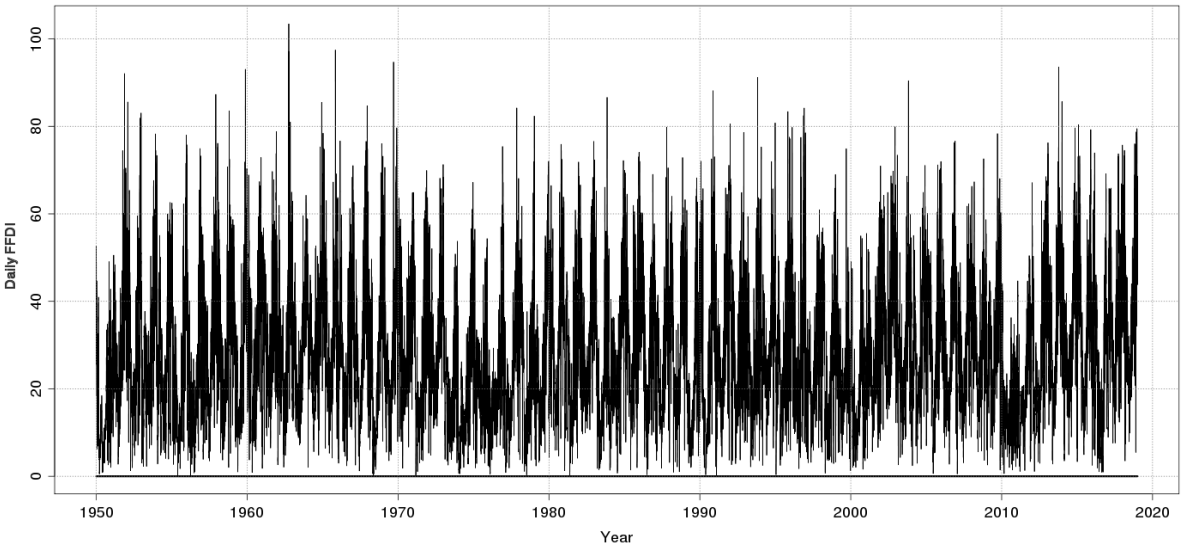

Figure J7: Time series of daily FFDI averaged across the South West subregion (1950-2018). The day with the highest spatial average for the subregion was 4 October 1962.

Discussion

The pattern of changes in the fire-weather characteristics of Queensland, as measured by the Forest Fire Danger Index (FFDI) is complicated. In part this a reflection of the climatology. In some parts of the State, the fire-weather season divides reasonably cleanly into an active part and an inactive part (e.g., the Cape York Peninsula subregion), while in other parts of the State, fire weather is more of an all-year-round proposition although with more intensity in some parts of the year than in other parts (e.g., the South West subregion).

Despite the complexity, it is apparent that the overall pattern is of an increased severity in the fire-weather season, with only small pockets of the north and west not showing an increase. In the South East Coast subregion, the increase since 1950 is particularly large, amounting to more than a 50% increase in the annual accumulated FFDI value (Figure B2). Accompanying the overall increase in severity has been a rise in more dangerous days, and an expansion of the fire-weather season, including a tendency for earlier onset and later cessation.

At the large scale, the fire weather since 2000 has been unusually severe compared to the previous five decades, with 2002, 2013 and 2018 (see Figure 35, also Figure A2) all standing well above previous years. These three years were years of significantly low rainfall: State-averaged annual rainfall percentages relative to the 1961-1990 base period were 55% (2002), 68% (2013) and 75% (2018). They also experienced well-above average temperatures: for annually averaged maximum temperature in the Jones et al. (2009) dataset, they were the third-warmest (2002), second-warmest (2013) and fourth-warmest (2018) years in the 1950-2018 period (behind 2017 as the warmest year).

The changes in FFDI are also reflective of what is happening with rainfall and temperature. Temperature has risen across the study period, consistent with global warming trends due to increasing greenhouse gas concentrations in the atmosphere. These temperature changes have a significant degree of spatial coherence across the State (Figure 17). Rainfall changes in contrast are much more spatially variable, with some parts of the State showing increasing rainfall and other parts declining rainfall (Figure 18). Afternoon windspeed over Queensland as a whole has tended to decline, particularly so during the Spring period (Figure 44) which is generally the windiest part of the year.

While the Bureau has confidence in the analyses presented here, understanding the background drivers (the interannual/interdecadal variability *versus* climate-change question) and projecting into the future poses significant challenges. The increases in the annual accumulated FFDI, particularly in the southeastern half of the State (Figure 20), in part reflect recent poor rainfall (Figure 18). Formally attributing these changes to the enhanced greenhouse effect will require significant work, and would be a necessary first step in projecting how these might further change into the future. The limited amount of published relevant climate change information available to the authors at the time of writing is assessed in the following section.

Looking Forward

The *Climate Change in Australia* project (CSIRO and Bureau of Meteorology 2015) has reported on projections of basic climate change variables. The reporting is not given on a State/Territorial basis, but rather on a climatologically driven geographical basis. The Natural Resource Management (NRM) regions have been aggregated into subclusters, clusters and superclusters. At the large scale, Australia is divided into four superclusters (Figure 46). Two of those superclusters, the Eastern Australia and Northern Australia superclusters, are particularly relevant to Queensland, although the large Rangelands supercluster encompasses the southwest of the State.

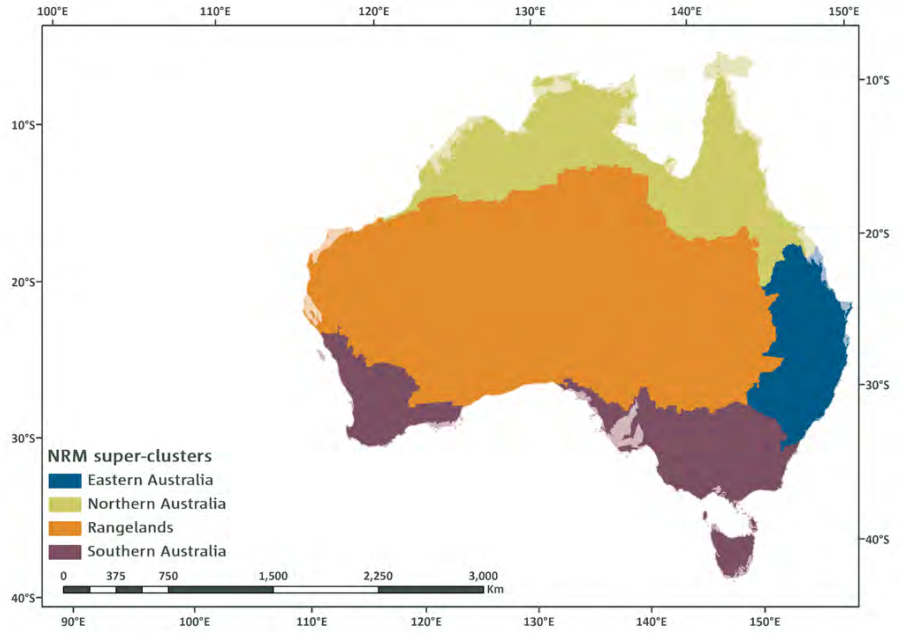

Figure 46: Map of the superclusters used in the *Climate Change in Australia* reporting. From CSIRO and Bureau of Meteorology (2015).

Figure 47 shows projections of annual maximum temperature change for the Eastern Australia supercluster, for two representative concentration pathways (RCP4.5 and RCP8.5). The RCP4.5 pathway has slow emission reductions that stabilise the CO_2 concentration at about 540 ppm by 2100, while RCP8.5 which assumes increases in emissions leading to a CO_2 concentration of about 940 ppm by 2100 (CSIRO and Bureau of Meteorology 2015). A temperature rise of more than 2 °C above the reference period by 2100 is projected under the RCP4.5 pathway. For the RC8.5 pathway, the projected temperature rise is more than 4 °C by 2100. Other things remaining the same (drought factor, wind speed, relative

humidity), a 2 °C increase in average daily maximum temperatures amounts to a 7% increase in average daily FFDI values. Such a calculation though should be treated with caution. It is unlikely, for example, that the drought factor *would* remain unaffected by a temperature rise of 2 °C.

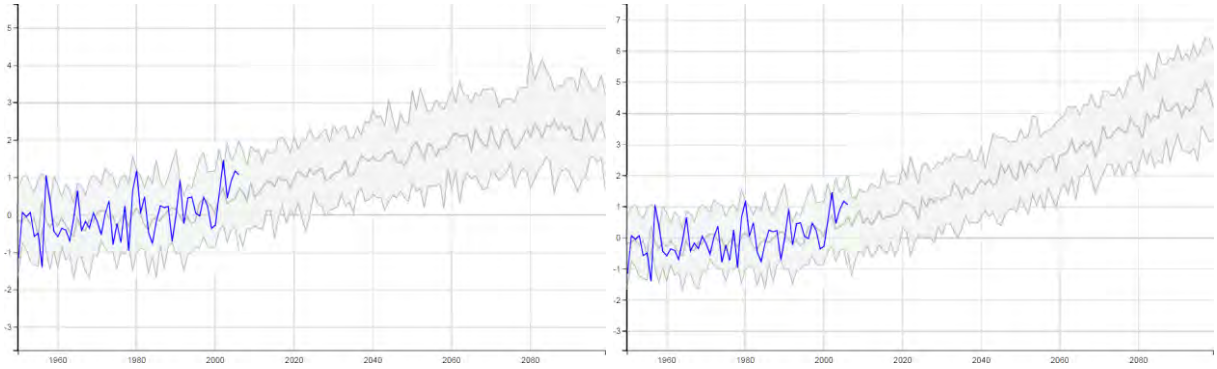

Figure 47: Projections of annual maximum temperature change (in °C) for the Eastern Australia supercluster, RCP4.5 representative concentrations pathway (left), and RCP8.5 representative concentrations pathway (right). The base period for the changes is 1950-2006. The grey band shows the range of model results. It is summarised using the median (central grey line) and 10th to 90th percentile range of the projected change in all available CMIP5 simulations. The blue line shows the AWAP analyses of the observations. From CSIRO and Bureau of Meteorology (2015).

Figure 48 shows the analogous results for the Northern Australia supercluster. The annual maximum temperature changes projected for the Northern Australia supercluster are similar to those projected for the Eastern Australia supercluster. Hence these results may be taken as indicative of the changes projected for Queensland, except possibly for the southwest of Queensland where the changes are likely to be larger.

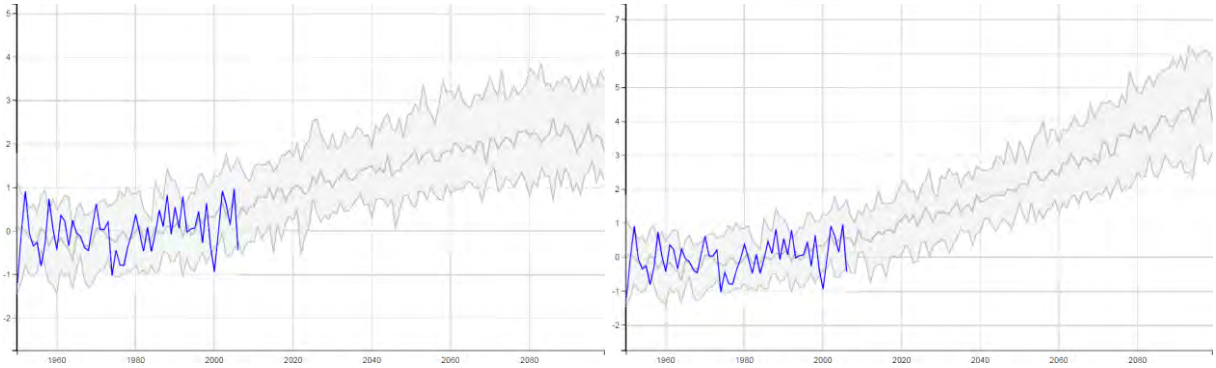

Figure 48: As per Figure 47, but for the Northern Australia supercluster. From CSIRO and Bureau of Meteorology (2015).

For annual maximum temperature the projected changes, as shown in Figures 47 and 48, are large compared with the current range of interannual variability. [For example, the 10th to 90th percentile model ranges around 1950 largely do not even overlap with those around 2100.] This is *not* the case with annual rainfall, where the projected changes even out to 2100 remain small compared with the current range of interannual variability. Figure 49 shows the annual rainfall projections for the Eastern Australia supercluster, while Figure 50 shows the corresponding projections for the Northern Australia supercluster. The projections are shown as percentage departures from the 1950-2006 mean.

As noted in the previous paragraph, the projected changes show little in the way of trends in the ensemble ranges. There is a small indication of an expansion of the ensemble range under the RCP8.5 pathway for the Northern Australia supercluster.

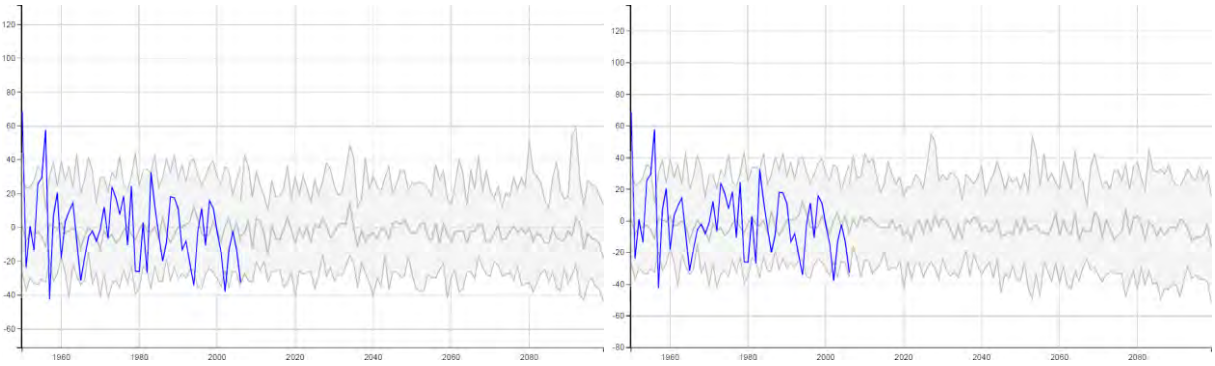

Figure 49: As per Figure 47, but for annual rainfall. Changes are shown as percentage departures from the 1950-2006 mean. From CSIRO and Bureau of Meteorology (2015).

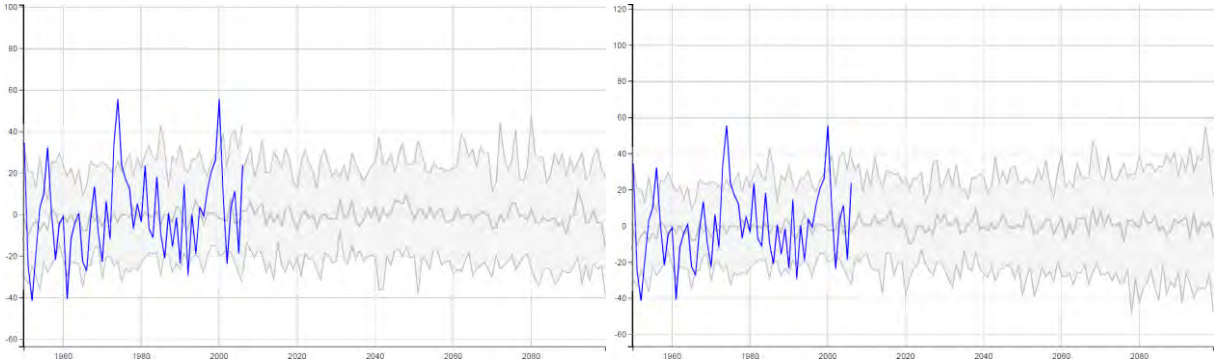

Figure 50: As per Figure 49, but for the Northern Australia supercluster. From CSIRO and Bureau of Meteorology (2015).

In the CSIRO and Bureau of Meteorology (2015) reporting, additional results are given at the cluster and subcluster spatial scale. Figure 51 shows the cluster and subcluster spatial scales. Three clusters and subclusters are of immediate importance for eastern Queensland; the Wet Tropics cluster, the Monsoonal North (East) cluster, and the East Coast (North) cluster.

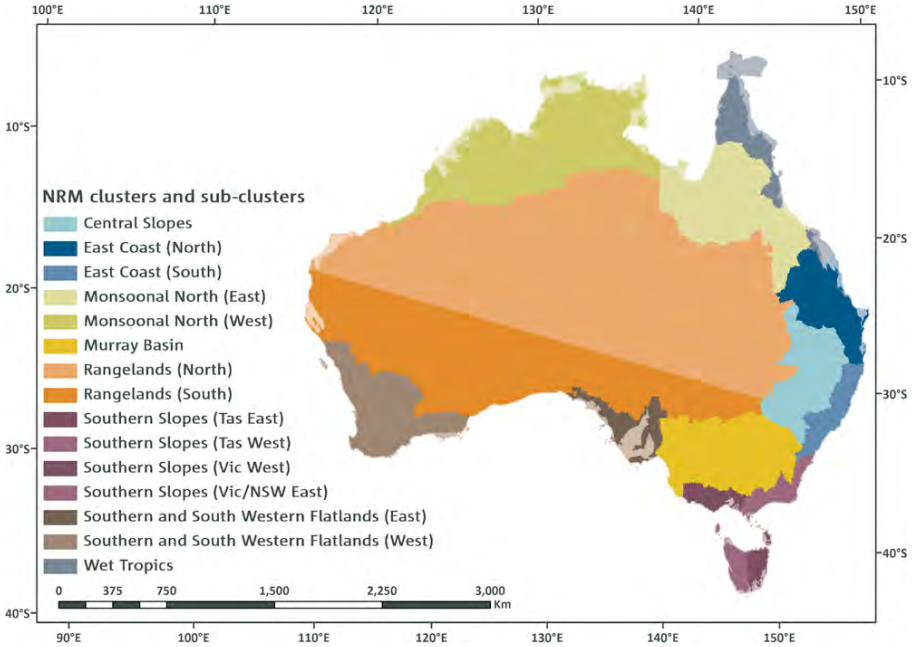

Figure 51: Map of the clusters and subclusters used in the *Climate Change in Australia* reporting. From CSIRO and Bureau of Meteorology (2015).

Figure 52 shows the projections for annual rainfall across the Wet Tropics cluster, with Figures 53 and 54 showing the analogous results for the Monsoon North (East) and East

Coast (North) subclusters, respectively. The projected changes for the Wet Tropics cluster are modest, although with a suggestion of increased annual variance under the RCP8.5 pathway. The projected changes for the Monsoon North (East) subcluster are even more minimal. In contrast, declines in annual rainfall of around 10 to 20% by 2100 are projected for the East Coast (North) subcluster.

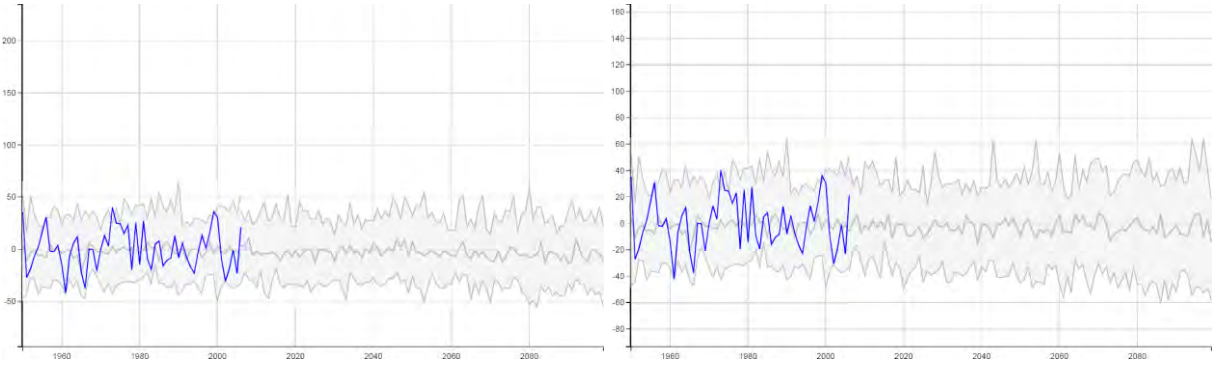

Figure 52: As per Figure 49, but for the Wet Tropics cluster. From CSIRO and Bureau of Meteorology (2015)**.**

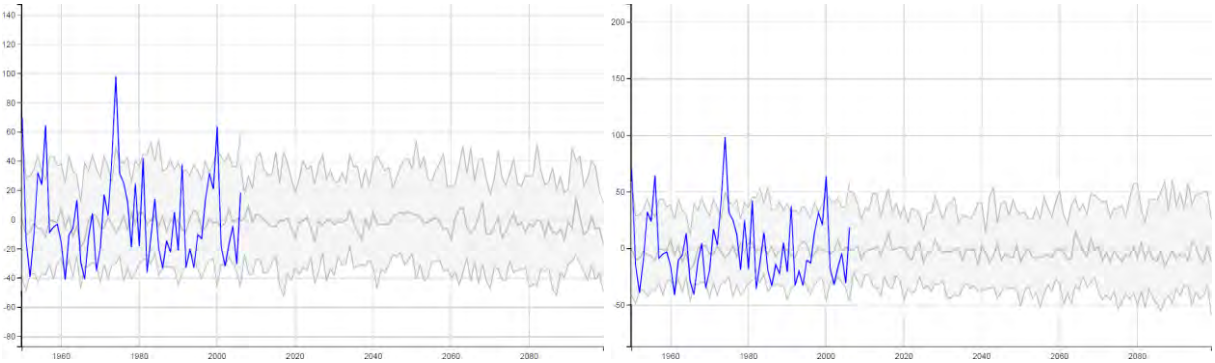

Figure 53: As per Figure 49, but for the Monsoon North (East) subcluster. From CSIRO and Bureau of Meteorology (2015).

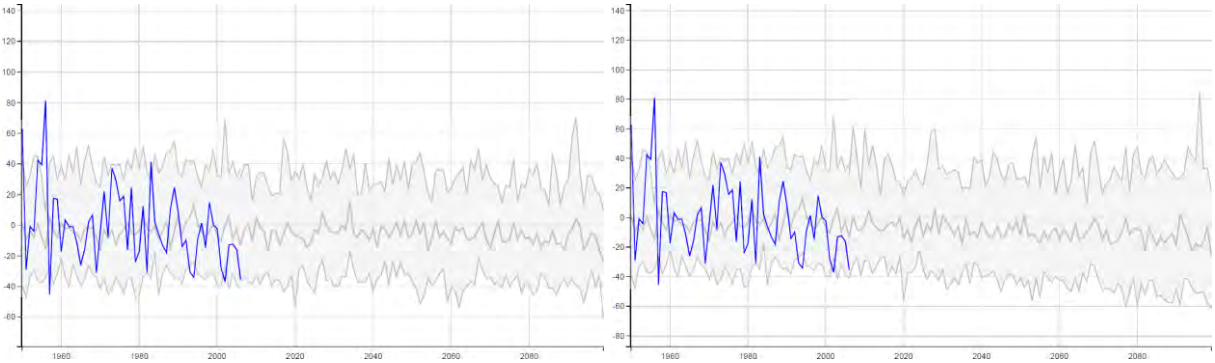

Figure 54: As per Figure 49, but for the East Coast (North) subcluster. From CSIRO and Bureau of Meteorology (2015).

FFDI projections for five Queensland locations are taken from the Eastern Australia (CSIRO and Bureau of Meteorology 2015ea) and Northern Australia (CSIRO and Bureau of Meteorology 2015na) cluster reports (Table 2 therein). The results, along with the projections for related climate variables, are shown in Table 5. The table shows results for a baseline period or 1981-2010, centred on 1995, together with two 30-year time slices centred on 2030 and 2090 for the RCP4.5 and RCP8.5 representative concentration pathways.

Table 6 shows the changes in the multi-model means for the five locations in Table 5. Annually averaged maximum temperatures are projected to rise by around 1 to 4 °C above the 1981-2010 baseline, while annual rainfall is generally projected to decline. In consequence, small increases in the annually averaged drought factor are projected. This flows through to moderately large increases in the annually accumulated FFDI, particularly for the four east-coastal locations, and large increases in the relative frequency of severe FFDI days.

A very recent report (Dowdy et al. 2019) assesses projected changes in the FFDI and Continuous Haines (CH) index across Australia. The CH index, not previously mentioned in the present assessment, is used in Dowdy et al. (2019) to "represent lower to mid-tropospheric vertical atmospheric stability and humidity measures relevant to dangerous wildfires and pyroconvective processes". They find that the "projections show a clear trend towards more dangerous near-surface fire weather conditions for Australia based on the FFDI". "Broadly consistent with previous projections of fire weather for Australia (e.g., CSIRO and Bureau of Meteorology 2015), new projections recently produced of FFDI throughout Australia show a future change towards more severe conditions including throughout Queensland, including based on an ensemble of GCMs as well as two different ensembles of finer-resolution downscaling from GCMs" (Dowdy, *pers. comm.*).

Station	Variable	1995 Baseline	2030 RCP4.5			2030 RCP8.5			2090 RCP4.5			2090 RCP8.5		
			CESM	GFDL	MIROC	CESM	GFDL	MIROC	CESM	GFDL	MIROC	CESM	GFDL	MIROC
Brisbane Airport	T	25.4	26.1	26.8	26.4	26.6	26.9	26.9	27.8	27.7	27.4	29.5	29.5	28.6
	R	1185	1043	809	1038	1080	767	934	1040	782	988	1063	638	1062
	DF	6.4	6.3	6.8	6.3	6.3	7.0	6.6	6.5	7.0	6.5	6.7	7.6	6.6
	SEV	0.6	0.7	1.0	0.7	0.7	1.2	0.8	0.9	1.0	0.7	1.4	1.7	0.8
	AccFFDI	2016	1960	2523	2032	2074	2636	2262	2179	2636	2190	2539	3327	2207
Amberley	T	27.2	28.0	28.6	28.2	28.4	28.7	28.7	29.6	29.5	29.2	31.3	31.3	30.4
	R	854	761	597	741	777	569	671	752	585	716	759	467	760
	DF	7.1	7.1	7.5	7.1	7.1	7.7	7.4	7.3	7.7	7.3	7.4	8.2	7.3
	SEV	1.3	1.3	2.2	1.7	1.6	2.5	2.0	2.0	2.4	1.8	3.1	4.1	2.1
	AccFFDI	3113	3065	3743	3179	3221	3888	3472	3371	3898	3390	3845	4755	3419
Rockhampton	T	28.7	29.5	30.2	29.7	29.9	30.3	30.3	31.1	31.1	30.8	32.9	32.9	31.9
	R	805	719	564	705	732	532	648	710	549	679	728	450	736
	DF	7.5	7.5	7.9	7.5	7.4	8.0	7.7	7.6	8.0	7.6	7.7	8.4	7.6
	SEV	0.6	0.7	1.0	0.8	0.8	1.4	0.9	0.9	1.3	0.8	1.8	2.4	1.0
	AccFFDI	3355	3305	4020	3400	3459	4142	3712	3603	4150	3622	4070	4991	3647
Townsville	T	29.3	30.1	30.6	30.2	30.4	30.9	30.7	31.4	31.6	31.6	33.2	33.7	32.5
	R	1111	1122	926	1085	1155	907	1005	1141	1083	951	1178	788	1093
	DF	7.7	7.6	7.9	7.6	7.5	7.9	7.7	7.6	7.8	7.8	7.6	8.2	7.7
	SEV	0.2	0.2	0.3	0.2	0.2	0.3	0.3	0.3	0.3	0.3	0.4	0.4	0.3
	AccFFDI	2704	2576	3299	2728	2609	3338	2999	2685	3194	3144	3022	4017	2920
Mt Isa	T	32.1	32.9	33.5	33.0	33.2	33.7	33.6	34.2	34.4	34.4	36.0	36.5	35.3
	R	452	475	405	471	495	404	440	494	489	420	505	344	478
	DF	8.4	8.4	8.6	8.4	8.3	8.6	8.5	8.4	8.4	8.6	8.4	8.8	8.5
	SEV	12.9	12.5	18.9	16.7	14.0	19.0	20.2	16.9	16.3	22.1	25.5	31.6	22.2
	AccFFDI	8118	7935	8917	8211	8035	8993	8633	8295	8730	8974	9055	10270	8833

Table 5: Annual values of maximum temperature (T; °C), rainfall (R; mm), drought factor (DF; no units), the number of severe fire danger days (SEV: FFDI greater than 50 days per year) and cumulative FFDI (AccFFDI; no units) for the 1995 baseline and projections for 2030 and 2090 under RCP4.5 and RCP8.5. Values were calculated from three climate models (CESM, GFDL and MIROC).

Station	Variable	2030 RCP4.5	2030 RCP8.5	2090 RCP4.5	2090 RCP8.5
Brisbane Airport	T	1.0	1.4	2.2	3.8
	R	-18.7%	-21.8%	-21.0%	-22.3%
	DF	1.0%	3.6%	4.2%	8.9%
	SEV	33.3%	50.0%	44.4%	116.7%
	AccFFDI	7.7%	15.3%	15.8%	33.5%
Amberley	T	1.1	1.4	2.2	3.8
	R	-18.1%	-21.3%	-19.9%	-22.5%
	DF	1.9%	4.2%	4.7%	7.5%
	SEV	33.3%	56.4%	59.0%	138.5%
	AccFFDI	6.9%	13.3%	14.1%	28.7%
Rockhampton	T	1.1	1.5	2.3	3.9
	R	-17.7%	-20.8%	-19.8%	-20.7%
	DF	1.8%	2.7%	3.1%	5.3%
	SEV	38.9%	72.2%	66.7%	188.9%
	AccFFDI	6.6%	12.4%	13.0%	26.3%
Townsville	T	1.0	1.4	2.2	3.8
	R	-6.0%	-8.0%	-4.7%	-8.2%
	DF	0.0%	-0.0%	0.4%	1.7%
	SEV	16.7%	33.3%	50.0%	83.3%
	AccFFDI	6.1%	10.3%	11.2%	22.8%
Mt Isa	T	1.0	1.4	2.2	3.8
	R	-0.4%	-1.3%	3.5%	-2.1%
	DF	0.8%	0.8%	0.8%	2.0%
	SEV	24.3%	37.5%	42.9%	104.9%
	AccFFDI	2.9%	5.4%	6.8%	15.6%

Table 6: As per Table 5, but showing the multi-model-mean changes for temperature (T; in °C) and percentage changes for the remaining four variables.

Appendix: The November/December 2018 Fires

During late November / early December 2018, there was a prolonged period of severe fire weather, with consequent fire activity, across Queensland, particularly in southeast and central parts of the State (Bureau of Meteorology 2018b). The fires were scattered across a large area. Figure P1 shows a satellite image for 26 November 2018. Smoke plumes are evident along the east coast of Queensland between Bundaberg and Mackay.

Figure P1: Satellite image for 26 November 2018, obtained from the USA's NASA Earth Observatory. The image shows smoke plumes along the east coast of Queensland between Bundaberg and Mackay.

A comprehensive report has been prepared for the Bushfire and Natural Hazards Cooperative Research Centre (Mills 2019) on the meteorology and antecedent climate relating to the period, and the reader is primarily referred to that report. This Appendix presents some additional details of interest.

Figure P2 shows the highest daily FFDI within the Wide Bay and Burnett and Central Coast subregions from 1 November to 31 December 2018. FFDI values in the *Severe* category or

higher were seen in the Wide Bay and Burnett and/or Central Coast subregions from 25 November to 3 December 2018.

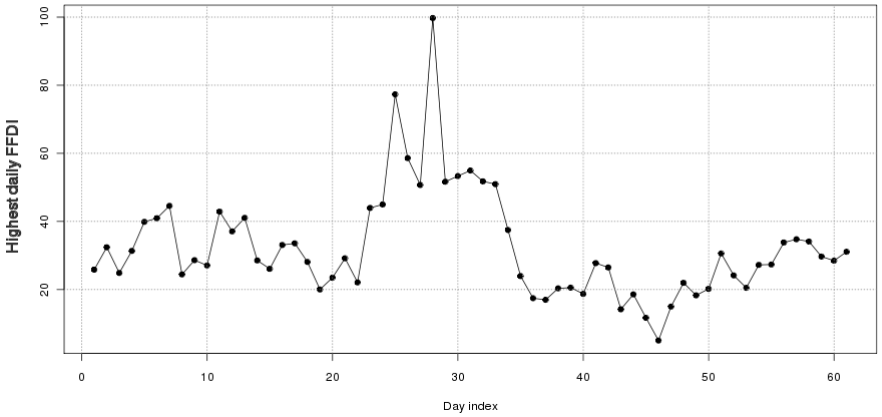

Figure P2: Highest daily FFDI within the Wide Bay and Burnett and Central Coast subregions from 1 November to 31 December 2018.

Figure P3 shows maximum temperature deciles for November 2018 across Queensland. This calculation is based on the Bureau of Meteorology's operational whole-network high-resolution monthly maximum temperature analyses of Jones et al. (2009). For most of the east coast of the State, November 2018 average maximum temperatures were in the top 10 percent of historical outcomes (from 1910 to the present; orange shades), with some parts (dark orange) showing highest on record outcomes.

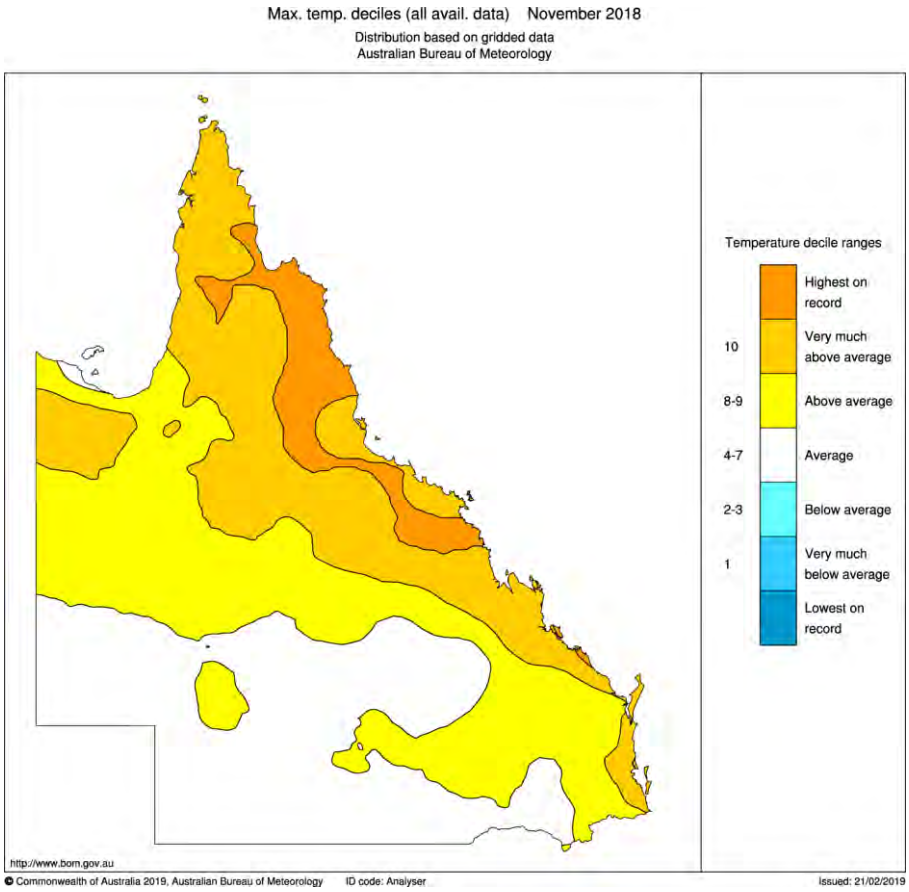

Figure P3: Maximum temperature deciles across Queensland for November 2018. The calculation compares November 2018 averaged maximum temperature against the Novembers from 1910 to 2018.

Figure P4 shows the places where the highest daily maximum temperature in November 2018 exceeded the previous highest November daily maximum temperature across the Novembers 1911 to 2017, and the amount of that exceedance (in °C). New November records were set along more than half of the east coast of Queensland. In several places, the existing records were broken by more than 2 °C.

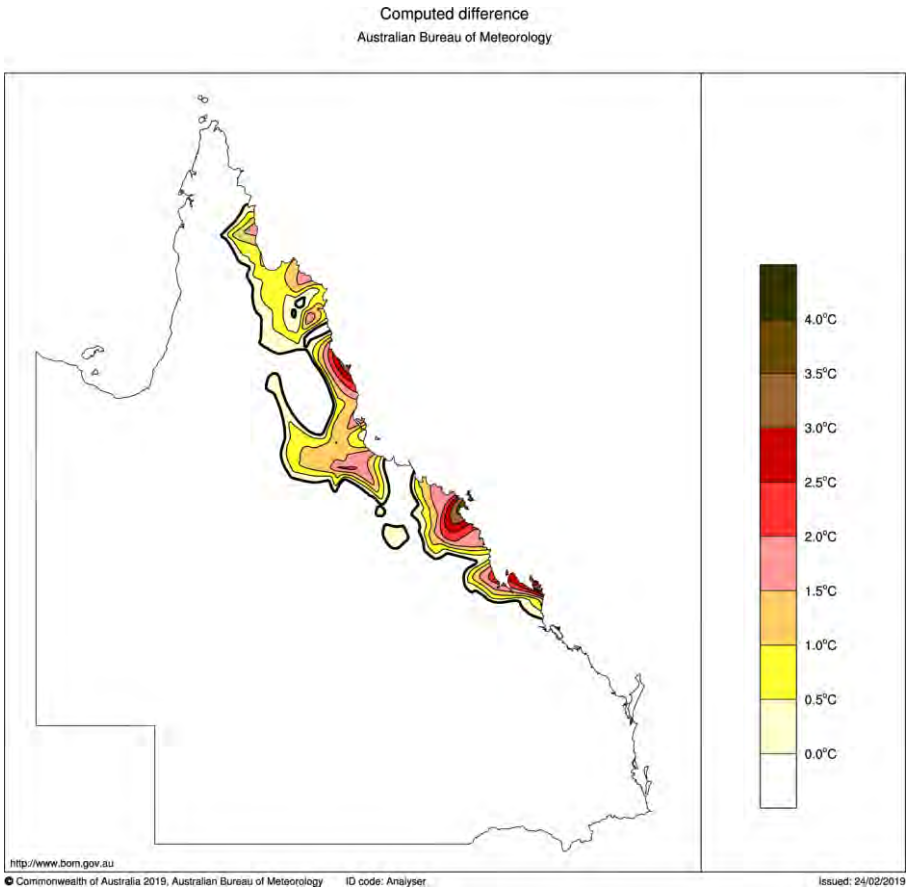

Figure P4: Places where the highest daily maximum temperature in November 2018 exceeded the previous highest November daily maximum temperature (Novembers 1911 to 2017), and the amount of that exceedance (in °C). White-shaded areas are where the highest daily maximum temperature in November 2018 did not exceed the previous highest November daily maximum temperature.

Figure P5 shows an analogous calculation to that shown in Figure P4, but for three-day-averaged maximum temperatures in November 2018. Here again, new records were set for November three-day-averaged maximum temperatures along more than half of the east coast of Queensland. In several places, the existing records (across the Novembers 1910 to 2017) were broken by more than 3 °C. The areas of record breaking in Figure P5 appear to be more extensive than those in Figure P4.

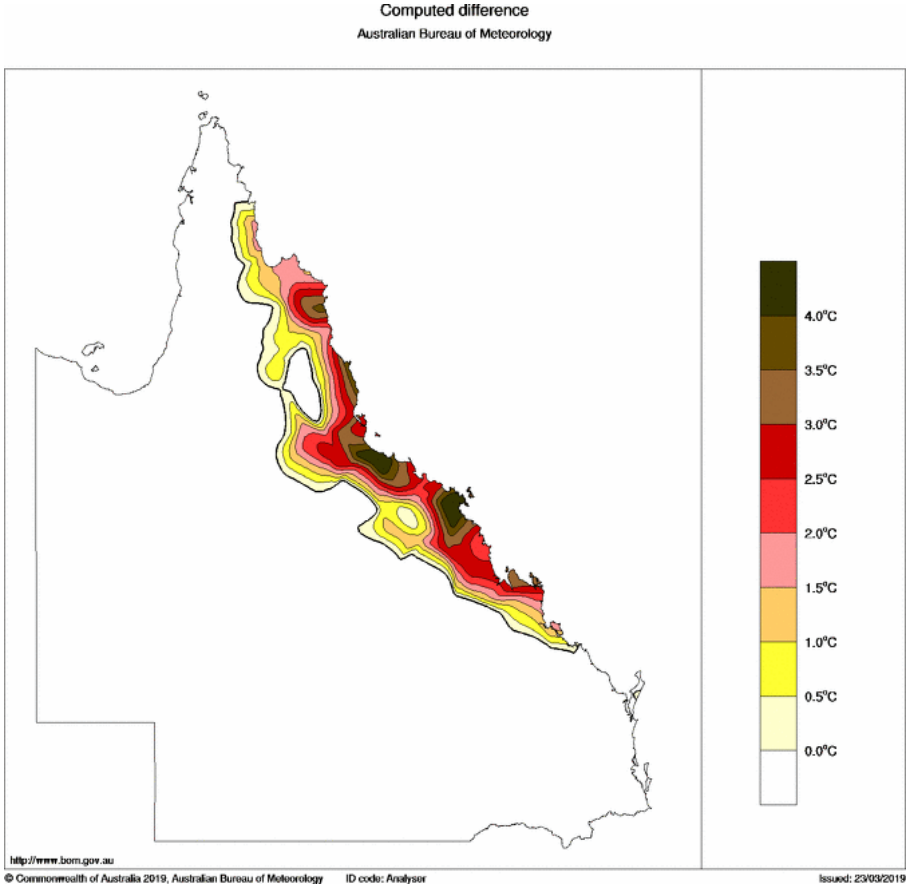

Figure P5: Places where the highest three-day maximum temperature in November 2018 exceeded the previous highest November three-day maximum temperature (Novembers 1910 to 2017), and the amount of that exceedance (in °C). White-shaded areas are where the highest three-day maximum temperature in November 2018 did not exceed the previous highest November three-day maximum temperature.

Figure P6 shows an analogous calculation to that shown in Figures P4 and P5, but for five-day-averaged maximum temperatures in November 2018. The areas of record breaking in Figure P6 are comparable to those shown in Figure P5 for three-day maximum temperature.

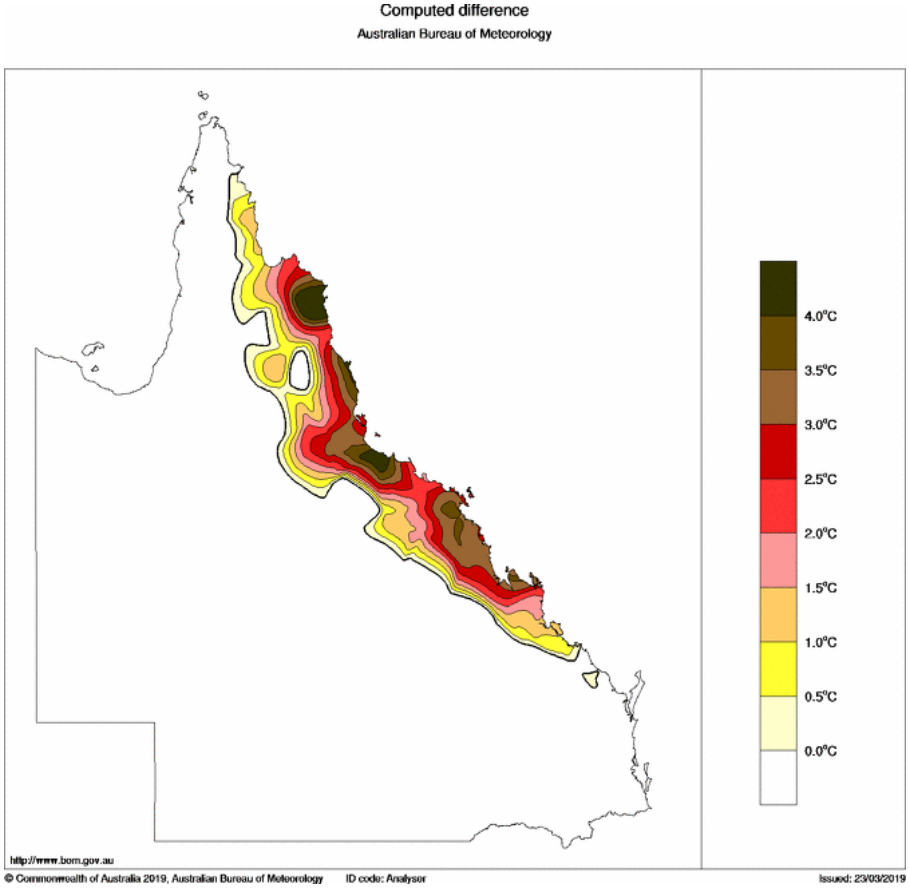

Figure P6: Places where the highest five-day maximum temperature in November 2018 exceeded the previous highest November five-day maximum temperature (Novembers 1910 to 2017), and the amount of that exceedance (in °C). White-shaded areas are where the highest five-day maximum temperature in November 2018 did not exceed the previous highest November five-day maximum temperature.

Figure P7 shows FFDI deciles for November 2018 across Queensland. The comparison is made for accumulated November 2018 FFDI against accumulated November FFDI for the Novembers 1950 to 2018. Accumulated FFDI values were above average (deciles 8 to 9) to very much above average (decile 10) across a broad swathe of eastern Queensland, and highest on record for Novembers across an area in central Queensland.

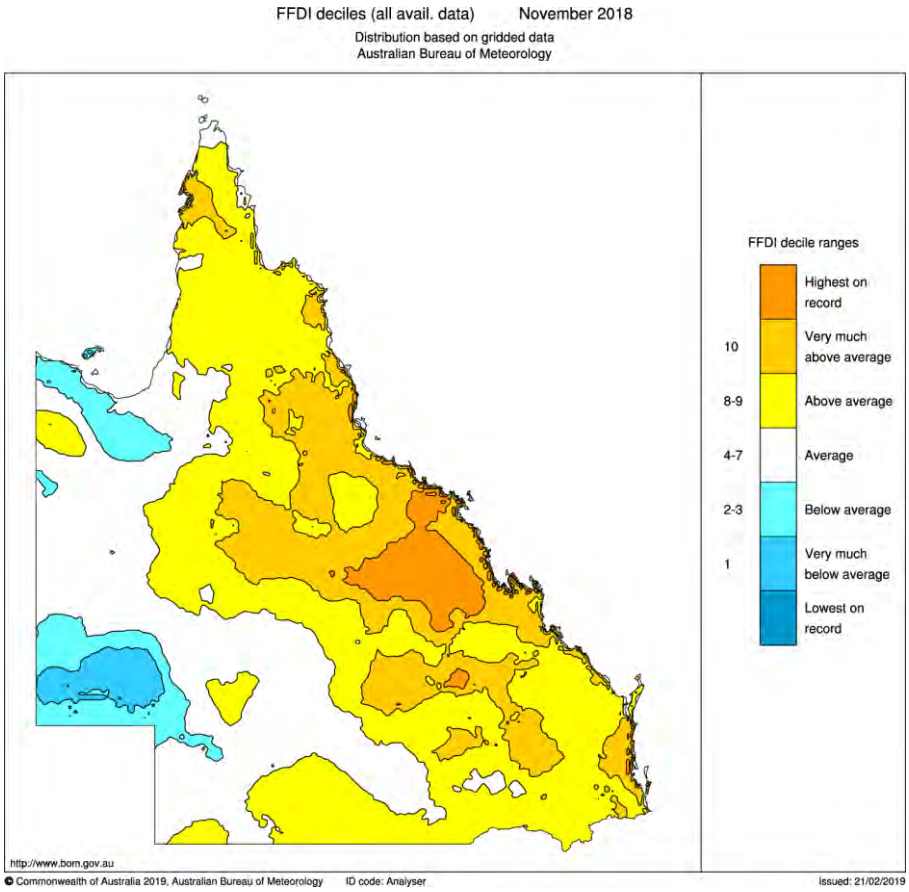

Figure P7: FFDI deciles across Queensland for November 2018. The calculation compares November 2018 accumulated FFDI against the Novembers from 1950 to 2018.

Figure P8 shows the highest daily FFDI across Queensland in November 2018, mapped in terms of the standard McArthur categories. Note that this calculation is based, as indicated in the Data and Methods section, on afternoon maximum temperature, relative humidity and windspeeds. A notional instantaneous calculation using synchronous temperature, relative humidity and windspeed (e.g., by using high frequency NWP forecast data) might well yield higher values at particular locations than are seen in the Dowdy (2018) gridded dataset (and mapped here).

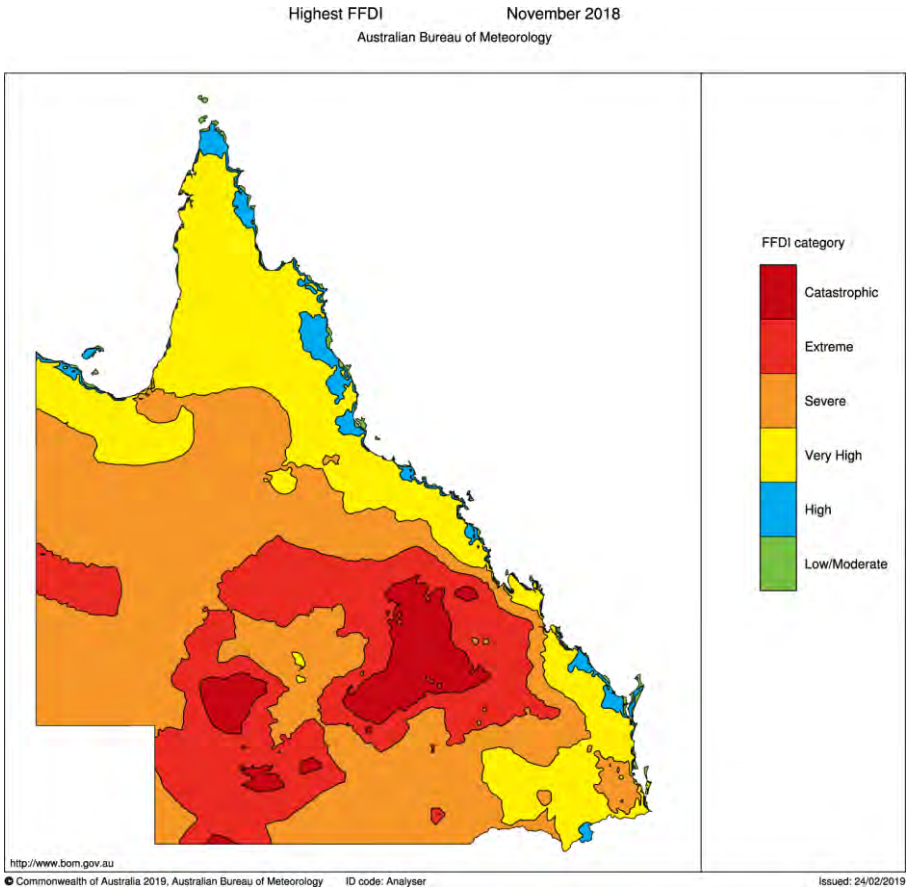

Figure P8: Highest daily FFDI in November 2018.

Another way in which FFDI values above these gridded values might be seen is through the use of site data, whether in the traditional afternoon FFDI calculation which forms the basis for the gridded dataset or the notional instantaneous calculation using synchronous data. [One potential cause for such higher values comes from the use of site wind speeds, which could be locally higher than the areal averages implicit in NWP modelling and gridded datasets like the Dowdy (2018) dataset.] The results of one such calculation is shown in Figure P9 for Rockhampton (Bureau site number 039083). High-frequency data from the AWS are used to calculate notional instantaneous FFDI values throughout the day. The values shown in the figure are accordingly the daily maximum for each day. In the gridded dataset, the highest daily value at the AWS location is 76 FFDI points, while the highest instantaneous site value exceeds 125 FFDI points (Figure P9). It should be noted that these two values are *not* a like-for-like comparison.

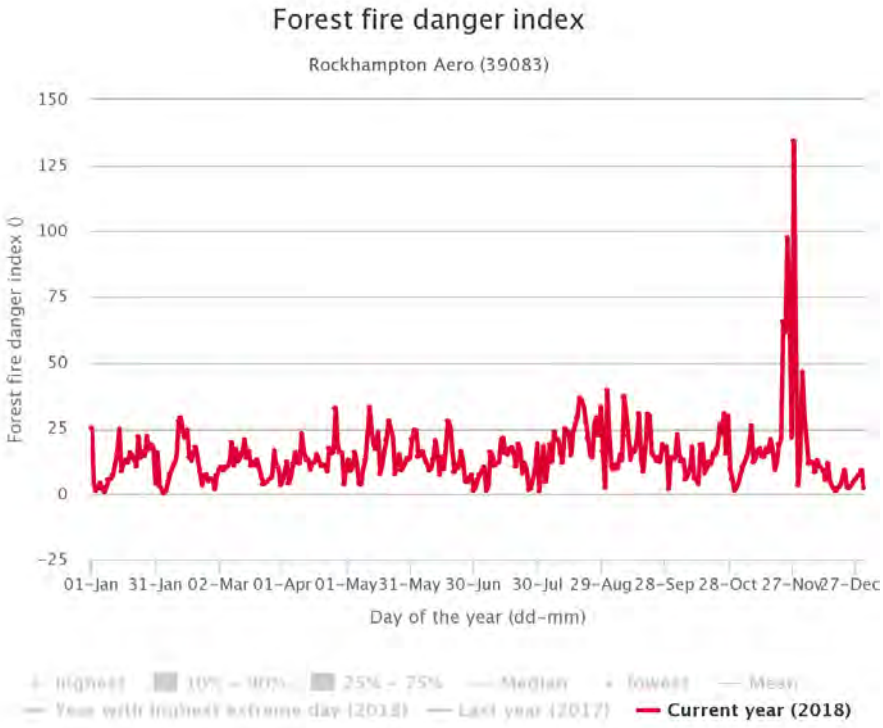

Figure P9: Highest calculated FFDI for each day in 2018 at Rockhampton (Bureau station 039083).

Figure P10 shows the places where the highest daily FFDI in November 2018 exceeded the previous highest November daily FFDI (across the Novembers from 1950 to 2017). In some places, the previous November record was exceeded by more than 30 FFDI points.

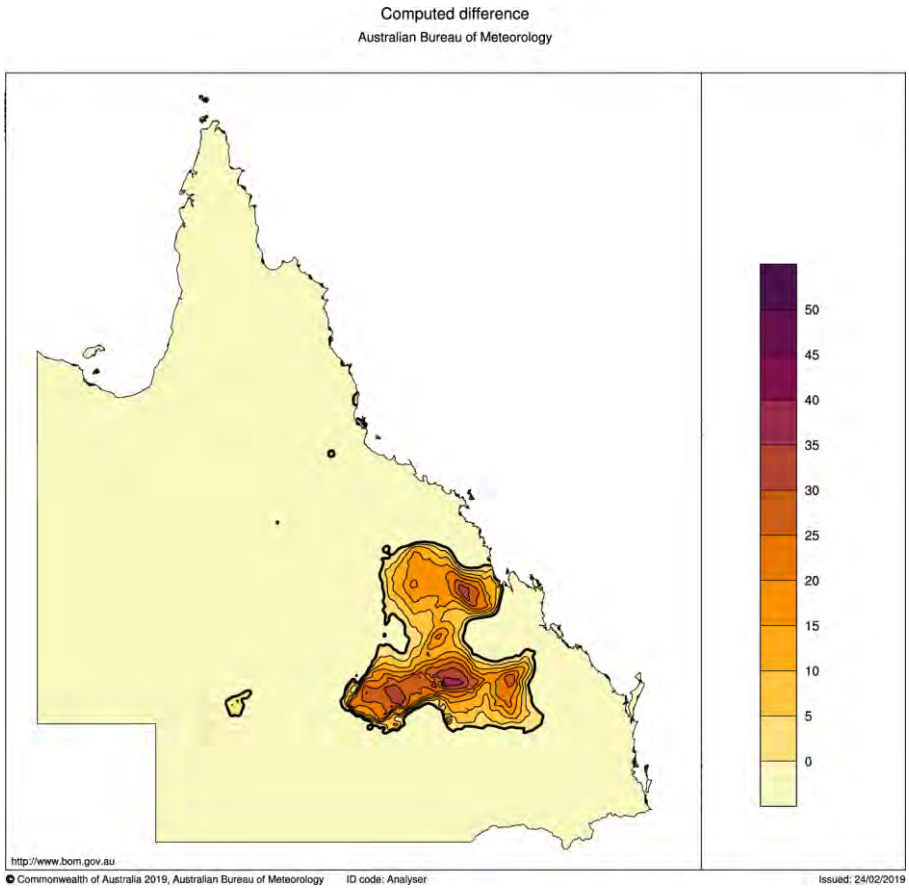

Figure P10: Places where the highest daily FFDI in November 2018 exceeded the previous highest November daily FFDI (Novembers 1950 to 2017), and the amount of that exceedance (in FFDI units). The pale yellow shade denotes places where the previous highest on record November daily FFDI was not exceeded during November 2018.

References

Blanchi R, Lucas C, Leonard J and Finkele K (2010), *Meteorological conditions and wildfire-related house loss in Australia*, International Journal of Wildland Fire, **19(7)**, 914-926.

Bureau of Meteorology (2008), *Climate of Australia*, Bureau of Meteorology, Melbourne, Australia, 214pp.

Bureau of Meteorology (2018a), *Climate Change and Bushfire Risk in New South Wales*, a report prepared for the New South Wales Rural Fire Service by the Bureau of Meteorology. 52pp.

Bureau of Meteorology (2018b), *Special Climate Statement 67 - an extreme heatwave on the tropical Queensland coast*, issued 12 December 2018, a report by the Bureau of Meteorology. 30pp. Available online at http://www.bom.gov.au/climate/current/statements/scs67.pdf.

Crompton R P, McAneney K J, Chen K, Pielke R A (Jnr) and Haynes K (2010), *Influence of Location, Population, and Climate on Building Damage and Fatalities due to Australian Bushfire: 1925-2009*, Weather, Climate, and Society, **2**, 300-310, doi.org/10.1175/2010WCAS1063.1.

CSIRO and Bureau of Meteorology (2015), *Climate Change in Australia Information for Australia's Natural Resource Management Regions: Technical Report*, CSIRO and Bureau of Meteorology, Australia, 218pp. Available online at https://www.climatechangeinaustralia.gov.au/. Time series projections taken from https://www.climatechangeinaustralia.gov.au/en/climate-projections/explore-data/time-series-explorer/.

CSIRO and Bureau of Meteorology (2015ea), *East Coast Cluster Report, Climate Change in Australia Projections for Australia's Natural Resource Management Regions: Cluster Reports*, lead author Dowdy A, eds. Ekström M et al., CSIRO and Bureau of Meteorology, Australia.

CSIRO and Bureau of Meteorology (2015na), *Monsoonal North Cluster Report, Climate Change in Australia Projections for Australia's Natural Resource Management Regions: Cluster Reports*, lead author Moise A, eds. Ekström M et al., CSIRO and Bureau of Meteorology, Australia.

CSIRO and Bureau of Meteorology (2018), *State of the Climate 2018*, CSIRO and the Australian Bureau of Meteorology, 24pp. Available online at http://www.bom.gov.au/state-of-the-climate/State-of-the-Climate-2018.pdf.

Dowdy A J (2018), *Climatological Variability of Fire Weather in Australia*, Journal of Applied Meteorology and Climatology, **57**, 221-234, DOI: 10.1175/JAMC-D-17-0167.1.

Dowdy A J, Ye H, Pepler A, Thatcher M, Osbrough S L, Evans J P, DiVirgilio G and McCarthy N (2019), *Future changes in extreme weather and pyroconvection risk factors for Australian wildfires*, Nature Scientific Reports, 9:10073, doi.org/10.1038/s41598-019-46362-x.

Fawcett R J B and Trewin B C (2003), *Seasonal climate summary southern hemisphere (autumn 2002): onset of El Niño conditions*, Australian Meteorological Magazine, **52**, 127-136.

Fawcett R, Trewin B and Jones D (2010), *On emerging droughts*, Bulletin of the Australian Meteorological and Oceanographic Society, **23**, 28-36.

Ganter C (2011), *Seasonal climate summary southern hemisphere (winter 2010): a fast developing La Niña*, Australian Meteorological and Oceanographic Journal, **61**, 125-135.

Harris S, Anderson W, Kilinc M and Fogarty L (2012), *The relationship between fire behaviour measures and community loss: an exploratory analysis for developing a bushfire severity scale*, Natural Hazards, **63(2)**, 391-415.

Hunt S, Hamwood R and Ollerenshaw S (1995), *Beerburrum Fires - September & November 1994*, Report by the Wildfire Investigation Committee. 58pp.

Jones D A (2003), *Seasonal climate summary southern hemisphere (winter 2002): consolidation of El Niño conditions in the Pacific*, Australian Meteorological Magazine, **52**, 203-212.

Jones D A, Wang W and Fawcett R (2009), *High-quality spatial climate data-sets for Australia*, Australian Meteorological and Oceanographic Journal, **58**, 233-248.

Mills G (2019), *The climate over northern Queensland leading to and including the fire period/heatwave of 23-11-2018 to 4-12-2018*, Bushfire and Natural Hazards Cooperative Research Centre (in preparation).